DIFFUSION OF RADIOGENIC HELIUM IN SHALLOW GROUNDWATER: IMPLICATIONS FOR CRUSTAL DEGASSING

by

Amy Lynn Sheldon

A dissertation submitted to the faculty of
The University of Utah
in partial fulfillment of the requirements for the degree of

Doctor of Philosophy

in

Geology

Department of Geology and Geophysics

The University of Utah

August 2002

THE UNIVERSITY OF UTAH GRADUATE SCHOOL

SUPERVISORY COMMITTEE APPROVAL

of a dissertation submitted by

Amy L. Sheldon

This dissertation has been read by each member of the following supervisory committee and by majority vote has been found to be satisfactory.

May 2, 2002 — Chair: D. Kip Solomon

May 2 2002 — John R. Bowman

May 9, 2002 — David S. Chapman

2 MAY 2002 — Thure E. Cerling

May 2, 2002 — Robert F. Poreda

THE UNIVERSITY OF UTAH GRADUATE SCHOOL

FINAL READING APPROVAL

To the Graduate Council of the University of Utah:

I have read the dissertation of Amy L. Sheldon in its final form and have found that (1) its format, citations, and bibliographic style are consistent and acceptable; (2) its illustrative materials including figures, tables, and charts are in place; and (3) the final manuscript is satisfactory to the supervisory committee and is ready for submission to The Graduate School.

July 9 2022
Date

D. Kip Solomon
Chair, Supervisory Committee

Approved for the Major Department

Ronald L. Bruhn
Chair

Approved for the Graduate Council

David S. Chapman
Dean of The Graduate School

ABSTRACT

The clay till of Sarnia and fractured bedrock of Smithville, Ontario provide well-characterized groundwater systems in which to examine the diffusive transport and crustal degassing of helium. Although poorly defined in the literature, the application of effective diffusion coefficients accurately describes the transport of ^4He in geologic media and is examined at both sites. In addition, the sites provide an opportunity to determine the crustal degassing flux in shallow groundwater systems for comparison to large sedimentary basins.

The effective diffusion coefficients of ^4He in clay till and fractured shale are examined by numerical simulation of measured groundwater ^4He concentrations at both sites. Effective diffusion coefficients of 6.3×10^{-6} cm^2/s and 1.48×10^{-7} cm^2/s were determined for the clay till and the Rochester Shale, respectively. A mass balance of methane substantiates that diffusion is the primary means of mass transport through the shale and define a CH_4 effective diffusion coefficient of 3.7×10^{-8} cm^2/s. The model results emphasize the importance of applying an effective diffusion coefficient to describe the transport of helium through geologic media.

The internal release rates and degassing fluxes are determined for both sites. The He degassing fluxes out of the clay till (2.7×10^8 atoms $^4He/m^2/s$) and Rochester Shale ($1.22 - 1.70 \times 10^8$ atoms $^4He/m^2/s$) are similar to the crustal degassing fluxes reported in the literature. The results of this study suggest the importance of the release of stored helium to the crustal degassing flux. Furthermore, the results indicate that a significant percentage of ancient stored helium is released to the atmosphere during erosional processes that cause grain size reduction and are not measurable in groundwater.

A new dissolved gas sampling method was developed to permit sample collection from small diameter peizometers and/or low permeability units. The results of field and laboratory analysis indicate that the samplers equilibrate in ~8 hours in advection-dominated systems, and within two weeks in a controlled diffusion-dominated system. The samplers allow for high quality

dissolved gas samples with minimal effort, time, and expense. The samplers eliminate sample loss and contamination common to other methods of obtaining dissolved gas samples.

TABLE OF CONTENTS

LIST OF TABLES

ACKNOWLEDGMENTS

The research performed at Sarnia was funded by an NSF research grant. Also supportive towards this research were John Cherry, Muin Husain, DaChang Zhang, and Lesley Sebol. DaChang Zhang and John Halleran provided field assistance on blistery cold days. The hospitality and friendship of Betty and Gord Tully made me feel at home in Petrolia, Ontario.

Gratitude is extended to the National Water Research Institute of Canada for their contributions. Kent Novakowski and Pat Lapcevic provided much understanding of the hydrogeology of the Smithville site, access to unpublished data, and cooperation with fieldwork. Sampling was greatly aided by the generous field assistance provided by Lavinia Zanini, Charles Talbot, and John Voralek. Ted O'Neill kindly provided access to Smithville Phase IV site photographs and documents. Sincere appreciation is extended to David Vacco for his assistance in reproducing lost documents. Finding for the Smithville research was provided by the U.S. EPA and the Smithville Phase IV project.

My sincerest appreciation is extended to my advisor Kip Solomon and committee members Bob Poreda, Thure Cerling, John Bowman, and Dave Chapman. Kip Solomon provided significant guidance and encouragement, and displayed enormous patience throughout this endeavor. Bob Poreda provided analyses of some dissolved gas samples and Andy Hunt performed most of those analyses. Thure Cerling, John Bowman and Dave Chapman were always encouraging and Thure frequently provided a greatly appreciated sense of humor to the monotony of laboratory analysis. Alan Rigby helped with the analysis of tritium and dissolved gas samples at Utah and Andy Manning provided valuable discussion.

Ronit Nativ and Brian Sheldon are responsible for encouraging me to pursue a Ph.D. I am grateful for their support and friendship.

CHAPTER 1

RADIOGENIC HELIUM IN SHALLOW GROUNDWATER WITHIN A CLAY TILL, SOUTHWESTERN ONTARIO

1.1 Abstract

Radiogenic helium-4 ($^4He_{rad}$) has been used in many studies to date groundwater ranging from 1,000 to a million years. Recently, residual ^4He released from aquifer solids has been identified as a potential groundwater dating technique for waters 10 to 1,000 years (Solomon et al, 1996). Radiogenic ^4He produced within shallow systems by the release from aquifer/aquitard grains often occurs at a rate greater than can be supported by U/Th series decay. In this study, ^4He is examined in a clay aquitard at two sites in SW Ontario. Fluid velocities at the sites have been negligible throughout most of the Holocene, resulting in diffusion controlled solute transport for up to 15,000 years (Husain, 1996). A steady state model of He transport resulting from spatially and temporally constant release rates failed to adequately reproduce observed concentration profiles. A transient numerical model that incorporates a constant ^4He concentration at the lower boundary, a near zero vertical fluid velocity, internal ^4He production that results from solid state diffusion out of aquitard solids, and an upper boundary ^4He concentration controlled by atmospheric exchange can reasonably reproduce measured concentrations. The measured concentration profiles are consistent with an effective ^4He diffusion coefficient of 0.02 m^2/yr (6.3 x 10^{-6} cm^2/s), that is 10% of the free-solution diffusion coefficient for helium at 15 ^oC. A comparison of model concentration profiles to measured ^4He data indicates the radiogenic ^4He release rate of 0.03 to 0.13 μcc/kg/yr is comparable to measured release rates from core samples, and to release rates determined at other aquifer sites. Although the aquitard was deposited approximately 15,000 years ago, rates of He release from solids are consistent with estimates of the amount of ^4He present in the protolith only if the

solids were losing ^{4}He for 50,000 to 60,000 years. The internal release of radiogenic helium can account for the He degassing flux out of the till and is comparable to continental crust degassing fluxes in the literature. Model results support the hypothesis of the internal release of ancient helium from aquifer/aquitard grains at a rate significantly greater than can be supported by U/Th series decay. Furthermore, the study supports the argument for the use of radiogenic helium as a groundwater dating technique provided the internal release from grains is properly quantified.

1.2 Introduction

He-4 occurs naturally in the atmosphere and subsurface. Subsurface radiogenic ^{4}He production results from the α-decay of U/Th-series elements in rocks and sediments ($^4He_{rad}$). A recent investigation (Solomon et al., 1996) into shallow groundwater systems indicates that ^{4}He may be released from aquifer solids at rates that are: a.) orders of magnitude greater than rates due to U/Th decay, and b.) quantifiable using mass spectrometric techniques (Solomon et al., 1996). Thus, Solomon and others (1996) propose that ^{4}He may be a useful groundwater dating technique for waters 10^1 - 10^3 years in age.

^{4}He in groundwater can be of atmospheric or subsurface origin. Subsurface production of ^{4}He often results in groundwater concentrations that are several orders of magnitude greater than water in equilibrium with the atmosphere (Davis and De Wiest, 1966; Andrews and Lee, 1979; Marine, 1979; Torgersen, 1980; Stute et al., 1992). Mass transport of $^4He_{rad}$ out of aquifer solids results in increased groundwater concentrations. The ^{4}He content of groundwater is therefore a result of the $^4He_{rad}$ release (mass transport) rate and the elapsed time since the water entered the saturated zone. If the release occurs at the rate of U/Th series decay, then measurable amounts of ^{4}He will accumulate after about 1000 years, and theoretically continue for millions of years. The steady state production of ^{4}He from the decay of U/Th-series elements is described by Pearson and others (1991) as

$$G = \rho N_L \left\{ 8\left[{}^{238}U\right]\left(\frac{\lambda_{238}}{M_{238}}\right) + 7\left[{}^{235}U\right]\left(\frac{\lambda_{235}}{M_{235}}\right) + 6\left[{}^{232}Th\right]\left(\frac{\lambda_{232}}{M_{232}}\right)\right\} \qquad (1.1)$$

where

G ^{4}He release rate per unit volume of solids per unit time

ρ density of solids

N_L Avogadro's Number

λ_i decay constants for radioactive isotopes, *i*, of U and Th

M_i molecular weights of radioactive isotopes, *i*, of U and Th

[*i*] decimal fraction of radioactive isotopes, *i*, of U and Th in solids.

He-4 has thus traditionally been used as a groundwater tracer over a long time scale (Andrews and Lee, 1979; Marine, 1979; Torgersen, 1980; Andrews et al., 1982; Torgersen and Ivey, 1985; Balderer and Lehmann, 1989; Bottomley et al., 1990; Ballentine et al., 1991; Mazor and Bosch, 1991; Stute et al., 1992; Marty et al., 1993). Recent investigations of shallow groundwater systems (Solomon et al., 1996), however, demonstrate ^{4}He accumulation rates that are 100-200 times greater than the production of $^4He_{rad}$ from U/Th series decay.

Elevated concentrations of ^{4}He in shallow groundwater have been well documented (Davis and De Wiest, 1966; Andrews and Lee, 1979; Marine et al., 1979; Torgersen and Ivey, 1985; Stute et al., 1992) and previously interpreted as the result of ^{4}He diffusion from older underlying units (external source). Previous research indicates that helium produced within the continental crust and the mantle is released to the atmosphere by migrating upward into groundwater flow systems. The crustal and mantle helium fluxes are dependent on several factors, including groundwater advection rates, diffusion coefficients, U/Th concentrations, and geologic history. Estimates of the crustal and mantle helium fluxes have been determined for various large-scale aquifer systems, such as the Great Hungarian Plain, Paris Basin, and the Great Artesian Basin, in various tectonically active regions (primarily mantle fluxes), and from atmospheric helium budgets.

The measured He degassing fluxes from continental crust vary spatially and temporally (O'Nions and Oxburgh, 1988; Torgersen and O'Donnell, 1991). Generally, however, the crustal helium fluxes cluster within a factor of 4 of the estimated mean global flux of 8.4×10^9 atoms/m^2_e/yr (O'Nions and Oxburgh, 1988), where m_e refers to the 30% continental land surface area. Larger flux variations are expected at smaller scales compared to the large-scale aquifer

systems commonly studied. In addition, non-steady state cases may exist where local upper crustal rocks are young (Tertiary to Quarternary) in age (Stute et al., 1992). Thus, it is potentially more difficult to determine continental fluxes from small-scale, or localized, measurements (O'Nions and Oxburgh, 1988). Although the crustal helium fluxes vary between basins and methods of determination, there is general agreement. When the uncertainty of the data is considered, the range in helium fluxes is insignificant (Cserepes and Lenkey, 1999).

At the site studied by Solomon and others (1996), however, the downward vertical flow rate is sufficient to minimize upward diffusion of ^4He. Thus, the source of elevated ^4He in groundwater is proposed to be diffusion from aquifer solids (internal source) rather than the upward diffusion from underlying bedrock. Incremental heating studies of $^4He_{rad}$ release performed on aquifer solids extrapolated well to field measured values, supporting the hypothesis of diffusional $^4He_{rad}$ release from aquifer grains (Solomon et al., 1996).

Solomon and others (1996), interpret the high $^4He_{rad}$ release rate observed as the release of stored helium. Prior to erosion and deposition of the aquifer grains, the accumulation of $^4He_{rad}$ within grains was facilitated by the decay of U/Th-series elements, the low porosity of the protolith, and the relatively small surface area to volume ratio of protolith grains. After the erosion and deposition of aquifer grains having a large surface to volume ratio, $^4He_{rad}$ release rates greater than that resulting from U/Th production can occur for a finite period of time.

The release rate of ancient or stored helium from aquifer or aquitard grains is dependent on the grain size, mineralogy, temperature, initial helium content, and geologic history (Solomon and Cook, 2000). For a sediment having an initial ^4He concentration of 50 μcc/g, quartz grains having a diameter of 0.01 cm (100 μm; very fine sand) can release helium at rates significantly greater than the steady-state release from U and Th decay for up to 10^7 years provided the sediments are cooler than ~20°C (Figure 1.1; Solomon et al., 1996). Meanwhile, grains larger than 0.5 cm release helium at rates indistinguishable from the steady-state release from U and Th decay. Grain sizes smaller than 0.001 cm (silt) will release helium at very high rates for a shorter duration (~10^4 yrs). Thus, grain size significantly affects the rate and duration of ^4He released from grains. Because the release of helium from sediment grains

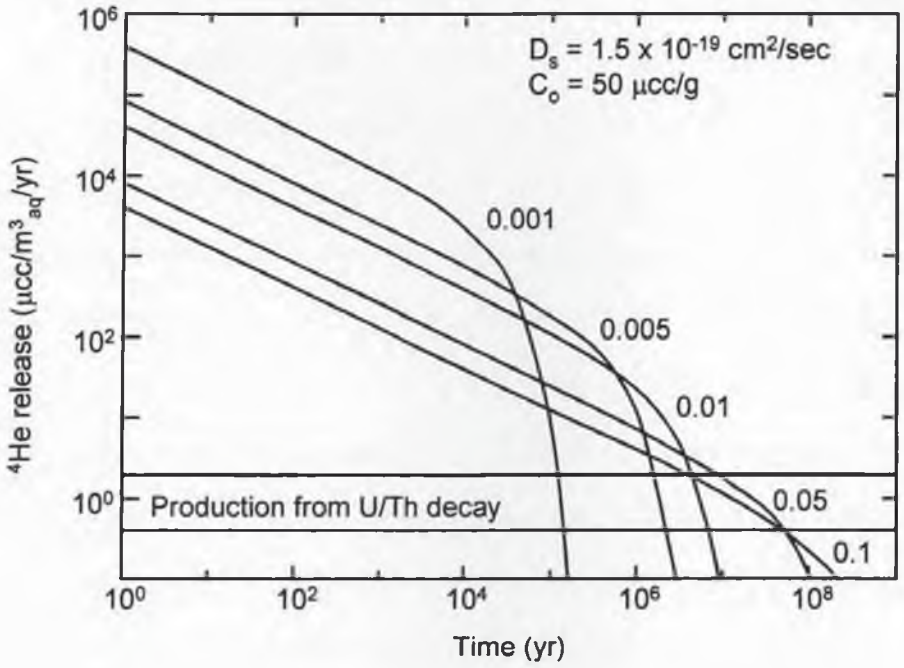

Figure 1.1. ^{4}He release rate from spherical grains. Model performed for grains having an initial concentration of 50 µcc/g. A solid-state diffusion coefficient of 1.5 x 10^{-19} cm^2/sec was applied, which is equal to the diffusion coefficient for quartz at ~20°C. Grain size diameters ranging from 0.1 to 0.001 cm are depicted.

is controlled by the solid-state helium diffusion coefficient, temperature is also an important factor in controlling the release rate (Solomon and Cook, 2000). Higher temperatures would result in larger solid-state diffusion coefficients and thus higher release rates. The solid-state diffusion coefficient for helium in quartz grains is 5.1×10^{-20} cm^2/s at 10 °C, 8.3×10^{-17} cm^2/s at 100 °C, and 1.1×10^{-14} cm^2/s at 200 °C. Therefore, grains that are or have been exposed to elevated temperatures may release the bulk of their stored helium over a shorter duration of time. Grain mineralogy is likely to have an effect on the helium release rate. Minerals such as zircon, apatite, and sphene contain U and retain helium much better than quartz, which more readily releases helium (Strutt, 1908a,b; Strutt, 1909; Hurley, 1954; Damon and Kulp, 1958). Finally, the geologic history of grains will affect the ^4He release rate through time. Small grains that have been reworked might have long ago exhausted their stored helium, whereas grains that have been recently reduced in size might release helium at rates significantly greater than the steady-state release from U and Th decay. Thus, recently deposited glacial sediments are potential candidates for the application of ^4He as a groundwater dating method for young waters because they are recently eroded, and then deposited in lacustrine settings.

In order to examine the internal release and transport of ^4He in the subsurface, I have measured the ^4He concentration in two clay-rich tills near Sarnia, Ontario. The sites were chosen because: 1.) mass transport is dominated by diffusion (rather than advection as at previous sites); 2.) the sites have been well characterized hydrologically; and 3.) previous research indicates the age of groundwater in the underlying aquifer to be modern at one site and Pleistocene at the second site (Desaulniers et al., 1981; Sklash et al., 1986; Baxter, 1987, Erdmann, 1987, Farvolden and Cherry, 1988; Crnokrak, 1990; Beaton, 1994; Remenda et al., 1994; Husain, 1996, Husain et al., in press). A companion study (Hunt, 2000) was designed to determine the grain sizes and mineralogy of the till and measure the ^4He release rate from bulk till samples. My study also provides an opportunity to compare the helium degassing flux resulting from the internal production of helium to the average continental degassing flux, and to evaluate the effective ^4He diffusion coefficient in the subsurface.

1.3 Field Site

The field sites are located in Lambton County, Ontario, between Lake Huron and Lake St. Clair (Figure 1.2). Brander Park is located near the St. Clair River, approximately 40 km south of the city of Sarnia. Warwick is located 30 km east of Sarnia. Each site consists of a cluster of peizometers and aquifer and bedrock wells (Husain, 1996). The topography of the area is flat and the region is referred to as the St. Clair Clay Plain.

1.3.1 Quaternary Aquitard

Both locations consist of clay till deposited in proglacial lakes (McKay and Fredericia, 1995; Klint, 1996) during the last Wisconsin glacial cycle (Lewis et al., 1994). The till thickens westward across Lambton County from 20 to 50 m. At the sites studied, the till consists of two distinct units (Fitzgerald et al., 1979) which are collectively referred to as the Quaternary Aquitard. The upper 10 to 15 m makes up the St. Joseph Till, which is underlain by the Black Shale Till (Figure 1.3; Fitzgerald et al., 1979). The Black Shale Till contains pebbles of black shale originating from the underlying Devonian Kettle Point Formation. Generally, the tills consist of 40 to 60% clay, 30 to 40% silt, 5 to 10% sand and less than 5% gravel-sized particles (Hanna, 1966; Soderman and Kim, 1970). The till is composed of carbonates, quartz, clay minerals, feldspars, and shale fragments (Desaulniers et al., 1981). The Black Shale and St. Joseph tills were deposited roughly 14,000 and 13,000 carbon-14 years ago in glacial lakes Maumee and Whittlesey (Lewis et al., 1994; Klint, 1996).

Collectively, the tills are divided into two hydraulic sections. The uppermost fractured section of the till (< 6 m) is the Active Zone in which water table fluctuations occur (D'Astous et al., 1989; McKay, 1991; Ruland et al., 1991). The rest of the till is hydraulically inactive (Figure 1.3). The hydraulic conductivity of the weathered till within the Active Zone ranges from 10^{-6} to 10^{-9} m/s, while the hydraulic conductivity of the underlying Inactive Zone is 10^{-10} m/s or less (Goodall and Quigley, 1977; Desaulniers et al., 1981; Desaulniers, 1986; D'Astous et al., 1989; McKay, 1991; Ruland et al., 1991; Harris, 1994; Murphy, 1994). Previous research (Desaulniers, 1986; Rowe et al., 1988; Johnson et al., 1989; Yanful and Quigley, 1990; McKay et al., 1993) indicates a porosity range of 0.37 to 0.44, with an average of 0.40 for the till.

Figure 1.2. Location map of the two field sites within Lambton County, Ontario (dashed line). Modified after Husain, 1996.

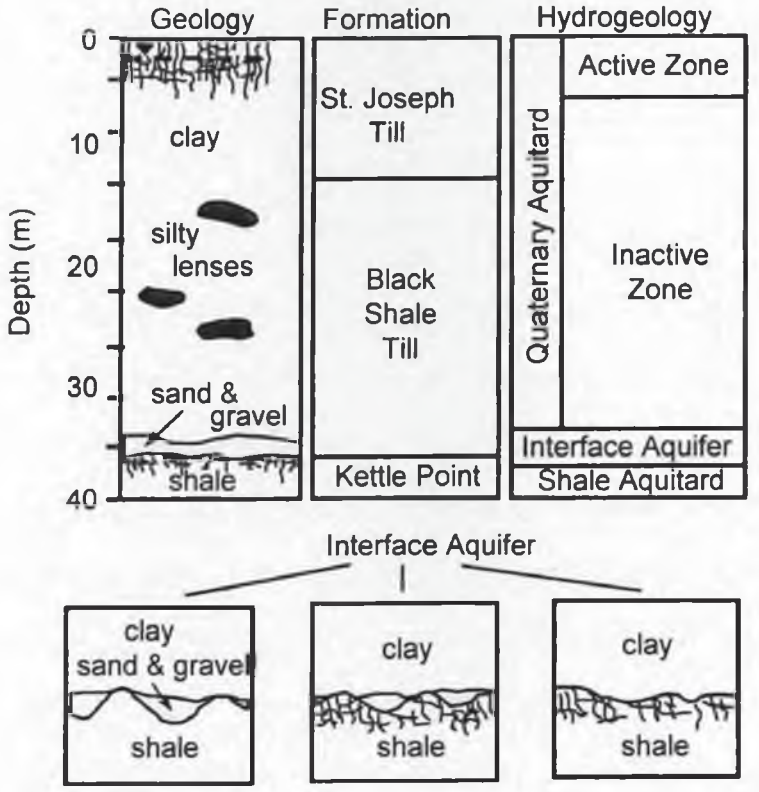

Figure 1.3. The geology and hydrogeology of the shallow Quaternary Aquitard and the Interface Aquifer. Modified after Husain, 1996.

Numerous studies have examined the hydraulic gradient within the till (Goodall and Quigley, 1977; Desaulniers et al., 1981, 1986; Crooks and Quigley, 1984). The downward vertical gradients observed today were previously considered representative of the conditions throughout the Holocene (Desaulniers et al., 1981, 1986). Recently, however, Weaver (1994), suggested the downward vertical hydraulic gradient is a response to increased aquifer pumping during the 1940s and 1970s. Groundwater modeling performed by Husain (1996), suggests the hydraulic gradient in the aquitard was very small to negligible (<0.01 m/m) in an upward rather than downward direction throughout most of the Holocene. In either case, the groundwater velocity within the clay is believed to have been very small to negligible throughout the last 15,000 years (Goodall and Quigley, 1977; Desaulniers et al., 1981, 1986; Husain, 1996; Husain et al., 1998), making solute transport controlled primarily by diffusion.

Based on chloride and oxygen-18 profiles, Husain (1996) determined that groundwater within the till is Pleistocene in age. Where the till is thin (e.g., Warwick), diffusion of modern ^{18}O signatures from fresh water at the surface and within the underlying aquifer have over-printed the Pleistocene ^{18}O signature (Husain, 1996). Where the till is thick (e.g., Brander park), ^{18}O data suggest a diffusive profile from modern signatures (~-10‰) near the surface to Pleistocene signatures (~-17‰) at depth.

1.3.2 Interface Aquifer

The Interface Aquifer lies below the till and occurs as discontinuous sand and gravel deposits overlying the fractured bedrock surface (Mellary and Kilburn, 1969; Husain, 1996). The Interface Aquifer consists of fractured bedrock at Warwick, and silty sand and gravel at Brander Park (Husain, 1996). Typically, the aquifer is 1-3 m thick and is bounded above by the clay till and below by the shale bedrock aquitard (Figure 1.3; Desaulniers et al., 1981).

The Interface Aquifer is recharged at topographically high areas located 45 km northeast of the St. Clair River and through sand plains near the eastern border of Lambton County (Husain, 1996). Within Lambton County, the aquifer discharges to Lake Huron and Lake St. Clair (Husain, 1996). A portion of the aquifer is believed to be relatively stagnant due to a groundwater flow divide located between the two lakes and the thickness of the overlying clay

till. The average hydraulic conductivity of the aquifer at the Brander Park site is approximately 3 x 10^{-9} m/s and 10^{-5} m/s at the Warwick site (Husain, 1996). Two orders of magnitude range in the hydraulic conductivity is typical for the aquifer, with the highest conductivity measured in the east and the lowest near the St. Clair River (Interra, 1989; Jagger Hims Lt., 1994; Weaver, 1994).

The age of groundwater within the aquifer varies from modern to Pleistocene, based on oxygen isotope signatures present (Figure 1.4; Desaulniers et al., 1981; Sklash et al., 1986; Baxter, 1987; Erdmann, 1987; Farvolden and Cherry, 1988; Crnokrak, 1990; Beaton, 1994; Remenda et al., 1994; Husain, 1996; Husain et al., in press). Modern water exists in regionally active portions of the aquifer where the overlying till is thin (~20 m). Pleistocene age water exists within an inactive portion of the regional aquifer system overlain by ~40 m of till.

1.4 Dissolved Gas Sampling

The size (typically < 0.8 in ID) and low yield of the multilevel monitoring wells did not permit samples to be collected using conventional Cu tubes. In situ diffusion samplers (Figure 1.5) were used instead (see Appendix A for details). Diffusion samplers are gas-filled devices that equilibrate with dissolved gases in water. Because of changes in gas pressure and sampler volume when the devices are removed from a well, it is only possible to accurately determine the gas composition. In order to determine dissolved gas concentrations, the measured composition (or mole fraction) of a gas is multiplied by the total dissolved gas pressure as follows.

$$C_i = K_i X_i P_T \qquad (1.2)$$

where

C_i dissolved gas concentration

K_i Henry's Law coefficient

X_i measured mole fraction

P_T total dissolved gas pressure.

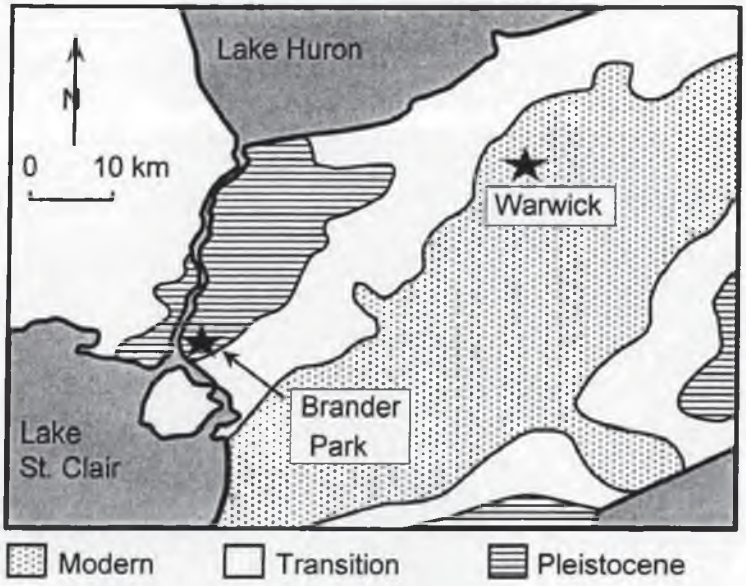

Figure 1.4. Groundwater age within the Interface Aquifer. Modified after Husain, 1996.

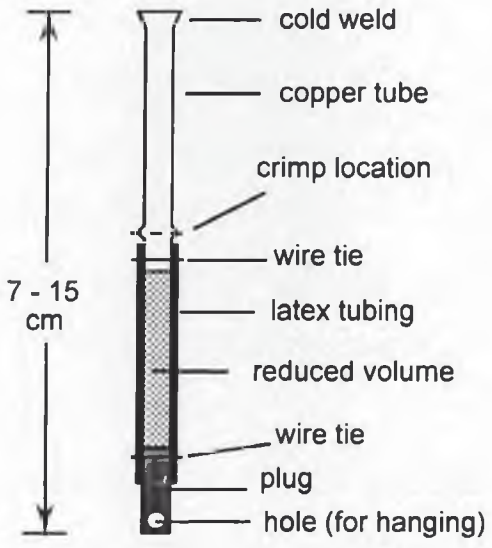

Figure 1.5. In-situ dissolved-gas headspace sampler.

Thus, the standard use of diffusion samplers requires a separate measurement of the total dissolved gas pressure which is normally done using a probe (Manning, 2000). However, it was not possible to make total dissolved gas pressure measurements in many of the small diameter wells as probes of this size do not exist. As a result, several methods that utilize optimization techniques were employed to estimate dissolved gas concentrations. The optimization techniques attempt to simultaneously fit measured mole fractions of various gases to a model of dissolved gas formation. See Appendix A for details.

1.5 Results

1.5.1 Total Dissolved Gas Pressure Measurements

Probe measurements of the dissolved gas pressure at both sites indicate that groundwater within the aquifer is over-saturated relative to groundwater in equilibrium with the atmosphere. The total dissolved gas pressure (P_t) of groundwater within the aquifer at the Warwick site was 1.39 atmospheres and 1.61 atmospheres at Brander Park. These measurements were obtained at hydrostatic pressures of 3.1 and 5.1 atmospheres, respectively. Thus, the in situ formation of bubbles is unlikely. The primary cause for over-saturation of dissolved gases at the sites is methane production.

1.5.2 Groundwater ^{4}He Concentration

R/R_a ratios (the $^3He/^4He$ ratio of the sample, R, compared to the ratio in air, R_a) decrease with depth at both sites (Figure 1.6; Appendix B). Groundwater at shallow depths (< 10 m) has an R/R_a ratio near 1.00, representative of groundwater at or near equilibrium with the atmosphere. The R/R_a ratio decreases with depth to ratios less than 0.20. Groundwater within the aquifer has an R/R_a ratio larger than groundwater in the base of the overlying till. Although the error was large for numerous samples (R/R_a ratios less than 0.20), the general trend of decreasing R/R_a with depth is clear.

The optimization technique resulted in a range of dissolved gas concentrations at each depth sampled (Figure 1.7). Erroneous results were readily identified by negative total dissolved-gas pressures or a greater than 5% error in the mole fraction of neon. The recharge temperature

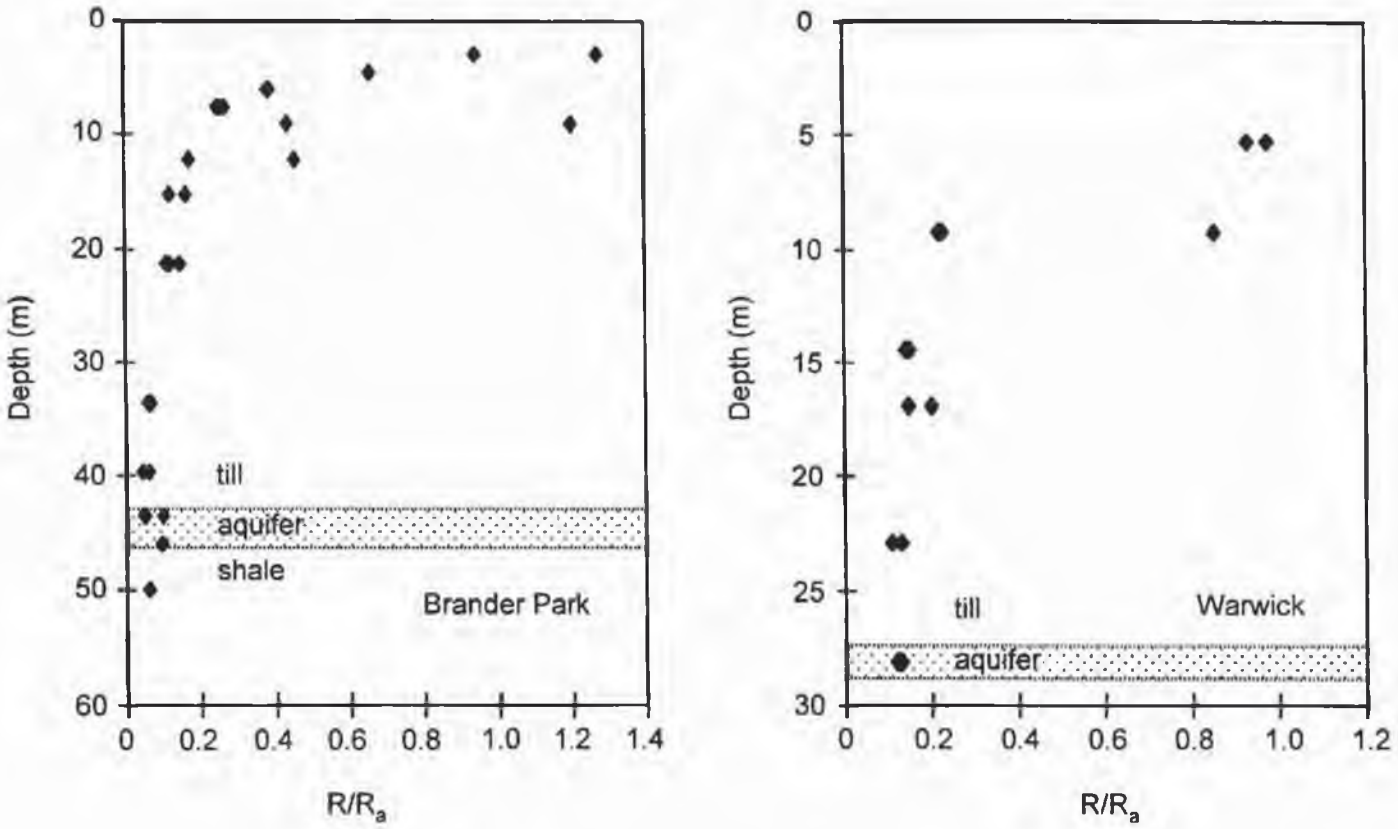

Figure 1.6. Measured groundwater R/R_a ratios.

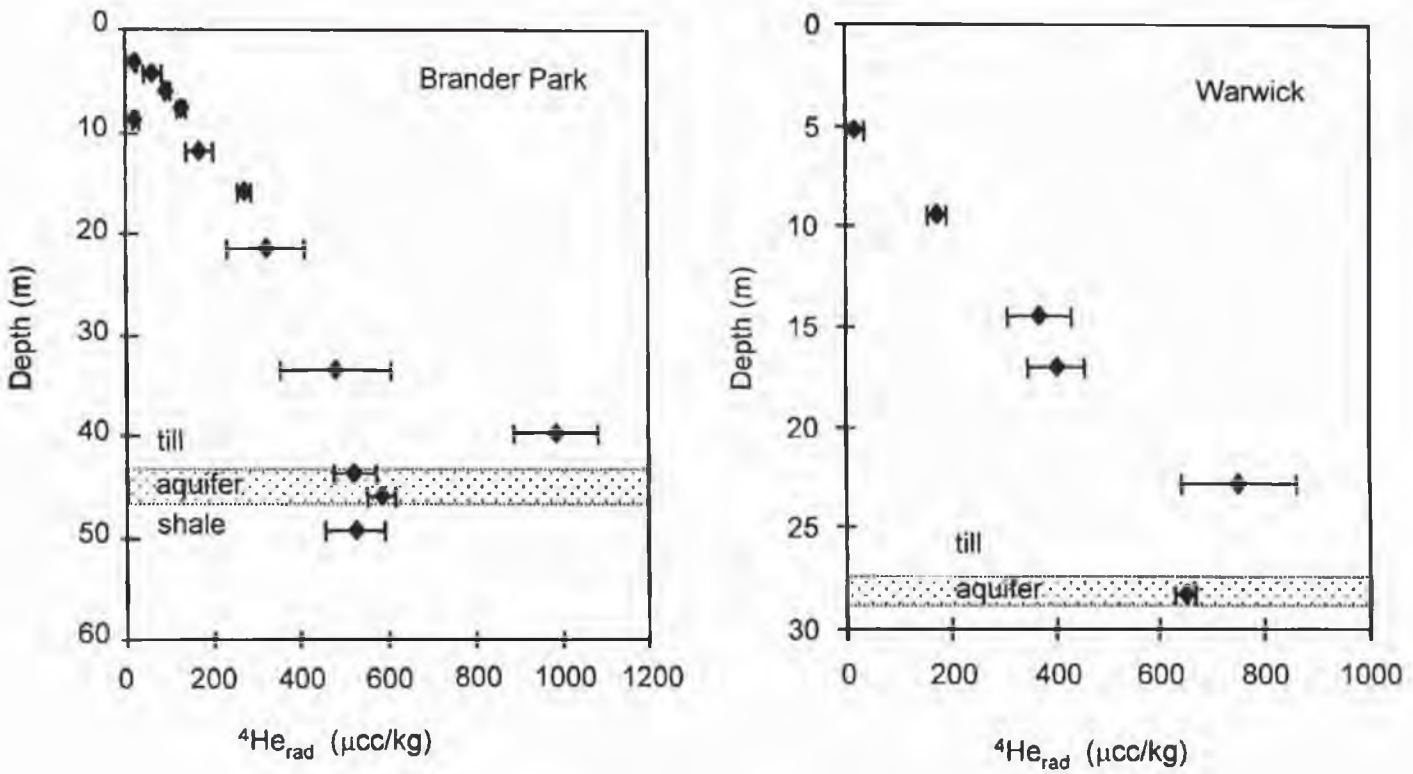

Figure 1.7. Groundwater $^4He_{rad}$ concentration.

was limited to 0 - 5 °C and in situ temperature to 9 - 14 °C. The largest source of variability in the modeled gas concentrations resulted from differences in the mole fractions of replicate samples from the same depth. In some cases, the range in $^4He_{rad}$ concentrations varied by as much as ~50% of the mean concentration (Figure 1.7). The largest range in $^4He_{rad}$ occurred at or near the base of the till where the methane concentration was greatest.

Groundwater radiogenic ^4He concentrations indicate a trend of increasing concentration with depth, with the maximum $^4He_{rad}$ concentration occurring within the clay till at both sites (Figure 1.7). Radiogenic helium is not detectable at the water table, increases to a maximum within the clay, and then decreases within the aquifer and underlying bedrock aquitard. $^4He_{rad}$ concentrations at depth within the clay till are significantly greater at the Brander Park site than at the Warwick site (Figure 1.7). Aquifer $^4He_{rad}$ concentrations are similar.

The vertical distribution of $^4He_{rad}$ at both sites indicates multiple sources of $^4He_{rad}$. The general trend indicates the influence of $^4He_{rad}$ diffusion from below the till, while the maximum in the $^4He_{rad}$ profile implies an internal (within the clay till) source. Hunt (2000), report the in-situ release rates obtained from step-heating experiments of core samples range from 0.02 to 1.17 $\mu cc/kg_{sed}/yr$ at 12°C (Table 1.1). This is greater than the $^4He_{rad}$ production from U and Th series elements in the till (Table 1.1). The U and Th concentrations averaged 2.73 ppm and 6.71 ppm, respectively (Hunt, 2000). The production of $^4He_{rad}$ from this amount of U and Th would be 5.08 $x10^{-4}$ $\mu cc/kg_{sed}/yr$. The average measured $^4He_{rad}$ release rate is roughly 600 times (ranges from 100 to 3200 times) the steady state $^4He_{rad}$ release from U and Th.

1.6 Modeling

The observed radiogenic $^4He_{rad}$ concentrations were modeled to evaluate the effective He diffusion coefficient, the rate of $^4He_{rad}$ released from grains, and the hydrologic parameters defined by previous research (e.g., historic head gradients). A steady-state analytical solution to the advection-dispersion equation (Solomon et al., 1996) and a one dimensional transient numerical model were used to evaluate the groundwater $^4He_{rad}$ concentrations at the two sites.

Table 1.1. Bulk till composition and $^4He_{rad}$ release rates resulting from the release of ancient helium and the production from U and Th series decay.

	Sampled Depth (m)	Percent Quartz (%)	^4He Quartz (µcc/g)	U (ppm)	Th (ppm)	^4He Release Rate (µcc/kg_{sed}/yr)	^4He Production from U & Th (µcc/kg_{sed}/yr)
Brander Park	2.98	86.5	13.64	1.51	3.64	0.047	0.00028
	4.34	83.8	8.30	2.60	7.86	0.217	0.00053
	8.83	89.9	8.15	3.71	8.82	0.148	0.00068
	11.85	73.3	5.14	5.28	12.36	0.308	0.00096
	33.51	74.8	6.58	1.36	3.28	0.801	0.00025
	39.83	89.0	2.27	5.13	10.37	1.166	0.00089
Warwick	5.25	54.7	7.39	3.17	6.46	.0116	0.00055
	9.36	51.5	8.15	3.16	9.40	0.063	0.00064
	14.39	51.9	22.74	2.04	2.55	0.140	0.00030
	16.97	57.0	6.02	1.65	6.44	0.112	0.00038
	22.76	57.7	5.02	1.25	3.77	0.250	0.00025
	28.25	58.4	11.56	1.92	5.56	0.019	0.00038

Both models included a velocity term, $^4He_{rad}$ diffusion from the underlying aquifer, and an internal $^4He_{rad}$ production term (Figure 1.8). An analytical model was used within the transient model to address the internal release of $^4He_{rad}$ from till grains at Brander Park and Warwick (Solomon et al., 1996), assuming the initial grain ^4He concentrations and sizes determined by Hunt (2000).

1.6.1 Steady-State Model

The steady-state one dimensional advection-diffusion model with an internal ^4He production term is similar to the equation of transport for reactive solutes that includes a source/sink term (Misra et al., 1974; Selim and Mansell, 1976). Specifically, the equation has been defined for the internal production of ^4He as (Solomon et al., 1996)

$$V_z \frac{\partial C}{\partial z} = D_h \frac{\partial^2 C}{\partial z^2} + \frac{G^*}{\theta} \qquad (1.3)$$

where

V_z vertical groundwater velocity [LT^{-1}];

C concentration of $^4He_{rad}$ [ML^{-3}];

z vertical spatial coordinate (positive downwards) [L};

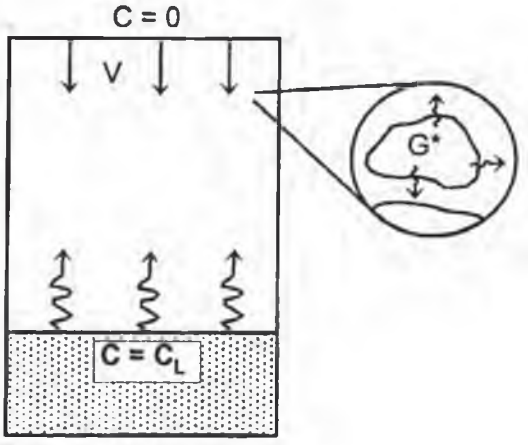

Figure 1.8. Conceptual model of the clay till. The boundary conditions and geometry used to evaluate groundwater $^4He_{rad}$ concentrations at Brander Park and Warwick are indicated. Modified after Solomon and others (1996).

D_h coefficient of hydrodynamic dispersion [L^2T^{-1}];

G^* $^4He_{rad}$ release rate from solids [$ML^{-3}T^{-1}$];

θ porosity [L^3L^{-3}].

The following boundary conditions were applied

$$C(0,t)=0 \qquad C(L,t)=C_L \tag{1.4, 1.5}$$

where L is the depth to the aquifer (Warwick) or underlying bedrock (Brander Park). The solution subject to boundary conditions and for spatially constant values of G*, , Vz, and Dh, is given by Solomon and others (1996) as

$$C(z)=\frac{C_L-\frac{G^*L}{V_z\theta}}{1-\exp\left(\frac{V_zL}{D_h}\right)}\left\{1-\exp\left(\frac{V_zz}{D_h}\right)\right\}+\frac{G^*z}{V_z\theta}. \tag{1.6}$$

The coefficient of hydrodynamic dispersion was defined as

$$D_h=\tau D_o+\alpha V_z \tag{1.7}$$

where τ is the tortuosity of the aquitard, D_o is the ^{4}He free-solution diffusion coefficient, and α is the vertical dispersivity. Generally, the dispersivity is at least an order of magnitude smaller than the field scale (Gelhar, 1986). Thus, the hydrodynamic dispersion coefficient (D_h) simplifies to the effective diffusion coefficient ($D_e = \tau D_o$) when velocity is small to negligible. With the tortuosity of the clay unknown, the approximation of

$$D_e \approx \theta^2 D_o \tag{1.8}$$

was applied, where θ is the porosity. Values for D_o at 5°C and 15°C are 5.10 x 10^{-5} cm^2/s (0.16 m^2/yr) and 6.30 x 10^{-5} cm^2/s (0.20 m^2/yr), respectively (Jähne et al., 1987). Equation 1.8 yielded an estimated ^{4}He effective diffusion coefficient (D_e) of 0.01 - 0.02 m^2/yr. Groundwater velocities could be defined as vertically upward (-) or downward (+).

Groundwater ^{4}He concentration profiles generated by the steady state model are particularly sensitive to the velocity and internal ^{4}He production terms. The effects of these parameters are demonstrated through an example that assumes a porosity of 40%, a saturated thickness of 30 m, and a hydrodynamic dispersion coefficient of 0.02 m^2/yr. An order of magnitude increase in the internal production term (from 0.01 to 0.10 $\mu cc/kg_{sed}$/yr, assuming a downward groundwater velocity of 0.005 m/yr) resulted in a ten-fold increase in the maximum ^{4}He concentration (Figure 1.9a). Meanwhile, an order of magnitude decrease in the groundwater velocity (from 0.01 m/yr to 0.001 m/yr, assuming an internal production rate of 0.075 μcc/kg/yr) resulted in a 2.5 times increase in the maximum helium concentration (Figure 1.9b). Unlike the production term, however, the location of the maximum ^{4}He concentration varied with depth depending on the magnitude and direction of the velocity term. This is also observed for the range in the hydrodynamic dispersion coefficient applied to the sites (Figure 1.9c).

1.6.2 Steady-State Model Results

The steady-state analytical solution yielded a fair fit of model profiles to measured $^4He_{rad}$ concentrations at the Warwick site when an effective diffusion coefficient of 0.02 m^2/yr, an upward velocity, and no internal release were applied (Figure 1.10a). The maximum groundwater ^{4}He concentration, however, was not predicted. Furthermore, internal release within the clay has been independently determined; thus the model is not an adequate representation of helium within the till. The modeled release rate ranged from 0.013 to 0.019 $\mu cc/kg_{sed}$/yr when an upward groundwater velocity of 0.01 to 1 mm/yr was applied (Figure 1.10a). However, the resulting concentration profiles poorly modeled the observed groundwater concentrations. Higher release rates (0.028 to 0.041 $\mu cc/kg_{sed}$/yr) were required when a downward velocity was used (2 to 3 mm/yr; Figure 1.10b). Of these, better results were obtained when a downward velocity of 2 mm/yr and internal release rate of 0.028 $\mu cc/kg_{sed}$/yr were applied.

The steady-state model was similarly successful at modeling the groundwater $^4He_{rad}$ concentrations at Brander Park. The best model results were obtained when an effective

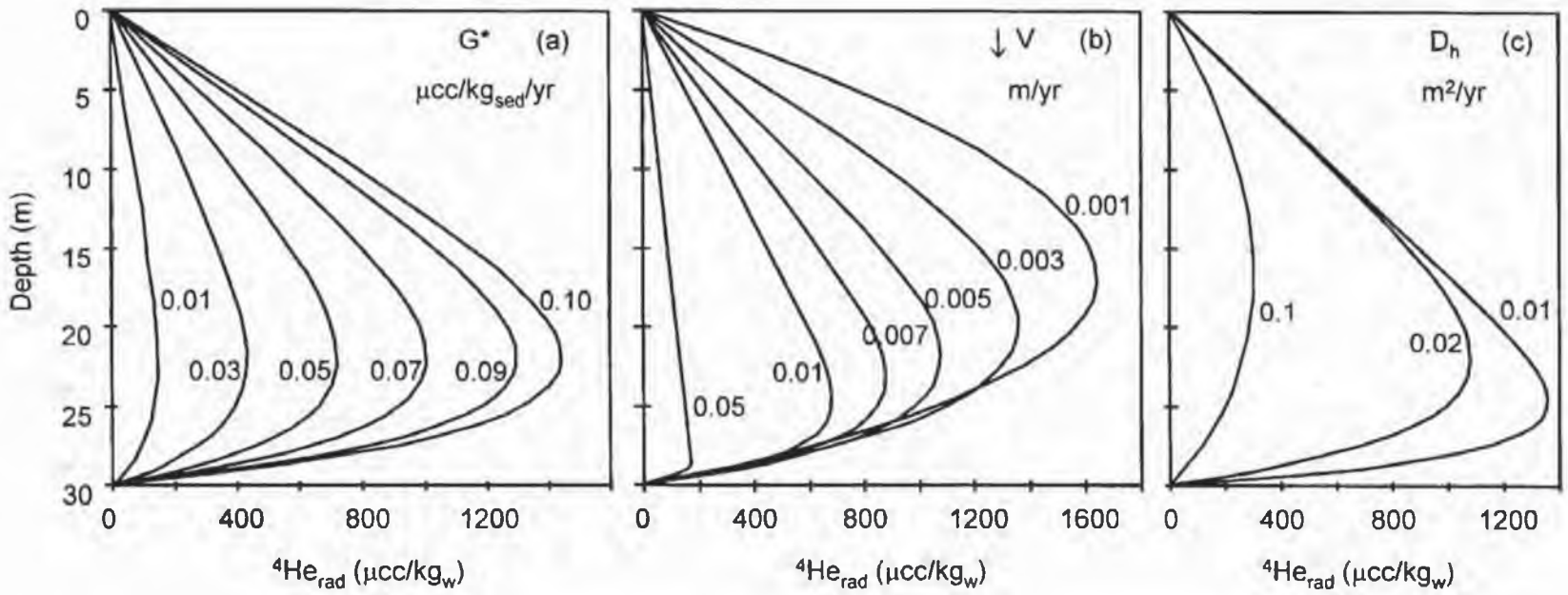

Figure 1.9. Sensitivity of modeled groundwater $^4He_{rad}$ concentration. Variables include: a.) the internal production of $^4He_{rad}$ (G*); b.) velocity (v); and c.) the hydrodynamic dispersion coefficient (D_h). The lower boundary concentration was defined as 0 µcc/kg$_w$ at 30 m depth. Parameters were varied over ranges reasonable for the field sites, and a dispersion coefficient equivalent to 50% of the free solution diffusion coefficient of helium at 15 °C (0.1 m^2/yr). When not the subject variable, the remaining parameters were held constant, (G* = 0.075 µcc/kg$_{sed}$/yr, v = 0.005 m/yr, and D_h = 0.02 m^2/yr).

diffusion coefficient of 0.01 – 0.02 m^2/yr was applied. The modeled release rates ranged from 0.003 to 0.006 $\mu cc/kg_{sed}$/yr with an upward velocity of 0.1 mm/yr (Figure 1.10c), with the best results requiring no internal release and thus not representative of the system. The best fit of modeled $^4He_{rad}$ concentration profiles using a downward velocity was obtained with a velocity of 3 mm/yr and an internal release rate of 0.013 to 0.019 $\mu cc/kg_{sed}$/yr (Figure 1.10d), which are reasonable values for the till. The spike in the groundwater $^4He_{rad}$ concentrations at the base of the till, however, could not be adequately reproduced in any of the model results. In either case, the overall fit of the model to observed data was poor.

The poor model results can be attributed to the assumptions of a spatially and temporally constant release rate and a steady-state condition existing at the sites. Noticeable differences were observed in the till composition and laboratory-determined $^4He_{rad}$ release rates for bulk till samples from the sites (Hunt, 2000). Thus, a spatially-constant release rate is not the condition within the tills. Furthermore, the modeled release rates were less than the actual release rates determined for bulk till samples from the sites (Table 1.1; Hunt, 2000). The model also assumes a steady state condition established in a 15,000 yr diffusion-dominated system. Although a fixed release rate might be suitable over the time period of 10^0 to 10^1 years, a release rate constant throughout 15,000 years is unlikely (Figure 1.1). For these reasons, a transient model was created to generate the observed $^4He_{rad}$ groundwater concentrations using initial $^4He_{rad}$ grain concentrations and grain sizes present (Hunt, 2000).

1.6.3 Transient Model

A one dimensional transient finite difference code was written that solves

$$\frac{\partial C}{\partial t} + V_z \frac{\partial C}{\partial z} = D_h \frac{\partial^2 C}{\partial z^2} + \frac{G^*}{\theta} \qquad (1.9)$$

using a modified Crank-Nicolson algorithm (Appendix C). Imposed were the boundary and initial conditions for $^4He_{rad}$

$$C(0,t)=0 \qquad C(L,t)=C_L \qquad C(z,0)=0. \qquad (1.10 - 1.12)$$

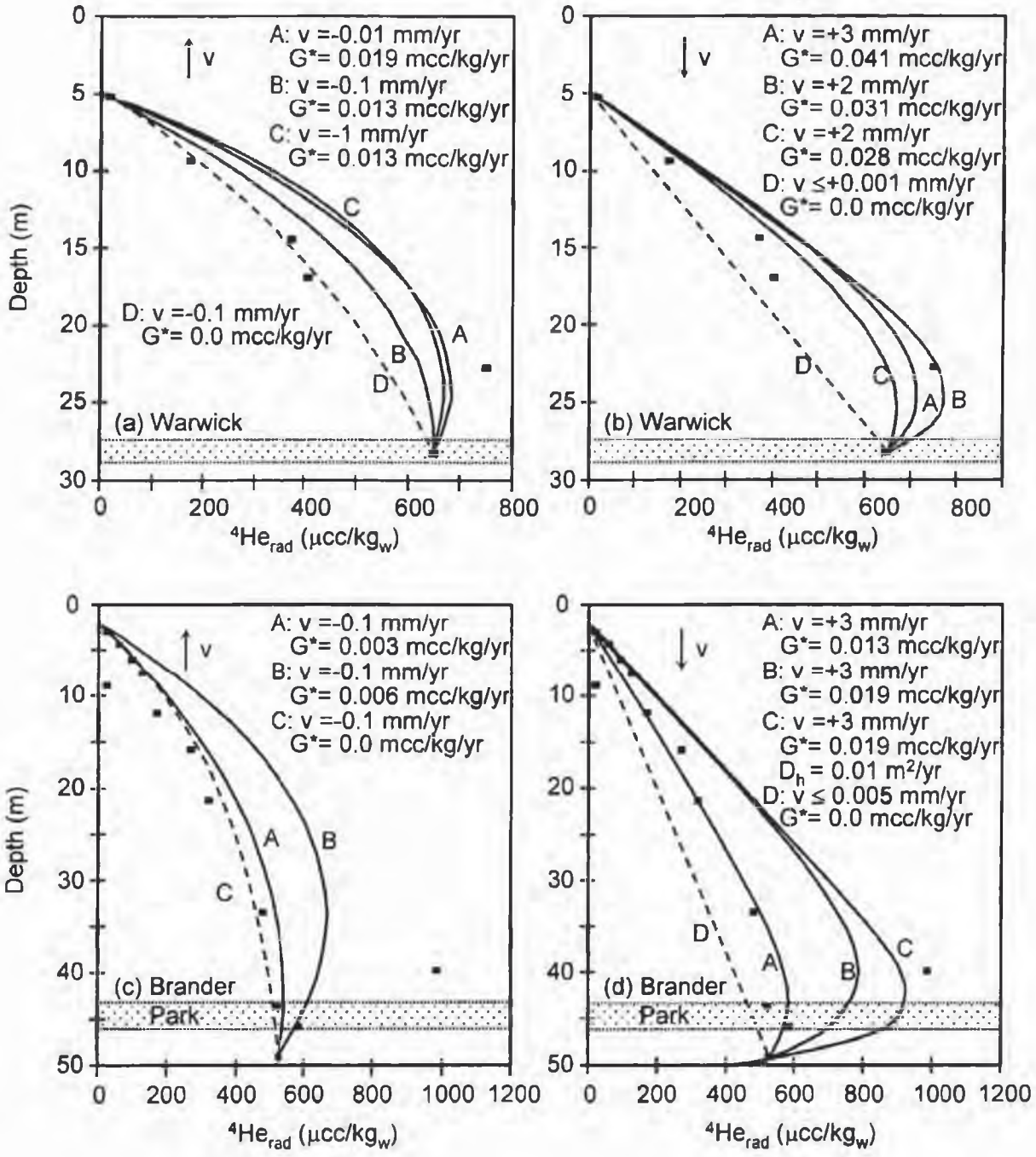

Figure 1.10. Modeled steady state groundwater $^4He_{rad}$ concentration. Profiles (lines) are drawn for Warwick (a & b) and Brander Park (c & d). Best-fit matches of modeled concentration profiles to measured data (squares) were obtained for both an upward (a & c) and a downward (b & d) groundwater velocity. A hydrodynamic dispersion coefficient (D_h) of 0.02 m^2/yr was applied, unless otherwise stated (d, case C). Dashed lines represent the model solution assuming no internal production. In general, a steady-state model poorly represents observed conditions.

The upper boundary was defined as the water table and the lower boundary was located at or near the bedrock &/or aquifer unit. The boundary concentrations were fixed through time. The upper boundary $^4He_{rad}$ concentration was zero, defined as water in equilibrium with the atmosphere. The lower boundary $^4He_{rad}$ concentration was determined using measured aquifer (Warwick) or bedrock (Brander Park) groundwater concentrations.

The transient model incorporated an analytical radial diffusion model (Solomon et al., 1996) to simulate the release of $^4He_{rad}$ from aquitard grains (G*) through time. Three options were provided within the numerical model to describe this release. The release rate could be determined for a.) each grain size present proportional to its abundance; b.) an average grain size at each depth increment; or c.) a fixed rate. A fixed release rate option was included for the purpose of model flexibility and future application. By the first method, the weighted average release rate for the bulk sediment was calculated at each time step using the proportion of each grain size present. This method is the most accurate and was applied to the sites studied. The model interpolated the release rates at depth increments for which measured data was not available. Experimentally determined solid-state diffusion coefficients of 5×10^{-20} cm^2/s and 1.9×10^{-19} cm^2/s were used to describe the diffusion of helium within aquitard grains at Warwick and Brander Park, respectively (Hunt, 2000). The radial diffusion model assumes a uniform initial helium distribution within grains.

The initial grain $^4He_{rad}$ concentrations were determined by Hunt (2000) using the Ne-He method (Yatsevich and Honda, 1997). Nucleogenic neon is produced as a result of the α-decay of U/Th-series elements. Yatsevich and Honda (1997) determined the radiogenic ^{4}He/nucleogenic ^{21}Ne production ratio to be $22 \times 10^{+6}$ in the crust. Diffusional loss of ^{4}He (with retention of Ne) out of grains results in a larger measured 4/21 ratio. Given the crustal production ratio and measured ^{21}Ne grain concentration, the initial grain ^{4}He concentration and percent of ^{4}He loss can be determined. Hunt (2000) determined the initial ^{4}He quartz grain concentrations as ranging from 49 to 77.8 μcc/g for the clay tills at the Lambton County sites.

The transient model also allows for the grains to have lost some ^{4}He through radial diffusion prior to their deposition in the shallow groundwater system. This "erosion" time is a

qualitative representation of the time during which grains may have been degraded in size by glacial processes, were re-worked, existed as a grain in a previous sediment, and/or were subjected to different thermal settings. Without the specific grain size and temperature histories, the erosion time cannot be a quantitative measure of the time throughout which the grains were altered or lost a portion of their original ^{4}He.

When possible, model parameters were defined using field measured or determined values. Measured grain size, abundance, and original ^{4}He content were used in the model and are given in Hunt (2000). Previously determined hydraulic properties such as hydraulic conductivity and porosity were incorporated. An effective helium diffusion coefficient was applied to describe the diffusion of helium within groundwater (see equations 1.7 - 1.8).

Model best-fits to measured $^4He_{rad}$ profiles were determined by varying the groundwater velocity and the erosion time. Minor adjustments were permitted to the effective diffusion coefficient and aquitard grain ^{4}He properties (e.g., initial ^{4}He concentration and grain sizes). Because only a handful of till samples were obtained for compositional and ^{4}He analysis, it is reasonable to assume some variation exists within the till between sampled depths. Model results were aided by the inclusion of up to three reasonable till compositions at depths for which the modeled data varied significantly from measured concentrations.

1.6.4 Transient Model Results

The transient numerical model successfully simulated the observed groundwater $^4He_{rad}$ concentrations, measured release rates from bulk till samples, and ^{4}He grain concentrations when an effective He diffusion coefficient was applied. Similar to the steady-state model (Figure 1.9c), the transient model was sensitive to the diffusion coefficient. The model results indicate that the estimated effective diffusion coefficient of 0.02 m^2/yr (6.3×10^{-6} cm^2/s) adequately describes the diffusive transport of helium in clay-rich till.

The modeled groundwater concentrations of $^4He_{rad}$ were significantly affected by the erosion time, or the length of time during which the aquitard grains lost some ^{4}He prior to deposition. An erosion time (Et) of 50,000 to 60,000 years resulted in the best graphical fit of modeled groundwater $^4He_{rad}$ concentrations at the Brander Park site (Figure 1.11). A similar

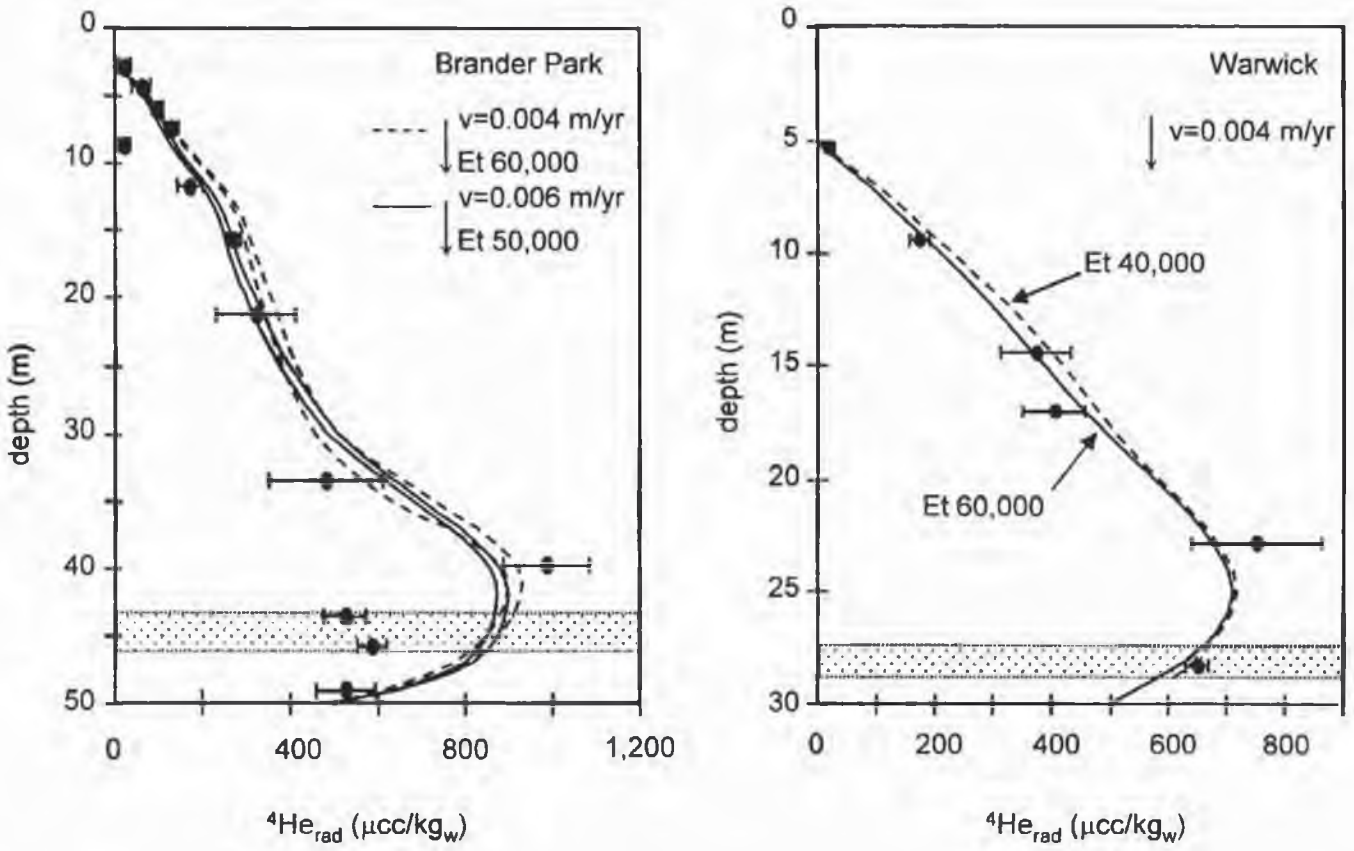

Figure 1.11. Modeled groundwater ^4He concentrations using a transient model after 15,000 years. The erosion time (Et) and velocity were varied to match modeled concentration profiles (lines) to measured data (circles).

erosion time of 40,000 to 60,000 years provided the best fit of modeled $^4He_{rad}$ concentrations at the Warwick site (Figure 1.11).

Generally, the range in modeled release rates agreed with helium release rates determined through step-heating experiments (Hunt, 2000). After 50,000 years erosion time and 15,000 years in situ, the modeled $^4He_{rad}$ release rates ranged from 0.01 to 0.13 $\mu cc/kg_{sed}/yr$ at the Brander Park site (Figure 1.12). The modeled release rate after 75,000 years (60,000 yrs Et and 15,000 in-situ) ranged from 0.01 to 0.11 $\mu cc/kg_{sed}/yr$. The release rates determined by Hunt (2000) ranged from 0.05 to 1.17 $\mu cc/kg_{sed}/yr$, with the majority falling between 0.10 and 0.30 $\mu cc/kg_{sed}/yr$ (Table 1.1). Thus, the model-determined release rates were slightly less but similar in range to those measured (Figure 1.13). After 40,000 years erosion time and 15,000 years of in-situ release, the modeled ^4He release rate from bulk till samples ranged from 0.06 to 0.13 $\mu cc/kg_{sed}/yr$ at the Warwick site (Figure 1.12). After 60,000 years erosion time, the release rate was slightly less (0.03 to 0.10 $\mu cc/kg_{sed}/yr$). These release rates are comparable to the measured release rates, which ranged from 0.02 to 0.25 $\mu cc/kg_{sed}/yr$ at the Warwick site (Figure 1.13; Table 1.1). The majority of measured bulk till release rates were less than 0.12 $\mu cc/kg_{sed}/yr$.

Modeled ^4He grain concentrations are dependent on the initial grain concentration, the initial ^4He distribution within the grain, and the release of stored helium through time. As might be expected based on the general agreement between the measured and modeled range of $^4He_{rad}$ release rates, the modeled ^4He grain concentrations also agreed with measured values. The ^4He concentration was determined for quartz grains after an erosion time and 15,000 years in-situ release. The modeled present-day grain ^4He concentration at Brander Park ranged from 1 to 16 $\mu cc/g$ after 50,000 years erosion time, and 1 - 13 $\mu cc/g$ after 60,000 years erosion time (Figure 1.14). After 60,000 years erosion time, the grain ^4He concentration ranged from 0.70 to 17.0 $\mu cc/g$ at the Warwick site, only slightly less then the grain concentrations after 40,000 years (0.90 to 18.0 $\mu cc/g$; Figure 1.14). In both cases, the majority of samples had grain concentrations greater than 5 $\mu cc/g$ and less than 20 $\mu cc/g$. Measured grain concentrations

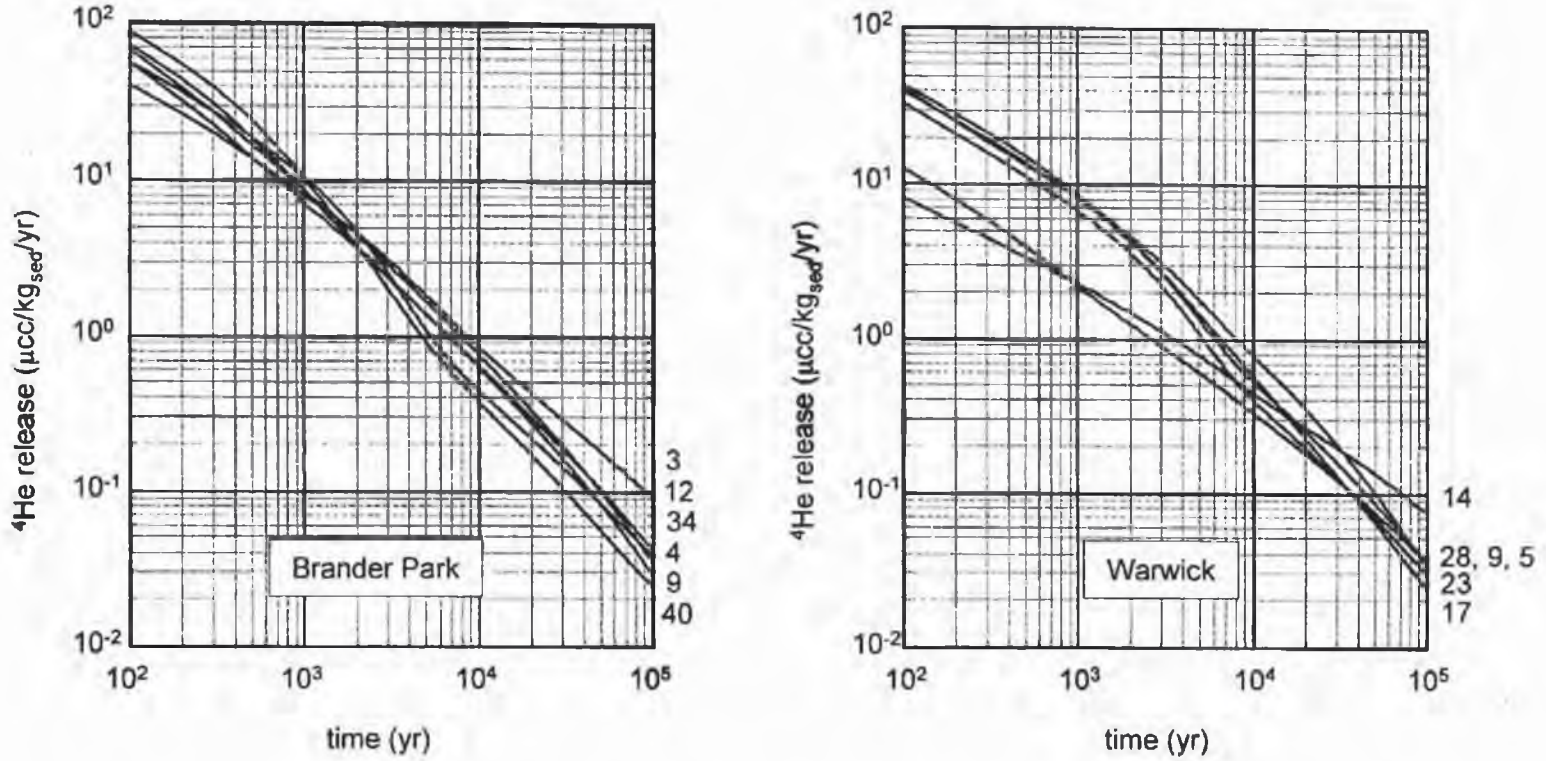

Figure 1.12. Modeled ^{4}He release rates from bulk-till samples through time. Each line represents the release rate for bulk till samples obtained at specified depths (meters below ground surface).

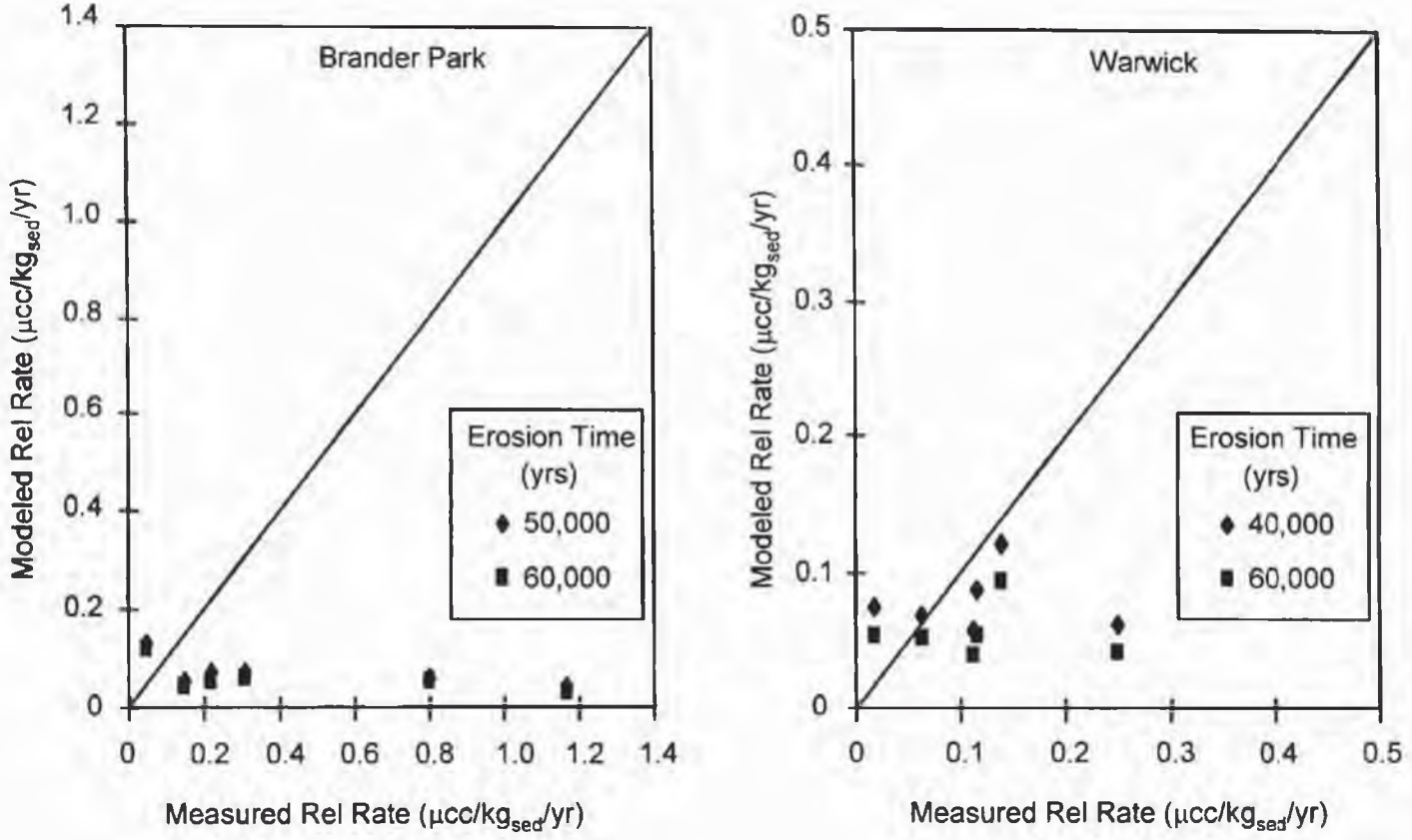

Figure 1.13. Comparison of modeled ^{4}He release rates to the laboratory-determined release rates of bulk till samples. The large values measured at the Brander Park site do not appear to be respresentative of the entire till.

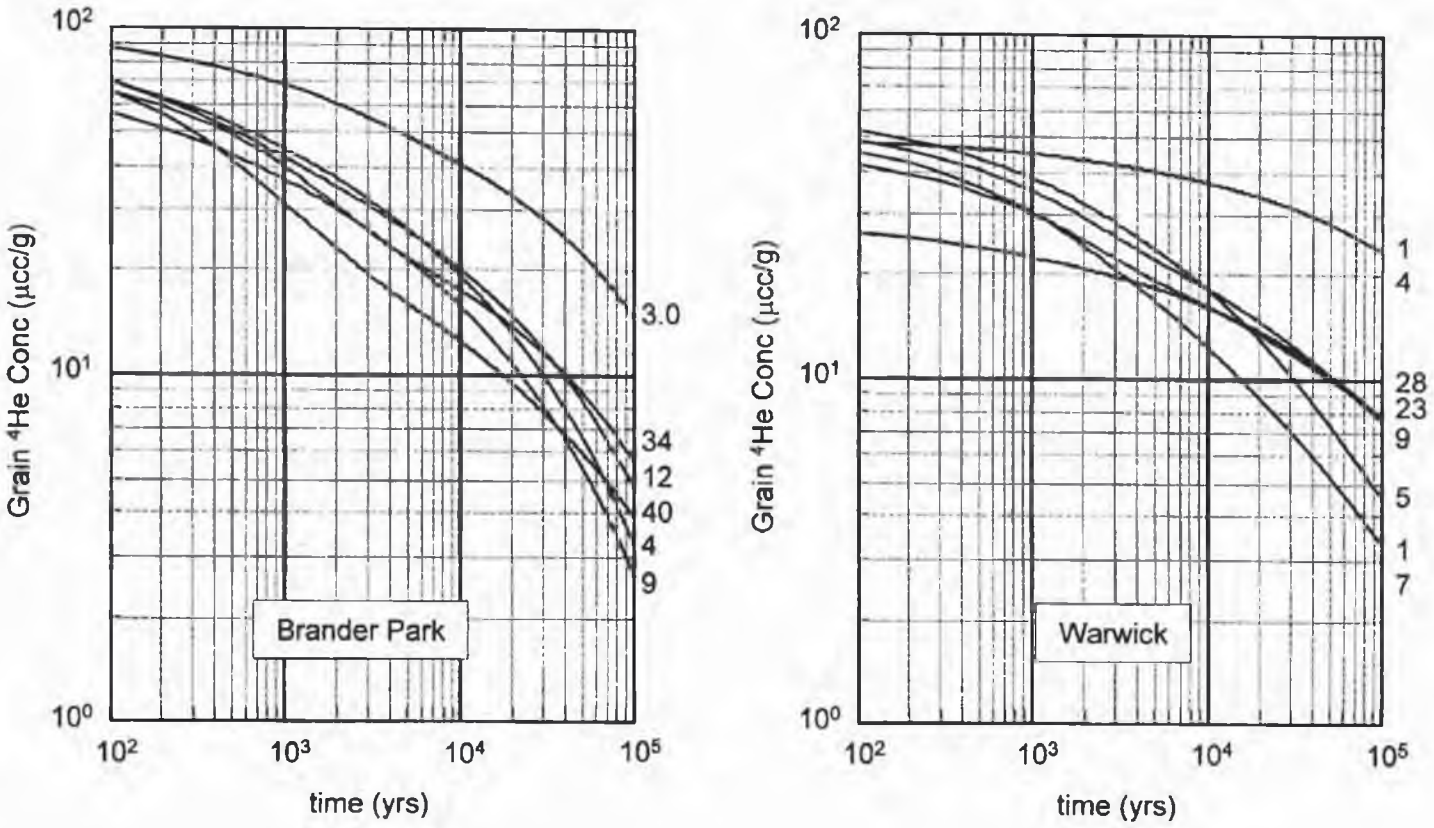

Figure 1.14. Analytical solution to the ^4He concentration of till quartz grains through time. Each line represents the grain concentration for bulk till samples obtained at specified depths (meters below ground surface).

ranged between 5.02 and 11.56 μcc/g at the Warwick site, with one exception (22.74 μcc/g; Table 1.1). There was good agreement between the modeled and measured grain $^4He_{rad}$ concentrations at both sites (Figure 1.15).

A downward vertical groundwater velocity was required to obtain modeled groundwater $^4He_{rad}$ concentrations similar to those observed. Similar to the steady-state model, the direction and magnitude of the velocity term influenced the location of the bulge in the modeled $^4He_{rad}$ concentration profile. A downward fluid velocity of 0.004 to 0.006 m/yr was required at both sites. This velocity is consistent with a hydraulic conductivity on the order of 10^{-10} m/s and the measured vertical hydraulic gradient (on the order of 10^{-1} m/m; Husain, 1996) at the Warwick site. The vertical hydraulic gradient determined at Brander Park (Husain, 1996) is an order of magnitude lower, suggesting the hydraulic conductivity at this site is on the order of 10^{-9} m/s.

1.7 Discussion

The peak in ^4He that exists near the base of the till can be explained by an internal production of ^4He within the till. However, the lower $^4He_{rad}$ concentrations observed within the aquifer could be explained as the result of aquifer flushing related to recent groundwater pumping. Indeed, some degree of aquifer flushing or increased groundwater flux may have resulted from groundwater pumping during a recent 30 year period (Husain et al., 1998). Assuming aquifer flushing has occurred, the present-day He concentrations of the aquifer would be the result of diffusion during the roughly 25 years since pumping ceased.

Presumably, a downward gradient would have been established from the till, while an upward gradient existed from the underlying shale. Using Crank's (1956) solution

$$C(x,t) = C_o erfc\left(\frac{x}{2\sqrt{D_e t}}\right) \qquad (1.13)$$

where erfc is the complementary error function, the length of time (t) required to diffuse a solute a given distance (x) can be estimated. The following boundary and initial conditions are required

$$C(x,0) = 0 \qquad C(0,t) = C_o \qquad (1.14, 1.15)$$

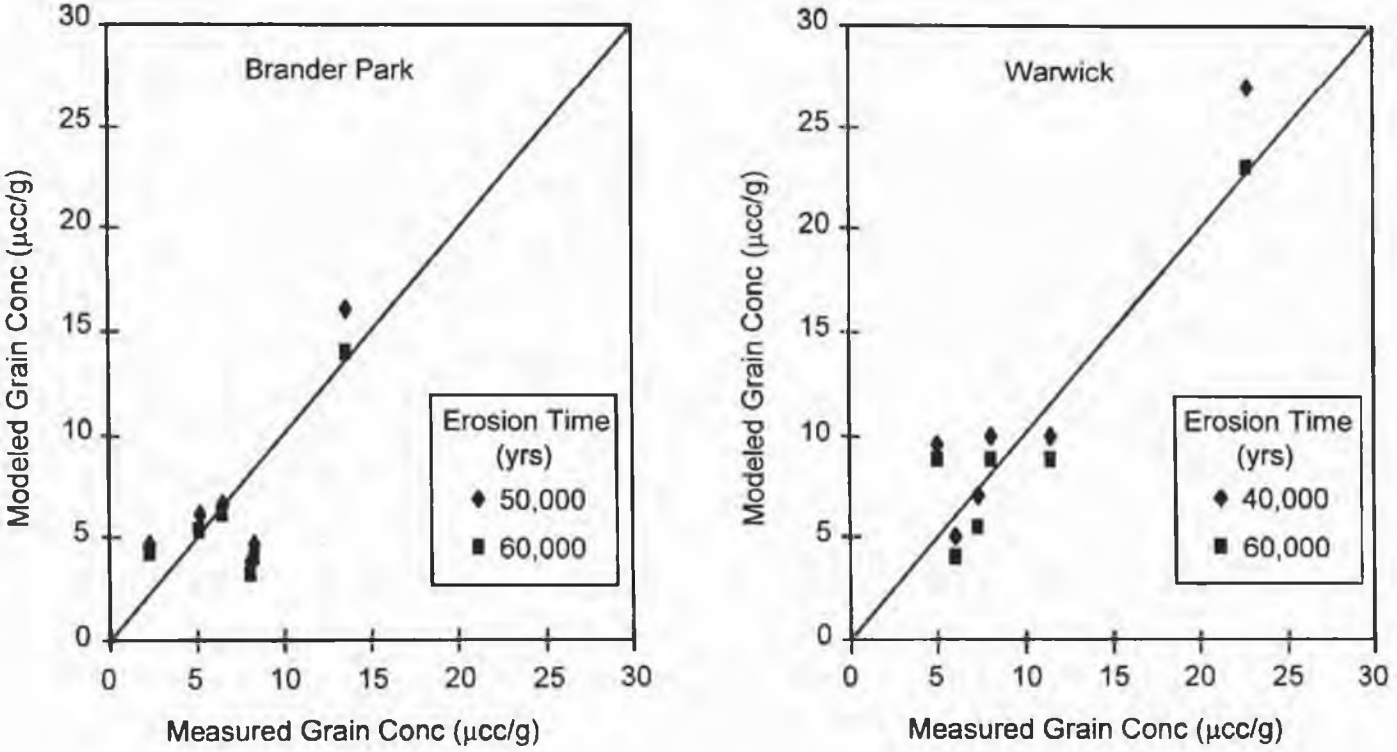

Figure 1.15. Comparison of modeled to measured grain ^4He concentrations.

where C_o is the ^4He concentration in either the till or shale (x = 0). According to the core logs for the sites, the Interface Aquifer is roughly 3 m thick at Brander Park and 2 m thick at Warwick (Husain, 1996). The effective diffusion coefficient determined in the transient model for He in a clay-rich till (0.02 m^2/yr) was applied. Based on this model, the current groundwater $^4He_{rad}$ concentration in the middle of the aquifer would be roughly 13% and 32% of the source concentrations in the shale and till (C/C_o), respectively, at Brander Park and Warwick. The length of time required to achieve a 50% C_o concentration would be ~125 years at Brander Park and ~55 years at Warwick. Ninety percent equilibration would be achieved after 2000 (Warwick) to 5000 (Brander Park) years.

Although the above equilibration model presents an argument for the reduced aquifer $^4He_{rad}$ concentration due to recent pumping followed by diffusion into the aquifer from the till above and bedrock below, it is probable that the situation is more complex. It is unlikely that groundwater introduced to the aquifer at the Warwick site would have the same helium content as groundwater at the Brander Park site. The aquifer hydraulic conductivities and locations with respect to the regional flow field indicate that while Warwick might see an input of fresh water, groundwater within the aquifer at Brander Park might have been affected only minimally. The water flushed into the aquifer at this location would still likely be Pleistocene in age and have a high $^4He_{rad}$ concentration. A complicated history of aquifer flushing, diffusion and internal production is the probable cause for the similar helium content observed in groundwater of vastly differing age.

Regardless of the groundwater history within the aquifer at the two sites, the release of helium from aquitard grains has played a major role in determining the groundwater $^4He_{rad}$ concentrations within the Quaternary Aquitard. Measured release rates ranged from 100 to 3200 times the in-situ steady-state production from U and Th present within the till. Thus, the bulge in the $^4He_{rad}$ profiles can be attributed to the internal $^4He_{rad}$ production, rather than solely from the recent input of water into the underlying aquifer creating an apparent bulge.

The transient numerical model predicted a groundwater velocity similar to the steady-state model. A prevailing downward gradient throughout the last 15,000 years was required to

model the groundwater $^4He_{rad}$ concentrations with depth. As indicated, the helium models were particularly sensitive to the velocity term. The models required grains that would generate a high release rate at depth within the till at both sites. Thus, the downward velocity necessary to model the groundwater concentrations cannot simply be attributed to inadequate low release rates at depth. The ability of the model to replicate the system throughout the last 15,000 years was dependent on the model assumptions. The downward velocity term may have been affected by the boundary and initial conditions estimated for the system. The results of a recent study by Husain and others (1998) indicate the hydraulic gradient within the till was previously vertically upwards (and essentially negligible, ≤ 0.01) and the present-day downward gradient is the result of recent aquifer pumping. Although the results of these studies are opposed, diffusion remains the dominant method of transport through the till. Regardless of direction, the velocity term is extremely low.

The transient numerical model simulated the observed groundwater $^4He_{rad}$ concentrations at both sites using an effective He diffusion coefficient of 0.02 m^2/yr (6.3×10^{-6} cm^2/s) which was estimated by $\theta^2 D_o$. The effective helium diffusion coefficient describes the diffusive transport of helium in clay-rich tills and similar sediments. The model results emphasize the importance of considering effective diffusion coefficients to describe the transport of dissolved gases in other low permeability media.

The model generated the observed range in $^4He_{rad}$ release rates from bulk till samples and grain ^4He concentrations using a radial diffusion model that incorporated the initial grain concentrations and grain sizes present. The model was particularly successful at generating the observed grain concentrations (Figure 1.15). Although the model predicted the observed range in the helium release rates, the modeled release rates were lower than the rates determined for specific bulk till samples (Figure 1.13). The modeled release rates were dependent on the solid-state diffusion coefficient determined by Hunt (2000). Similar to the results of this study, Hunt (2000) also observed a poor fit of modeled to measured release rates for Brander Park. Hunt (2000) attributes the variance to a potential sampling bias and a poor representation of the population of larger grain sizes, including rock fragments, in the model.

The study presented in this paper provides an additional opportunity to investigate the influence of other factors that affect the modeled release of ^{4}He. In addition to the grain size population, the geologic and thermal history of grains and mineralogy affect the release of stored helium. The following discussion will address these factors and their impact on the numerical model results.

The mineralogy and thermal history of the grains are represented in the numerical model by an average solid-state diffusion coefficient. The coefficient represents the average thermal setting for the grains since erosion from the protolith(s). In addition, the solid-state diffusion coefficient is an average of the coefficients for the various minerals present. If only quartz were present, the solid-state diffusion coefficients determined through modeling by Hunt (2000) would correspond to average temperature settings of 10°C at Warwick and 23°C at Brander Park. It is unlikely that the till grains have undergone significantly different thermal histories at the two sites. The till at both locations is composed of re-worked sediments derived from the same nearby Silurian and Devonian sedimentary deposits. Rather, the inconsistent solid-state diffusion coefficients for Warwick and Brander Park are more likely the result of their differing mineralogy and local differences in their source rocks (see Hunt, 2000). Thus, we can assume that the till grains have not undergone significantly different thermal histories and the differences in mineralogy are accounted for in the solid-state diffusion coefficients.

The geologic history of aquitard grains is represented in the numerical model by the erosion time and the solid-state diffusion coefficient (see discussion above). The model presented in this paper assumed a common erosion time for all till grains. It is unlikely that individual grains at a given depth within the till would have the same erosion time. It is perhaps even more unlikely that grains at depth would have an equal erosion time to grains deposited afterwards at shallower depths, particularly since the sediment grains have been re-worked. Hunt (2000) assumed only the former in his model of helium release rates, allowing for the erosion time to vary with depth within the tills. The resulting modeled release rates agreed with measured values at Warwick but were not equal to those measured for the Brander Park site. The assumption of a common erosion time is the only difference between the model presented

in this paper and that by Hunt (2000). Thus, the assumption of a common erosion time is the likely cause for the variance observed between the modeled and measured release rates presented in this paper for the Warwick site.

The assumption of equivalent radial release from all mineral grains is another potential factor affecting the modeled release rates. The model assumes radial release of helium from spherical grains in which helium is initially evenly distributed. Because all grains are not spherical, evaluating the release from bulk till samples of varying mineral content would indicate whether this assumption greatly affects the modeled release rates, causing the inequality with measured release rates. A till containing a greater percentage of flat or elongate minerals should reflect this potential error. The till samples obtained from the Warwick site contain a larger percentage of clay and carbonate minerals than till samples from the Brander Park site, which has a larger percentage of quartz grains (Hunt, 2000). Since the radial release model adequately predicted the measured release models at the Warwick site, the assumption of spherical grains appears to have little effect on the model results.

The model predicted the groundwater $^4He_{rad}$ concentrations and present ^4He release rates from bulk aquitard grains. The boundary and initial conditions, complex history of ^4He within the aquifer due to flushing and subsequent diffusion, and the geologic history of aquitard grains represented by the "erosion time" were unknown and therefore estimated. Despite these limitations, the model was able to predict the observed groundwater $^4He_{rad}$ concentrations and ^4He release rates.

1.7.1 Helium Degassing Flux

Although the scale of the till examined in this study is limited in its vertical and horizontal extent, the current degassing flux from the till can be compared to the continental radiogenic helium fluxes in the literature. In this study, the degassing flux is the result of the internal release of ancient helium stored in till grains rather than continental crust degassing from depth.

The ^{4}He flux out of the till was determined using Fick's 1st law of diffusion:

$$F = -\theta D_e \left.\frac{\partial C}{\partial z}\right|_{z=0} \quad (1.16)$$

where θ is the porosity, D_e is the effective diffusion coefficient, and $\partial C/\partial Z$ is the ^{4}He gradient at some depth, z, within the till. Applying the till porosity of 0.40 and the model-determined effective ^{4}He diffusion coefficient of 0.02 m^2/yr, the flux of ^{4}He from the top and base of the till were determined (Appendix D). The ^{4}He gradient at the till surface (40 μccSTP/kg$_w$/m) equates to a degassing flux of 2.7 x 10^8 atoms/m^2/s (Appendix D). The ^{4}He gradient at the base of the till (10 μccSTP/kg$_w$/m) equates to a lower degassing flux of 6.8 x 10^7 atoms/m^2/s. Applying an internal ^{4}He production rate of 0.1 μccSTP/kg$_{sed}$/yr, the internal ^{4}He flux out of till grains would be approximately 2.7 x 10^9 atoms/m^2/s (Appendix D), 10 times higher than the flux out of the till. Thus, the internal release of ^{4}He can account for the current ^{4}He fluxes out of the top and the bottom of the till. Furthermore, the production rate indicates that ^{4}He is accumulating within the till.

The degassing fluxes determined for the till in this study can be compared to continental degassing fluxes determined by various means, including those determined for the Great Hungarian Plain (GHP), the Paris Basin (PB), and the Great Artesian Basin (GAB). The till fluxes are multiplied by 30% (continental land surface area) to compare them to the crustal degassing fluxes, which range 0.09 - 9.2 x 10^6 ^{4}He atoms/m^2_e/s (Table 1.2). The corresponding crustal degassing flux determined for the glacial till is 8.1 x 10^7 ^{4}He atoms/m^2_e/s. This flux is two orders of magnitude less than the average crustal degassing flux determined for the Earth assuming a steady-state production from U/Th decay (O'Nions and Oxburgh, 1983) and the majority of crustal degassing fluxes determined for large sedimentary basins (Table 1.2). It is approximately half the crustal degassing flux determined by Stute and others (1992) for the GHP and it is equivalent to the degassing flux determined for the Saijo Basin in Japan (Takahata and Sano, 2000). It is important to note that the crustal degassing fluxes found in the literature were not determined at the surface as in the case of the till.

Table 1.2. Estimated continental helium fluxes. All crustal fluxes are referred to the entire surface area of the Earth (30% continental).

Site	Crustal Flux $\left(x10^9 \frac{^4He\ atoms}{m_e^2 s}\right)$	Reference
Continents	8.4	O'Nions and Oxburgh, 1983
Auob Sandstone, Namibia	7.8	Torgersen and Ivey, 1985;
Kanto Plain, Japan	2.7 – 3.0	Sano, 1986
Chinasui gas field, Taiwan	5.1 – 7.2	Sano and others, 1986
GAB, Australia	9.3	Torgersen and Clarke, 1987
Continents	8.1	Torgersen, 1989
GHP, Hungary	24	Martel and others, 1989
GHP, Hungary	0.2 – 1.4	Stute and others, 1992
PB, France	1.4	Marty and others, 1993
GHP, Hungary	4.4	Cserepes and Lenkey, 1999
Saijo Basin, Japan	0.09	Takahata and Sano, 2000
Nigashi-Niigata, Japan	2.5	Takahata and Sano, 2000
Glacial till, Ontario	0.08 – 0.26	This study

A portion of the difference between the degassing flux determined in this study and those determined for large-scale aquifer systems can be attributed to differing means of transport. The crustal degassing fluxes determined for the large-scale aquifer systems require advective He transport (Torgersen and Clarke, 1985; Torgersen, 1989). A hydrodynamic dispersion coefficient of 2 x 10^{-5} cm^2/s is used to describe the transport of helium in the upper crust (Torgersen, 1989). This is a factor of 3 greater than the effective He diffusion coefficient determined for till in this study.

The results of this study suggest that a significant percentage of ancient stored helium is released to the atmosphere during the erosional processes that cause grain size reduction. The release rate of helium from grains is greatest immediately upon size reduction and decreases as a function of time (Figure 1.1). The total loss of helium from till grains varied from ~60 to 87% of the original helium concentration within the grains. This helium was released to the atmosphere during weathering, transportation, and deposition, rather then accumulating in the groundwatersystem. Thus, the results of this study suggest that nonaccumulated helium could represent a substantial percentage of the continental degassing flux that cannot be directly measured.

The degassing flux determined for the till can be used to estimate the flux of ancient stored helium from recent glacial deposits. During the Pleistocene, 30% of Earth's land surface area was covered by glaciers, resulting in glacial deposits of variable thickness (0 – 150 m; Flint, 1971). Assuming an average thickness for the glacial deposits of 50 m and a release rate similar to what was observed in this study (2.7×10^8 ^{4}He atoms/m^3/s), the total flux of ^{4}He being released from glacial deposits would be 1.2×10^9 ^{4}He atoms/m^2/s. This is approximately 14% of the crustal degassing flux. It is important to note that this flux is based on the current degassing flux and does not include the ~60 - 90% loss of helium from the grains during the preceding "erosion time."

The results of this study suggest that the internal release of ancient stored helium from glacial deposits might contribute significantly to the continental helium degassing flux at other sites. The degassing flux from the till, while being comparable to the crustal degassing fluxes in the literature, is supported by the release of ancient stored helium in the upper 30 m of the crust. The results further suggest that the release of residual helium from fine-grained glacial materials over relatively limited thickness might be more significant than previously considered.

The ability to simplify the complex system of variables controlling the release of helium from aquifer/aquitard grains with a simple model provides a powerful method to use helium as a groundwater dating method for young shallow groundwater. The previous study performed by Solomon and others (1996) indicated that helium may present a method of dating waters 10^1 to

10^3 years in age. Based on the results of this study and the companion study performed by Hunt (2000), it appears that a simple spherical release model can be used to represent the release of helium from different mineral grains over large temporal scales. A constant release rate may be applied to younger groundwater. In addition, a solid-state diffusion coefficient representative of the bulk material can be determined from the measured release (see Hunt, 2000 for details).

The results of these companion studies indicate that the ^{4}He dating method for young groundwater requires a measurement of the in-situ $^4He_{rad}$ release rate and the groundwater $^4He_{rad}$ concentrations. An estimate of the length of time during which the grains lost some helium prior to being deposited in the aquifer/aquitard system and a measurement of the initial grain concentration may not be required for young groundwater systems in which the release rate decreases minimally through time. The same may be true for older groundwater systems depending on the length of the "erosion time" and the age of the groundwater. The release rate may change by orders of magnitude along a groundwater flow path, or it may change very little. Using the example in Figure 1.1, the release rate of a 0.001 cm grain changes by 1 order of magnitude in 100 years time, assuming no preceding loss. On the other hand, if the same grain underwent 1000 years of ^{4}He loss prior to deposition, the in-situ release rate would decrease by only ~20% in the following 1000 years. In this case, the present-day measured release rate could be applied as a constant to represent the release of helium for groundwater 1000 years in age.

The release rates determined for the Quaternary Aquitard and presented in this paper are similar to the release rates determined at other locations. The average measured release rate for the clay tills was 0.274 $\mu cc/kg_{sed}/yr$ (or 435 $\mu cc/m^3_{aq}/yr$). The exclusion of the two high release rates observed at depth at the Brander Park location yields an average release rate of 0.132 $\mu cc/kg_{sed}/yr$ (209 $\mu cc/m^3_{aq}/yr$). Similar release rates have been determined for sites in Ontario, Germany, Tennessee, Wisconsin and Nebraska. Solomon and others (1996) determined a release rate of 130 $\mu cc/m^3_{aq}/yr$ for a sandy aquifer located at Sturgeon Falls, Ontario. The aquifer is of similar age compared to the clay tills near Sarnia, Ontario. However, the age of the aquifer source material is significantly greater (> 1 Ga compared to 360 to 420

Ma) and the grain size is larger (sand). Solomon and others (1996) report release rates of 200 $\mu cc/m^3_{aq}/yr$ for fractured saprolite in Tennessee and a Late Quaternary sand and gravel aquifer in Nebraska. A release rate of 230 $\mu cc/m^3_{aq}/yr$ was determined for a site in Germany. Preliminary results of a study in Dane County, Wisconsin indicate a release rate of roughly 0.11 $\mu cc/kg_{sed}/yr$ (or 100 to 200 $\mu cc/m^3_{aq}/yr$) in a Cambrian sandstone and recent glacial outwash deposits (Swanson, pers. commun., 2000). The elevated release rates observed at other locations support the hypothesis for the release of stored helium. Additional investigations at other localities may determine whether generic solid-state diffusion coefficients and/or release rates can be defined to represent various geologic materials of varying age.

1.8 Conclusions

In-situ headspace or diffusion samplers provide a means of obtaining dissolved-gas samples from micro-wells screened in aquitards, an extremely difficult if not impossible task using conventional sampling methods. Although the over-pressurization of dissolved gases complicated sample collection at the sites investigated, measurements of the total-dissolved gas pressure using a specially-designed probe allowed for the direct calculation of dissolved-gas concentrations. The combined use of headspace samplers and a total-dissolved gas pressure probe is a fairly easy method of obtaining dissolved gas concentrations.

The vertical distribution of $^4He_{rad}$ at both sampling sites indicates multiple sources of $^4He_{rad}$. The general trend indicates the influence of $^4He_{rad}$ diffusion from below, while the bulge in the $^4He_{rad}$ profile implies an internal (within the clay) source. The measured $^4He_{rad}$ release rates obtained from bulk core samples support the hypothesis of internally released helium from aquitard grains. The measured release rates are 100 to 3200 times greater than can be supported by the steady-state production from U and Th present within the tills.

An effective diffusion coefficient of 0.02 m^2/yr (6.3 x 10^{-6} cm^2/yr), which is equal to $\theta^2 D_o$, can be used to describe the diffusive transport of helium through the clay-rich tills in this study. Modeling results emphasize the importance of applying an effective diffusion coefficient to describe the transport of dissolved gases through low permeability units.

The internal release of He from fine-grained sediments might contribute significantly to the continental degassing flux. Further research is required to determine which geologic media are subject to the release of stored helium and the significance of this helium source on the current understanding of the continental helium flux.

Helium-4 released from aquifer/aquitard grains at rates greater than can be supported by the decay of U and Th-series elements demonstrates its potential as a powerful groundwater dating method. Although groundwater dating is not meaningful at the Brander Park and Warwick sites due to the diffusion-controlled solute transport, ^4He may be useful in advection-dominated systems. Groundwater ages can be determined using the measured $^4He_{rad}$ concentration of groundwater and a mass transport rate of helium from aquifer/aquitard grains. The results of this study indicate that a constant ^4He release rate may be applied for young ($10^1 - 10^2$) groundwater systems as well as some older systems. The measured release rate may be applied for young systems in which the release rate changes minimally along a groundwater flowpath. For older groundwater, an average release rate representing the history of release rates encountered along a flowpath might need to be determined. A simple spherical release model can also be used to estimate the release of helium from aquifer/aquitard grains through time. In this case, a measurement of the initial grain concentration and an estimate of the duration of time during which grains lost some stored helium prior to deposition are required. The release of stored helium may provide a means of dating groundwater that is of an age for which there is no current dating method (50 – 1000 years).

CHAPTER 2

DISSOLVED GASES AND TRITIUM IN A FRACTURED DOLOSTONE: IMPLICATIONS FOR GROUNDWATER RECHARGE AND HELIUM DIFFUSION

2.1 Abstract

Measurements of dissolved gases (^3He, ^4He, CFCs, and CH_4) and tritium along with detailed hydraulic investigations (more than 1396 packer tests; Novakowski et al., 2000) provide estimates of the spatial location of recharge, and the effective ^4He diffusion coefficient through a fractured Silurian dolomite in Southern Ontario. CFC data indicate young water occurring at depth at the site, overlain by older water. The CFC data indicate recharge is occurring in spatially discrete areas located north of the site, where the overlying glacial till is thin or non-existent. Radiogenic ^4He and CH_4 exist at extremely high concentrations within the low-permeability Rochester Shale that underlies the site. Modest concentrations of ^4He and CH_4 also exist within the primary hydraulic units (Eramosa and Vinemount members of the Lockport Formation). Concentration profiles suggest that ^4He in the Lockport is derived from the underlying Rochester Shale rather than being produced by U/Th-series decay within the Lockport Formation itself. As a result, the groundwater concentration of ^4He within the Lockport is controlled by vertical dilution rather than travel time. A ^4He mass balance model which incorporates ^4He diffusion from below and the flushing of ^4He through horizontal fractures within the Lockport indicates an effective ^4He diffusion coefficient of 1.48×10^{-7} cm^2/s for the Rochester Shale and a flux of helium out of the Rochester Shale equal to $1.22 - 1.70 \times 10^8$ $atoms/m^2_{aq}/s$. The results of a CH_4 mass balance substantiate that diffusion is the primary means of mass transport in the Rochester Shale and define a CH_4 effective diffusion coefficient of 3.7×10^{-8} cm^2/s in the Rochester Shale. Observed groundwater helium concentrations within the Lockport were successfully simulated using a transient two dimensional numerical model

employing measured aquifer parameters. Results of mass balance, numerical and crustal degassing models indicate the importance of applying an effective ^4He diffusion coefficient to describe the transport of dissolved helium through geologic media. The combination of short-term tracers that enter the system from the upper boundary, and a long-term tracer that enters from the lower boundary, results in a powerful quantification of capture zones in this fractured carbonate flow system.

2.2 Introduction

In 1985 groundwater contamination was discovered in monitoring wells located near a PCB waste management site outside the town of Smithville, Ontario. PCB oils and solvents were subsequently detected within the upper bedrock units at the site (Golder Associates, 1995). Several studies were initiated to evaluate the extent of the contaminants and the hydrogeology of the site. Recent investigations have expanded upon the initial site characterization to: a) evaluate the location and magnitude of recharge; b) provide a detailed hydrologic description of the region; c) describe the bedrock fracture network and its influence on groundwater flow and solute transport; d) define a conceptual model for the site; e) create numerical models that can describe the hydrogeology of the site and assist in modeling the fate and transport of the PCB-related contaminants; and f) describe well head capture zones for the pump-and-treat wells. Investigators with the U.S. Environmental Protection Agency, the Canadian National Water Research Institute, Brock University, the University of Waterloo, McMaster University, and the University of Utah have performed individual studies towards these goals (Zanini et al., 1997, 2000; Ford and Worthington, 1998; O'Neill and Brindle, 1998; Sudicky et al., 1998; Worthington and Ford, 1998, 2001; Slough et al., 1999; Worthington et al., 1999; Novakowski et al., 2000). This paper presents the results of a study designed to evaluate the dissolved gases and tritium at the site in terms of groundwater recharge and residence times, and to determine the effective diffusion coefficients of ^4He and CH_4 in fractured bedrock.

Tritium has been a useful tracer of groundwater recharge, residence time, and fluid flux. Radioactive tritium (^3H) is produced naturally in the atmosphere by cosmic radiation. Above-ground thermonuclear testing between 1952 and 1962 resulted in a significant increase in the

atmospheric tritium concentration (Araguas et al., 1996), which has steadily declined since the mid-1960's to natural production levels (O'Brien, 1979; Weiss et al., 1979; Masarik and Reedy, 1995; Kim et al., 1998). Since tritium is readily incorporated into the water molecule, elevated atmospheric concentrations correspond to higher concentrations in precipitation (Figure 2.1, IAEA, 1992) and groundwater recharge. Thus, tritium has been used to date groundwater that has a residence time of <50 years.

Unfortunately, historical atmospheric tritium records are limited to a few locations (IAEA, 1992). Natural atmospheric variability and local ^{3}H sources, such as nuclear fuel facilities and landfills, can be significant and are generally not quantified. Thus, the local atmospheric ^{3}H concentration and resulting groundwater input may be poorly known. Since ^{3}H decays to ^{3}He (half-life of 12.43 years), measuring both ^{3}H and ^{3}He can allow the use of tritium as a groundwater age tracer without requiring the tritium source function be known (Tolstikhin and Kamensky, 1969).

Dissolved gases have been used as tracers of recharge temperature, elevation, groundwater residence times, and to evaluate groundwater flux and solute transport through saturated media. Dissolved gases in groundwater can be of atmospheric and subsurface origin. Rainwater equilibrates with gases in the atmosphere resulting in groundwater concentrations similar to those in air (Benson and Krause, 1976; Andrews, 1992). Notable exceptions are O_2 (consumed) and CO_2 (produced). Production of certain dissolved gases can occur as a result of processes such as radioactive decay and natural gas production.

Chlorofluorocarbons (CFCs) are man-made compounds that were first introduced to the atmosphere in the 1930s (Lovelock, 1971). The release of CFCs to the atmosphere has steadily climbed since the 1960s (Figure 2.2, Rasmussen and Khalil, 1986; Busenberg and Plummer, 1992; Elkins et al., 1993; AFEAS, 1997). Because CFCs are not produced in the subsurface, the CFC input function and time control CFC concentrations in groundwater. Thus, for a given groundwater sample, the dissolved concentration can be converted to an atmospheric concentration using the CFC solubility (Warner and Weiss, 1985; Bu and Warner, 1995) and recharge temperature. Comparing this concentration to the history of atmospheric CFC levels

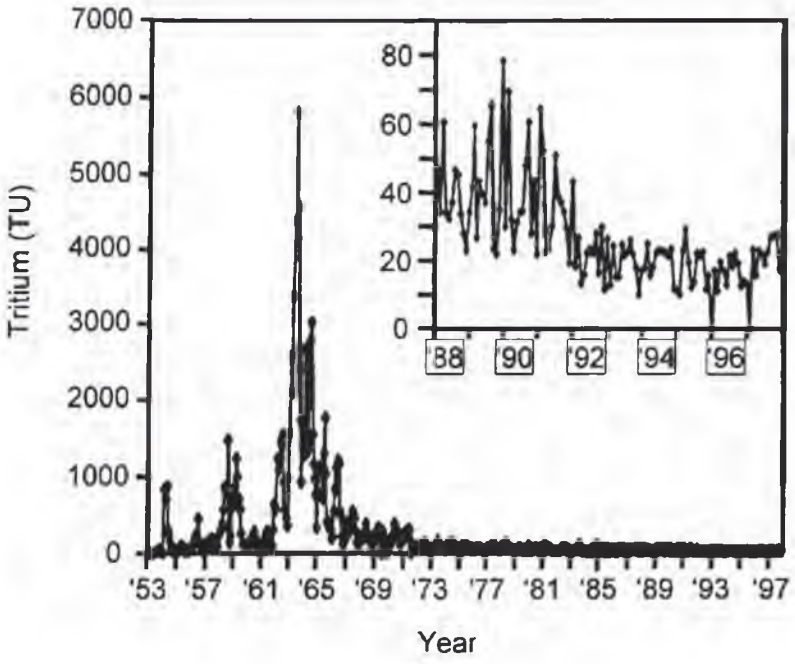

Figure 2.1. Tritium concentrations in rainfall at Ottawa, Canada. Data provided at www.iaea.or.at/programs/ri/gnip/gnipmain.htm.

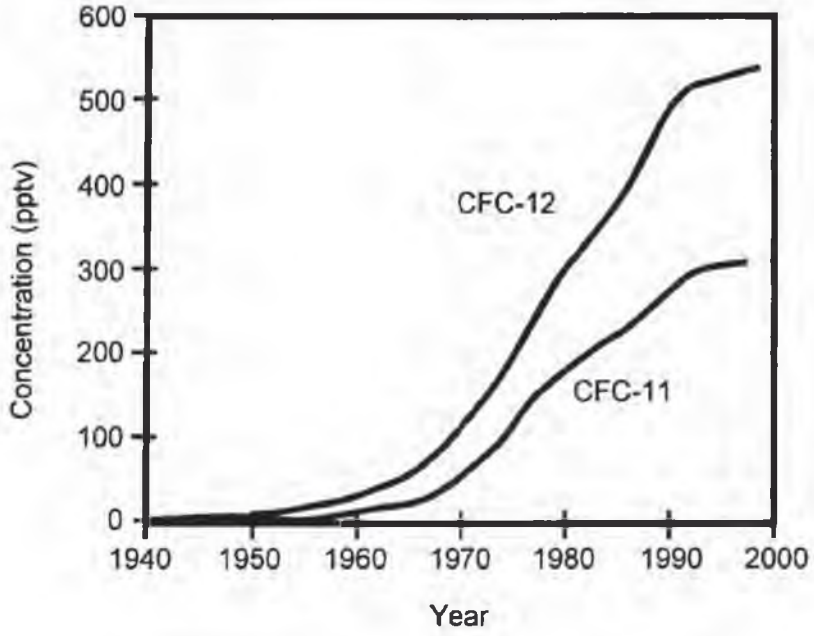

Figure 2.2. Atmospheric concentrations of CFC-11 and CFC-12 as a function of time (McCarthy et al., 1977; Rasmussen and Hkalil, 1986; http://www.cmdl.noaa.gov).

indicates the apparent groundwater recharge year. CFCs are therefore used to examine groundwater recharge and residence times (Thompson and Hayes, 1979; Busenberg and Plummer, 1992; Dunkle et al., 1993).

Plummer and Busenberg (2000), present a comprehensive description of the many factors that affect CFC concentrations in groundwater. Of particular concern at the site investigated in this study was the possibility of anaerobic microbial degradation of CFCs in sulfate-reducing groundwater, resulting in apparently older CFC ages. Recent studies, however, indicate that CFC-12 remains fairly stable in sulfate-reducing conditions, whereas CFC-11 and CFC-113 are significantly degraded (Semprini et al., 1990; Cook et al., 1995; Katz et al., 1995; Deipser and Stegmann, 1997; Plummer et al., 1998a,b). Thus, only CFC-12 was considered conservative in groundwater at the site.

The ^4He concentration of groundwater is acquired by atmospheric and subsurface processes. Subsurface processes can include mass transport from a source external to the hydrologic flow system, and/or internal production of radiogenic ^4He. $^4He_{rad}$ is produced in the subsurface as a result of either the decay of U/Th-series elements, or the release of stored $^4He_{rad}$ from aquifer grains (Solomon et al., 1996). In either case, the $^4He_{rad}$ concentration of groundwater can be orders of magnitude greater than water in equilibrium with the atmosphere (Davis and De Wiest, 1966; Andrews and Lee, 1979; Marine, 1979; Torgersen, 1980; Stute et al., 1992). He-4 released from aquifer solids at the rate of U/Th series decay has been used to date groundwater that is 10^3 to 10^6 yrs old (e.g. Mazor and Bosch, 1992).

Helium produced within continental crust is released to the atmosphere by migrating upward into the groundwater flow system. The crustal helium fluxes are dependent on several factors, including advection rates, diffusion coefficients, U/Th concentrations, and geologic history. Estimates of the crustal helium fluxes have been determined for various large-scale aquifer systems, such as the Great Hungarian Plain, Paris Basin, and the Great Artesian Basin, and from atmospheric helium budgets. Generally, the crustal helium fluxes range within a factor of 4 of the estimated mean global flux of 8.4×10^9 atoms/m^2_e/yr (O'Nions and Oxburgh, 1983).

Frequently, hydrodynamic and free-solution diffusion coefficients are used to describe the mass transport of helium through aquifer systems.

The occurrence and concentrations of tritium, CFCs and $^4He_{rad}$ were examined at the Smithville site to provide information about groundwater recharge and helium diffusion through the fractured bedrock. The combination of tritium, CFCs, and helium provide a powerful means to constrain the bulk groundwater flux. Tritium and CFCs represent "young" groundwater tracers entering the hydrologic system from above. Helium represents an "old" tracer, entering the system from below, and/or within. The results are constrained by a recently proposed conceptual model (Novakowski et al., 2000; Zanini et al., 2000) and a flow and transport model. The detailed hydraulic characterization of the site provides an opportunity to evaluate the necessity of applying effective diffusion coefficients to describe the diffusive transport of dissolved gases (helium) in fractured bedrock.

2.3 Site Characterization

The study site is located in southern Ontario near the town of Smithville (Figure 2.3), roughly 6 km south of the Niagara Escarpment. The surface topography at the site is relatively flat. A gentle swale occurs to the north of the site, oriented in a northwest to southeast direction (Golder Associates, 1988; Zanini et al., 2000). 20 Mile Creek exists south of the site and flows from northwest to southeast (Figure 2.3).

The geology of the site consists primarily of dolostones of the Lockport Formation overlain by a thin layer (5-10 m) of clay till (Golder Associates, 1995). The permeability of the clay is very low (roughly 10^{-9} to 10^{-11} m/s), although several vertical fractures exist which may extend to the underlying units (Golder Associates, 1995). Fine- to medium-grained dolostones dipping roughly 0.5 degrees southeast make up the members of the Lockport Formation (Eramosa, Vinemount, Goat Island, and Gasport members) and underlying Decew Formation (Golder Associates, 1995). A few shaley dolostone layers exist within the Vinemount and Gasport members, and the Decew Formation (Golder Associates, 1995). The low permeability Rochester Shale underlies the Decew Formation.

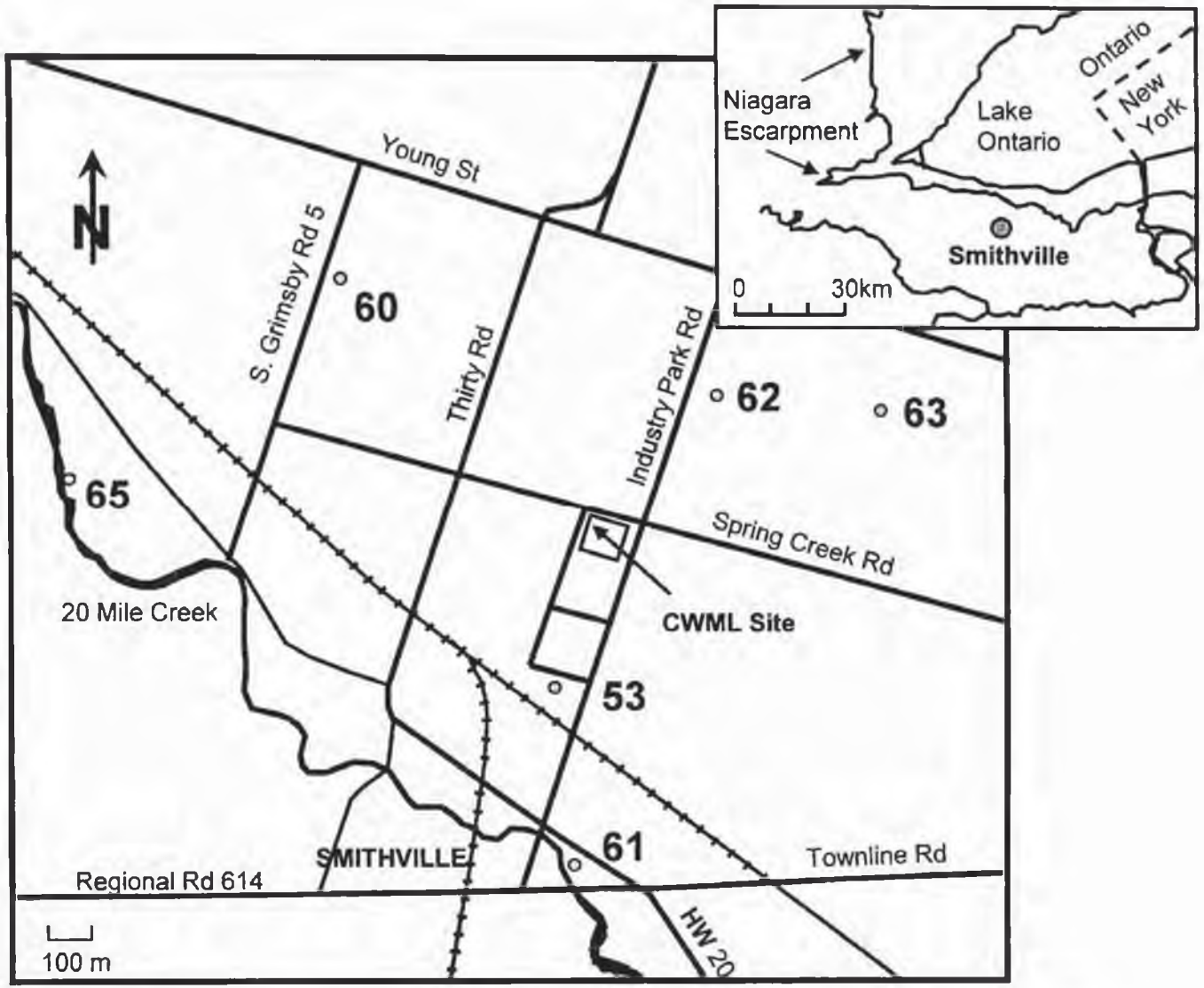

Figure 2.3. Site map (courtesy of Kent Novakowski). Borehole locations are marked with circles.

In addition to the initial site characterization performed by Golder Associates (1988, 1995), recent investigations have extensively characterized the site (Novakowski and Lapcevic, 1988; Lapeciv et al., 1996; Zanini et al., 1997, 2000; Novakowski et al., 2000). Novakowski and others (2000) provide a detailed list of the efforts made to define the fracture orientation and spacing and bedrock hydraulics of the site. From each of 18 boreholes, core has been collected and examined for structural and lithological features. Over 1396 packer tests were performed at 2.0, 0.5, and 0.1 m increments to provide a detailed description of the bedrock and fracture hydraulics of the site. Multiple local-scale tracer tests were also performed. Many of the boreholes were completed with multilevel piezometers from which routine measurements of hydraulic head were and continue to be obtained. The site is exceptionally well characterized compared to most field sites where ^{4}He studies have been performed.

The primary hydraulic zones coincide with laterally extensive bedding-plane fractures within the Eramosa/Vinemount members and to a lesser extent in the lower Gasport Member (Novakowski and Lapcevic, 1988; Golder Associates, 1995; Zanini et al., 2000). Flow within the fractures is in a southeast direction (Novakowski and Lapcevic, 1988; Golder Associates, 1995; Zanini et al., 2000) with fracture transmissivity as high as 10^{-2} m^2/s (Golder Associates, 1995). The vertical interconnection between major horizontal fractures is limited (Golder Associates, 1995). The Rochester Shale is a regional aquitard (Golder Associates, 1995) which marks the lower boundary of the groundwater flow domain. The conceptual model of the site (Zanini et al., 2000) describes the hydrologic framework with respect to the different lithologic units (Figure 2.4).

The inorganic geochemistry indicates a general progression from aerobic to sulfate-reducing conditions with depth at the Smithville site (Zanini et al., 1997). Aerobic conditions present within the clay till and upper portion of the Eramosa Member change to Fe-reducing within 20 m below ground surface (Zanini et al., 1997). Sulfate-reducing conditions exist within the Goat Island and Gasport Members (Zanini et al., 1997). Groundwater sampled from within the Rochester Shale indicated more anaerobic conditions in borehole 53, but less reducing conditions in boreholes 62 and 61 (Zanini et al., 1997).

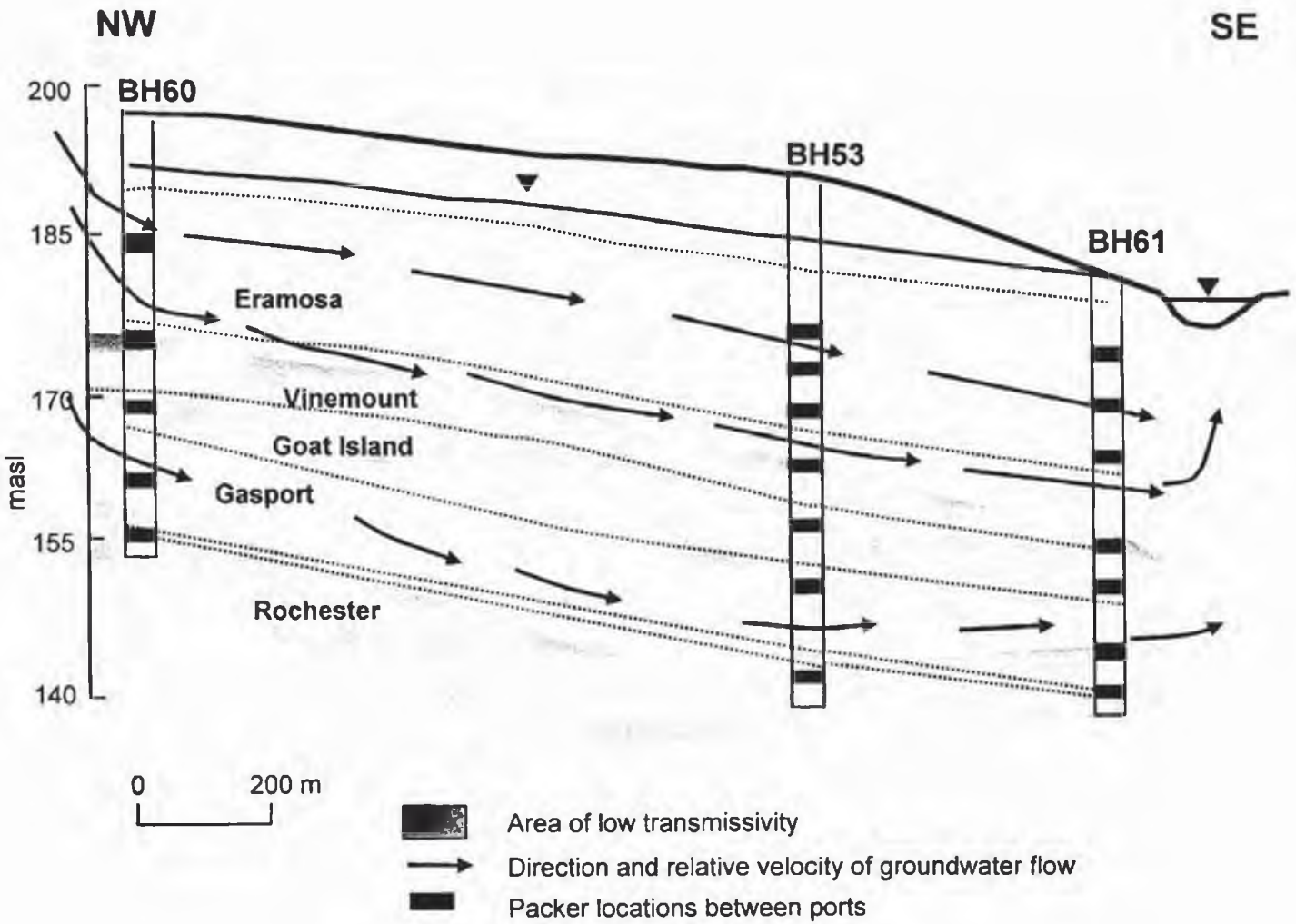

Figure 2.4. Site conceptual model (adapted from Zanini et al., 2000).

2.4 Site Investigation

During August 1997, regional groundwater dating commenced with the sampling of 6 boreholes (53, 60, 61, 62, 63, 65), which are completed with Westbay sampling devices (Zanini et al., 2000). From each well five to eight ports were sampled for dissolved gases (^{3}He, ^{4}He), CFCs, and tritium (^{3}H). Sampling ports that were either open to very low permeability zones or physically inaccessible were not sampled. Due to the length of the sampling string, occasionally the lowest port in a well could not be reached. Based on the results of this sample suite, three of the six wells were re-sampled during the following summer (August, 1998). The three wells were selected based on their relation to the regional groundwater flow direction and the site conceptual model (Novakowski et al., 2000; Zanini et al., 2000).

2.4.1 Sampling Method

The Westbay sampling device consists of a remotely controlled actuating device ("probe") and a sample chamber ("bottle"). Both probe and bottle are evacuated prior to installation with a hand held air pump. After the probe has been electronically located at a sampling port, a sealed connection is made between the borehole casing and probe (Zanini et al., 1997). The port valve is then opened remotely and groundwater from the formation enters the probe.

The standard Westbay sampling method described above presented a challenge for collecting dissolved gas samples. Due to the large increase in the internal cross-sectional area from probe to bottle, dissolved gases exsolve immediately as the water enters the larger diameter bottle. To minimize the ex-solution of dissolved gases, an additional bottle was created using 3/8 inch copper tubing. This Cu bottle was installed between the Westbay probe and bottle (Figure 2.5). This chamber made the change in cross sectional area more gradual, thereby limiting the amount of ex-solution to the leading front of water entering the Westbay bottle. Once located at a sampling port, the entire assembly was filled, sealed and removed. At the surface the Cu bottle was isolated from the probe and the probe was removed. The Cu sample tubes were then installed in-line with the Cu bottle. The water was pushed out of the bottles and through the sample tubes using a pump attached to the Westbay bottle. While the water was

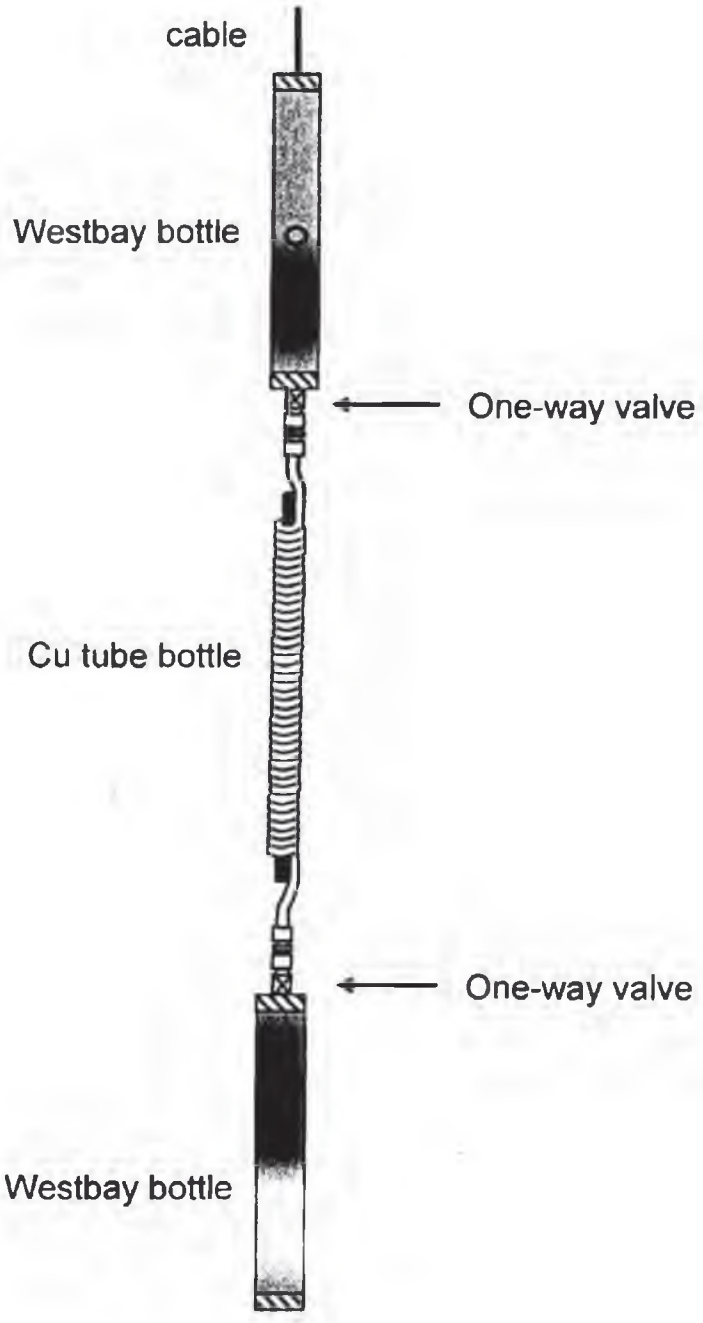

Figure 2.5. Sampling string. The Cu bottle was coiled around a central pipe for stability. Connections between the Cu bottle and Westbay devices were reinforced with wire and electrical tape.

being pushed through the sampling string, the sample tubes were tapped with a wrench to mobilize any gas bubbles adhered to the inside walls. Samples were only collected after no bubbles were observed in the effluent. Due to the limited volume of water contained in the chambers, only a small amount of water was allowed to purge the sampling tubes before samples were obtained. It was imperative that the exsolved water not be collected, nor any of the evolved gas bubbles. The ideal purge volume, the volume of water necessary to flush the sample tubes prior to sample collection, is far greater than this method could allow (Wilkowske, 1998). Duplicate and in many cases triplicate samples were collected to compensate for this potential error.

All dissolved gas samples were collected in copper tubes using refrigeration clamps (Ekwurzel et al., 1994; Wilkowske and Solomon, 1997; Wilkowske, 1998). Tritium samples were collected in glass bottles. Minimally one dissolved gas sample and duplicate CFC samples were collected from each port. The sampling method described above was used to sample all six wells in 1997, and the three wells sampled in 1998. As a means of evaluating the accuracy of this method, additional samples were collected during the 1998 season by a more traditional method. In this case, a few of the Westbay pumping ports were opened (individually) in each well allowing the borehole casing to fill. After purging three well volumes, a WaTerra pump was used to bring water to the surface where samples were collected in Cu tubes.

2.4.2 Sample Analysis

CFC samples were analyzed by a purge and trap gas chromatography method with an electron capture detector (Wilkowske, 1998), modified after Bullister and Weiss (1988). Atmospheric CFC concentrations were determined using Henry's Law and the solubility data of Warner and Weiss (1985).

$$C_i = H_k p_i \qquad (2.1)$$

where C is the solubility of CFC species *i* in water (measured), H_k is the Henry's constant (Warner and Weiss, 1985), and p is the partial pressure of CFC_i in the gas phase that is in

equilibrium with the water. Apparent groundwater recharge years were determined by comparing the CFC partial pressures in the gas phase (p_i) to the atmospheric growth curve (McCarthy et al., 1977; Rasmussen and Khalil, 1986; Busenberg and Plummer, 1992; Elkins et al., 1993; Plummer and Busenberg, 2000).

Tritium values were determined using a modified "in-growth" technique (Clarke et al., 1976). Approximately 250 g of degassed water was sealed in an evacuated copper bulb (Figure 2.6). The bulb stem was cold-welded on-line to form a leak-tight seal. Poor seals were detected by the lack of a "water hammer" when the bulb was gently shaken. Freezing of the water sample during storage is not necessary when using copper bulbs, unlike 1724 glass, since the diffusion of helium through copper is extremely low. Samples were stored at room temperature for six weeks prior to analysis. Standard lab waters prepared and stored in the same manner indicate a minimal helium blank corresponding to about 0.05 TU.

Dissolved gases were extracted from water samples and then introduced to a cleanup system, which removes condensable gases (H_2O, CO_2), reactive gases (O_2, N_2), high molecular weight noble gases (Ar, Kr, Xe), and finally Ne (absorbed onto charcoal at 35 K). The He was then introduced into a magnetic sector mass spectrometer for analysis. All samples were analyzed at the University of Utah.

Radiogenic ^4He concentrations were determined using measured Ne concentrations and the solubility of He and Ne (Schlosser et al., 1989).

$$^4He_{rad} = {}^4He_{aq} - {}^4He_{sol} - R_{He-Ne}\left[Ne_{aq} - Ne_{sol}\right] \qquad (2.2)$$

where

$^4He_{rad}$ radiogenic component of ^4He

$^4He_{aq}$ aqueous ^4He concentration

$^4He_{sol}$ solubility ^4He concentration

Ne_{aq} aqueous Ne concentration

Ne_{sol} solubility Ne concentration

R_{He-Ne} atmospheric He/Ne ratio.

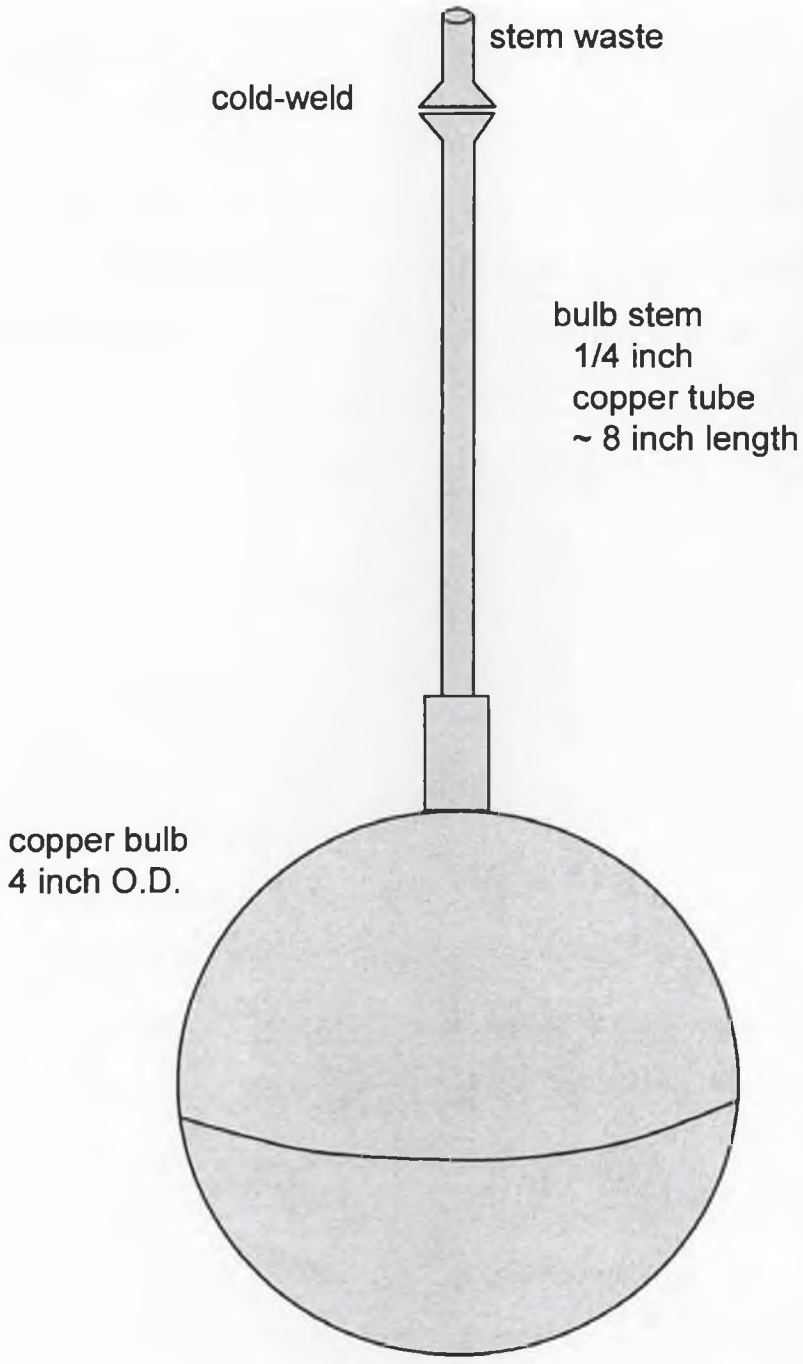

Figure 2.6. Copper bulb used for tritium in-growth technique.

A recharge temperature of 5°C was used to calculate $^4He_{sol}$ and Ne_{sol} using the solubility data of Weiss (1971). The $^3H/^3He$ age was determined by

$$t = \lambda^{-1} \ln\left[\frac{^3He^*}{^3H} + 1\right], \tag{2.3}$$

where t is the estimated groundwater age, λ^{-1} is the ^3H decay constant, ^3H is the tritium concentration in tritium units (TU), and $^3He^*$ is the tritogenic ^3He measured in TU (Tolstikhin and Kamensky, 1969; Torgersen et al., 1977; Takaoka and Mizutani, 1987; Poreda et al., 1988; Schlosser et al., 1988; Solomon and Cook, 2000). Tritiogenic ^3He concentrations were calculated according to Schlosser and others, (1989).

$$^3He^* = {}^4He_m R_o - R_{sol}\left[{}^4He_{sol} + \alpha' R_{He-Ne}(Ne_m - Ne_{sol})\right] - R_{rad}\left[{}^4He_m - {}^4He_{sol} - (Ne_m - Ne_{sol})R_{He-Ne}\right] \tag{2.4}$$

where

^4He_m	measured ^4He concentration
Ne_m	measured Ne concentration
R_o	measured $^3He/^4He$ ratio
R_{sol}	$^3He/^4He$ ratio of groundwater in equilibrium with the atmosphere
R_{rad}	$^3He/^4He$ ratio of radiogenic ^4He and nucleogenic ^3He
α'	He air-water isotope fractionation factor (R_{gas}/R_{water}).

2.5 Results

2.5.1 CFCs

The apparent recharge year determined from concentrations of CFC-12 ranged from 1954 to 1990 (Table 2.1, Figure 2.7). The specially designed Cu bottle appears to have minimized dissolved gas stripping during sampling. Duplicate samples generally agreed to within 4 years. The CFC-12 concentrations were within the range expected for natural waters that obtain CFCs from the atmosphere (which is the basis for the CFC dating method), indicating that

Table 2.1. Dissolved gas data for samples collected in 1997 and 1998. *- a sample that might have degassed, p- pumping port, **- apparent recharge year.

Borehole ID	Depth (mbTOC)	Year Sampled	CH_4 (ucc/kg)	N_2 (cc/kg)	Ar40 (cc/kg)	Kr (ucc/kg)	Ne20 (ucc/kg)	He4 (ucc/kg)	R/Ra	$4He_{rad}$ (ucc/kg) air corr	CFC-12 pmoles/kg	CFC-12 Recharge Year**	T (T.U.)	T +	T -	T/3He Recharge Year**
60	15	1997	88.10	33.22	0.87	74.35	411.72	109.44	1.01	7.99	0.19	<1960				
60	18	1997	34.02	30.86	0.83	69.18	355.36	113.50	1.07	25.94	0.10	<1960				
60	18	1997	51.24	30.68	0.83	67.32	359.13	119.77	1.11	31.27						
60	27	1997	48.34	31.03	0.89	82.08	437.47	10745.63	0.03	10637.83	0.62	1968				
60	36	1997	163.18	33.02	0.90	90.72	467.37	7621.52	0.03	7506.36	1.09	1972				
60	46	1997	59.78	33.84	0.90	81.79	488.76	6295.44	0.04	6175.00	1.30	1974				
60	50	1997	254.10	55.91	1.17	82.05	707.46	27190.66	0.02	27016.34	0.98	1971				
60	15	1998									0.14	<1960	3.73	0.19	0.19	
60	18	1998	20.19	31.42	0.93	89.76	341.06	110.19	1.06	26.15	0.15	<1960	4.69	0.23	0.23	1960
60	21p	1998	399.92	38.80	1.05	101.54	421.88	121.75	1.02	17.80			6.11	0.31	0.31	1962
60	27	1998	47.70	14.27	0.42	41.64	153.94	5492.34	0.03	5454.40	0.12	<1960	2.04	0.10	0.21	
60	36	1998	29.65	34.48	0.95	89.37	501.05	6975.23	0.04	6851.77	0.91	1971	9.00	0.45	0.45	
60	39p	1998	27.70	33.19	0.94	92.75	400.90	5502.72	0.04	5403.93						
60	46	1998	47.45	32.09	0.95	83.45	477.15	17238.16	0.02	17120.58	1.21	1973	5.15	0.26	0.26	
60	50	1998	193.12	37.77	0.94	77.41	539.88	23009.55	0.02	22876.52	0.94	1971	3.43	0.17	0.17	
62	23	1997	14.21	19.49	0.64	47.64	268.07	87.89	0.83	21.83	1.34	1974				
62	30.5	1997	43.42	32.59	0.98	81.28	446.58	5687.77	0.01	5577.73	0.67	1968				
62	39.5	1997	54.14	36.36	1.02	90.68	634.41	7405.44	0.03	7249.12	0.81	1970				
63	15	1997	46.30	23.83	0.75	64.52	299.86	99.12	0.82	25.23	0.63	1968				
63	19.5	1997									0.51	1966				
63	25.5	1997	114.67	21.84	0.76	80.13	227.86	78.26	0.66	22.12	0.70	1969				
63	30	1997	148.05	31.11	0.91	79.52	367.39	1207.89	0.10	1117.36	0.34	1963				
63	34	1997	233.97	33.20	0.96	90.11	392.72	1238.77	0.11	1141.99	0.18	<1960				
63	41.5	1997	27.72	29.38	0.82	65.57	401.59	719.47	0.16	620.52	0.89	1971				

Table 2.1 Continued.

Borehole ID	Depth (mbTOC)	Year Sampled	CH_4 (ucc/kg)	N_2 (cc/kg)	Ar40 (cc/kg)	Kr (ucc/kg)	Ne20 (ucc/kg)
65	4	1997	19.97	18.99	0.60	48.98	269.11
65	7	1997	54.73	28.38	0.89	76.41	332.36
65	13.5	1997	83.70	24.28	0.67	62.87	312.68
65	24	1997	646.24	58.16	1.40	101.56	565.10
65	29.5	1997	1359.18	74.93	1.60	116.43	
65	35	1997	2091.10	117.80	2.34	170.52	1045.28
65	39	1997	143.80	19.78	0.59	48.50	344.80
53	16.5	1997	3415.00	69.03	0.99	90.30	372.38
53	19.5	1997	94.03	21.48	0.64	58.28	233.57
53	22.5	1997	20.77	28.39	0.85	79.16	305.76
53	30	1997	431.10	31.93	0.89	77.07	116.82
53	36	1997	654.65	51.12	1.26	124.25	599.99
53	42	1997	9.47	19.07	0.57	42.99	245.66
53	49.5	1997	101.00	38.12	0.95	85.67	510.58
53	55.5	1997	174.45	31.01	0.80	69.35	0.16
53	60	1997	10081.23	89.24	1.16	90.50	
53	16.5	1998	367.97	32.46	0.82	80.85	347.52
53	19.5	1998	5.94	26.62	0.78	67.23	306.27
53	22.5	1998	24.65	31.77	0.88	79.66	398.49
53	30	1998	140.45	27.51	0.79	72.72	334.27
53	33p	1998	219.13	32.14	0.86	77.06	345.11
53	33p	1998	218.51	26.77	0.89	80.95	207.54
53	36	1998	338.13	38.39	1.07	104.80	432.41
53	36	1998					
53	42	1998	199.86	47.23	1.26	105.63	291.87
53	45p	1998	64.72	30.94	0.87	71.33	377.53
53	49.5	1998	73.48	34.26	0.91	90.12	494.75
53	51p	1998					
53	55.5	1998	193.41	49.85	1.24	132.55	773.38
53	60	1998	7100.59	66.44	1.02	81.46	

He4 (ucc/kg)	R/Ra	$4He_{rad}$ (ucc/kg) air corr	CFC-12 pmoles/kg	CFC-12 Recharge Year**	T (T.U.)	T +	T -	T/3He Recharge Year**
418.25	0.24	351.93	2.35	1982				
237.47	0.39	155.57	1.50	1975				
2285.37	0.06	2208.32	0.82	1970				
58724.44	0.02	58585.20	1.10	1972				
		114063.69	0.24	1961				
127320.26	0.02	127062.70	0.28	1962				
48732.35	0.02	48647.39	1.80	1977*				
105.78	1.03	14.02	0.14	<1960				
201.15	0.37	143.59	0.09	<1960				
162.05	0.62	86.70	0.18	<1960				
3416.49	0.05	3387.70	0.46	1965				
14782.89	0.03	14635.05	1.76	1977				
23472.92	0.02	23412.38	0.89	1971*				
47878.26	0.02	47752.45	1.90	1979				
			2.40	1982				
			0.53	1967*				
94.30	1.13	8.66	0.07	<1960	8.27	0.41	0.41	1971
282.52	0.27	207.05	0.14	<1960	3.01	0.21	0.41	1966
186.63	0.65	88.44	0.21	1960	4.35	0.22	0.22	1958
3479.21	0.04	3396.85	0.39	1964	7.06	0.35	0.68	
3112.32	0.05	3027.28			5.75	0.29	0.29	
4879.44	0.02	4828.30						
3919.99	0.05	3813.44	1.85	1978	1.02	0.05	0.05	
					3.46	0.17	0.17	
10115.46	0.02	10043.54	0.64	1968	1.21	0.06	0.06	
16967.34	0.02	16874.31						
35201.23	0.02	35079.32	0.51	1966	0.69	0.03	0.04	
83373.54	0.01	83182.98	0.50	1966	0.33	0.02	0.02	
			0.49	1966	0.67	0.03	0.06	

Table 2.1 Continued.

Borehole ID	Depth (mbTOC)	Year Sampled	CH_4 (ucc/kg)	N_2 (cc/kg)	Ar40 (cc/kg)	Kr (ucc/kg)	Ne20 (ucc/kg)	He4 (ucc/kg)	R/Ra	$4He_{rad}$ (ucc/kg) air corr	CFC-12 pmoles/kg	CFC-12 Recharge Year**	T (T.U.)	T +	T -	T/3He Recharge Year**
61	7	1997									1.25	1974				
61	10	1997									0.45	1965				
61	16	1997									0.17	<1960				
61	22	1997	666.11	65.87	1.41	96.82	963.80	4025.02	0.11	3787.53	0.43	1965				
61	34	1997	68.81	28.15	0.77	63.32	81.20	14662.11	0.02	14642.10	1.49	1975				
61	38.5	1997	121.82	31.79	0.94	73.04	374.56	16684.72	0.02	16592.42	0.48	1966				
61	46	1997	68.56	21.08	0.62	57.86	48.07	17081.79	0.02	17069.94	1.87	1978*				
61	50.5	1997	145.04	5443.77	85.19	5049.23	13502.54	37510.73	0.01*	34183.70	3.74	1990				
61	50.5	1997	3588.18	4714.23	73.37	5475.80	22676.35	51710.18	0.007*	46122.72						
61	7	1998	695.58	35.40	0.79	74.63	328.45	505.35	0.24	424.42	2.16	1980				
61	10	1998	30.65	30.87	0.98	90.70	370.45	3367.19	0.05	3275.91	0.07	1963	0.39	0.02	0.04	
61	11.5p	1998	81.92	31.74	0.90	88.17	386.55	3512.34	0.05	3417.09						
61	16	1998									0.16	<1960				
61	22	1998	222.23	37.22	0.88	70.70	593.17	2565.27	0.09	2419.11	0.37	1964	4.61	0.23	0.23	1959
61	22	1998	232.67	82.40	1.09	110.07	599.21	4079.62	0.06	3931.97						
61	25p	1998	124.40	34.76	1.03	97.84	419.50	3740.95	0.05	3637.58			4.82	0.27	0.54	1959
61	34	1998	38.45	23.18	0.74	59.91	344.22	8810.06	0.02	8725.24	1.89	1978	2.08	0.1	0.1	
61	37.5	1998	29.51	27.95	0.86	76.49	358.06	12998.70	0.02	12910.47	0.20	1960	0.74	0.04	0.04	
61	46	1998	42.78	31.51	0.96	82.27	415.18	36547.03	0.02	36444.72	1.25	1974	1.53	0.08	0.08	

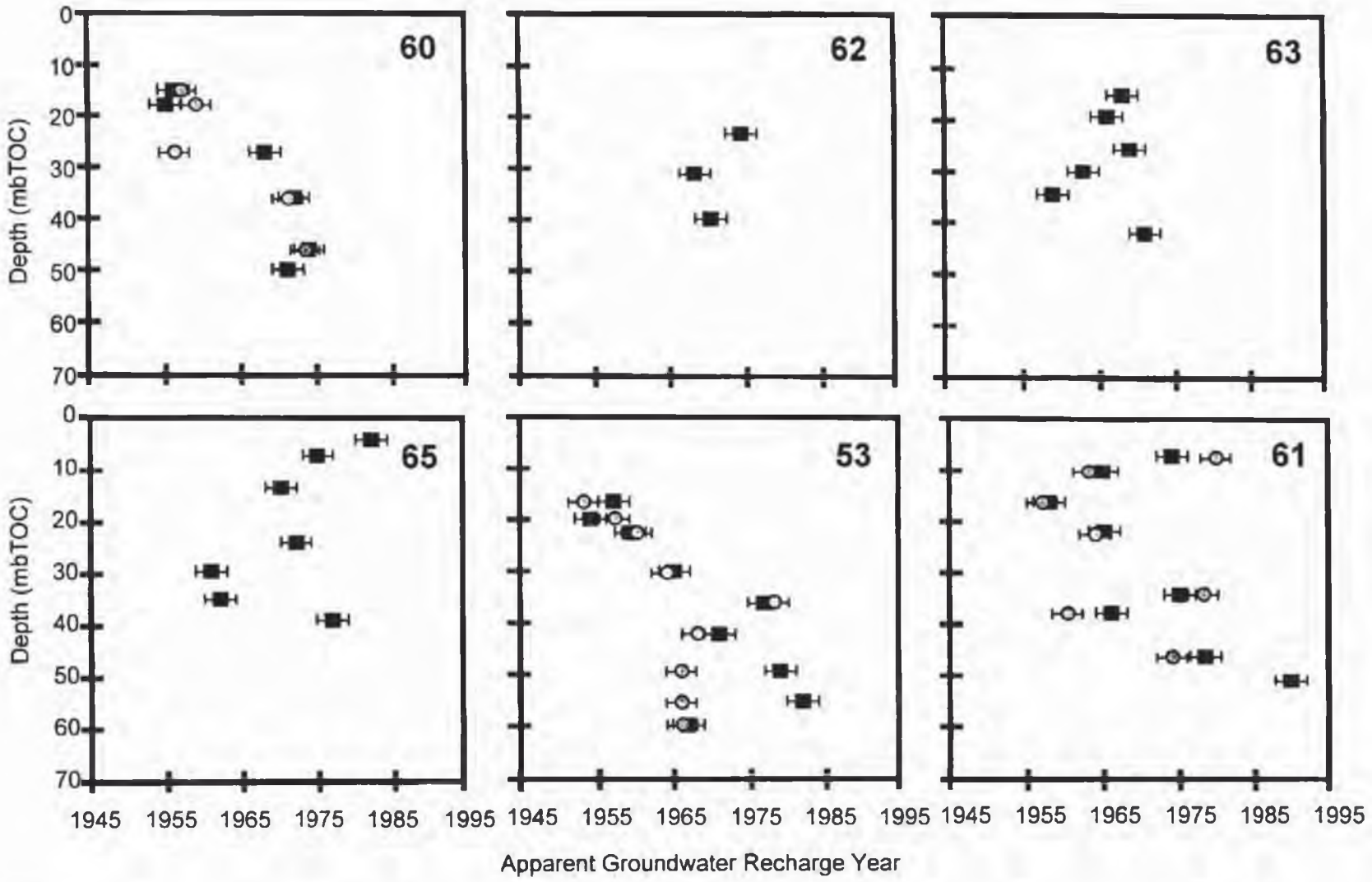

Figure 2.7. Groundwater CFC ages with depth. Boreholes 60, 62, and 63 are located up-gradient. Boreholes 65, 53, and 61 are located down-gradient. Squares represent samples collected in 1997, circles 1998.

CFC dating can be performed in Westbay installed wells at this site. Samples collected in 1998 generally show the same trend with depth as those collected in 1997 (Figure 2.7). Groundwater ages determined using CFC-11 were consistently older than those determined using CFC-12, suggesting that CFC-11 is degraded in the sulfate-reducing conditions at the site.

The CFC-12 data indicate a general trend of decreasing age with depth at the site, with the youngest waters commonly occurring at or near the greatest depth (Figure 2.7). Groundwater sampled in boreholes 61 and 65 show a trend of increasing age with depth from 0 to 15 m. In all three down-gradient boreholes (53, 61, and 65) there is a marked increase in CFC-12 (younger water) in the lower Vinemount Member, followed by a decrease in the underlying Goat Island Member. Also significant is a relatively "smooth" distribution of groundwater ages with depth, rather than a "noisy" profile which might be expected of a fracture-dominated flow system.

2.5.2 Tritium

Tritium was detected in all samples collected, with concentrations ranging from 0.3 to 9.0 TU (Figure 2.8, Table 2.1). Duplicate water samples were used to constrain the sampling error to within 1 TU. The analytical error was significantly less (Table 2.1). The larger sampling error is most likely due to the minor presence of drilling fluid, which was the in situ groundwater. The tritium concentrations determined in this study agree with tritium results determined by electrolytic enrichment (Zanini et al., 2000). Lower tritium concentrations are common in groundwater obtained from the Rochester Shale. This is particularly noticeable in borehole 53. Groundwater within the Rochester Shale at this location may represent pre-bomb water, although CFC-12 concentrations from the same location indicate the groundwater was recharged in 1965 +/- 3 years.

2.5.3 Helium

Since dissolved helium is more susceptible to ex-solution than CFCs, the ^{4}He results are a better validation of the sampling method. There is very good agreement between

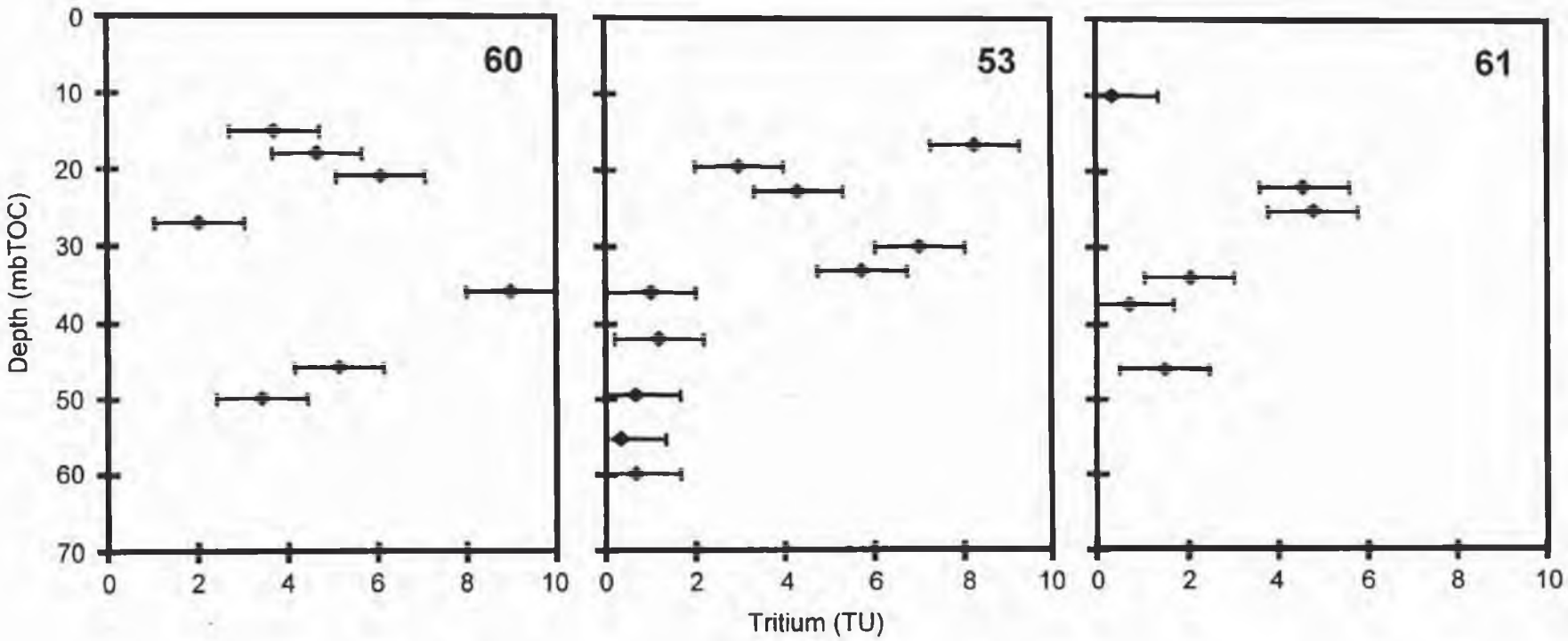

Figure 2.8. Tritium concentrations measured in boreholes 60, 53 and 61 during the 1998 sampling season.

groundwater samples collected in 1998 using the Cu bottle method and the more standard technique (Table 2.1). There is good agreement between samples collected in 1997 and 1998.

The ratio of $^3He/^4He$ in groundwater compared to the $^3He/^4He$ of air (R/Ra) decreases with depth in all sampled boreholes. Generally, shallow groundwater within the up- and mid-gradient boreholes (60, 62, 63, and 53) has a R/Ra ratio near or greater than 1.0, indicative of the presence of young tritiated water (Table 2.1, Figure 2.9). Down-gradient the R/Ra ratio of shallow groundwater is less than 1.0 (boreholes 61 and 65). The similar R/Ra ratios at 30 and 36 m in borehole 63 are the result of a compromise to the packer system resulting in a hydraulic connection between the screened zones (Zanini, pers. commun.).

The concentration of ^4He increases with depth in all sampled wells, from near atmospheric solubility (48 μcc/kg) to over 80,000 μcc/kg in the deepest sampled location (Table 2.1, Figure 2.10). Extremely high ^4He concentrations were observed in the lowermost Goat Island, Gasport, Decew and Rochester units. The greatest increase in concentration with depth occurs near the Rochester Shale. Groundwater ^4He concentrations within the Rochester Shale are not represented in boreholes 62, 63 and 65. Generally, the ^4He concentration increases downgradient (Figure 2.10). The similar ^4He concentrations at depths of 30 and 36 m in borehole 63 are a result of the failed packer.

The use of $^3H/^3He$ dating is limited at the site. High ^4He concentrations and low R/Ra ratios result in large errors in $^3H/^3He$ ages due to mass spectrometer counting statistics (only a very small split of the total gas from a 30 cm^3 water sample was inlet into the mass spectrometer). Indeed, $^3H/^3He$ ages could be obtained on a limited number of samples (Table 2.1). In general, $^3H/^3He$ ages agree with the CFC-12 results, indicating the presence of relatively young (post-bomb) water within the Lockport Formation.

2.6 Modeling ^4He

Groundwater ages were initially determined based on the internal production of $^4He_{rad}$ from the decay of U/Th-series elements. This method assumes the groundwater $^4He_{rad}$ concentration is a result of the steady-state U/Th→$^4He_{rad}$ production rate and the length of time the groundwater has been exposed to it (or its age). The steady-state ^4He release is described

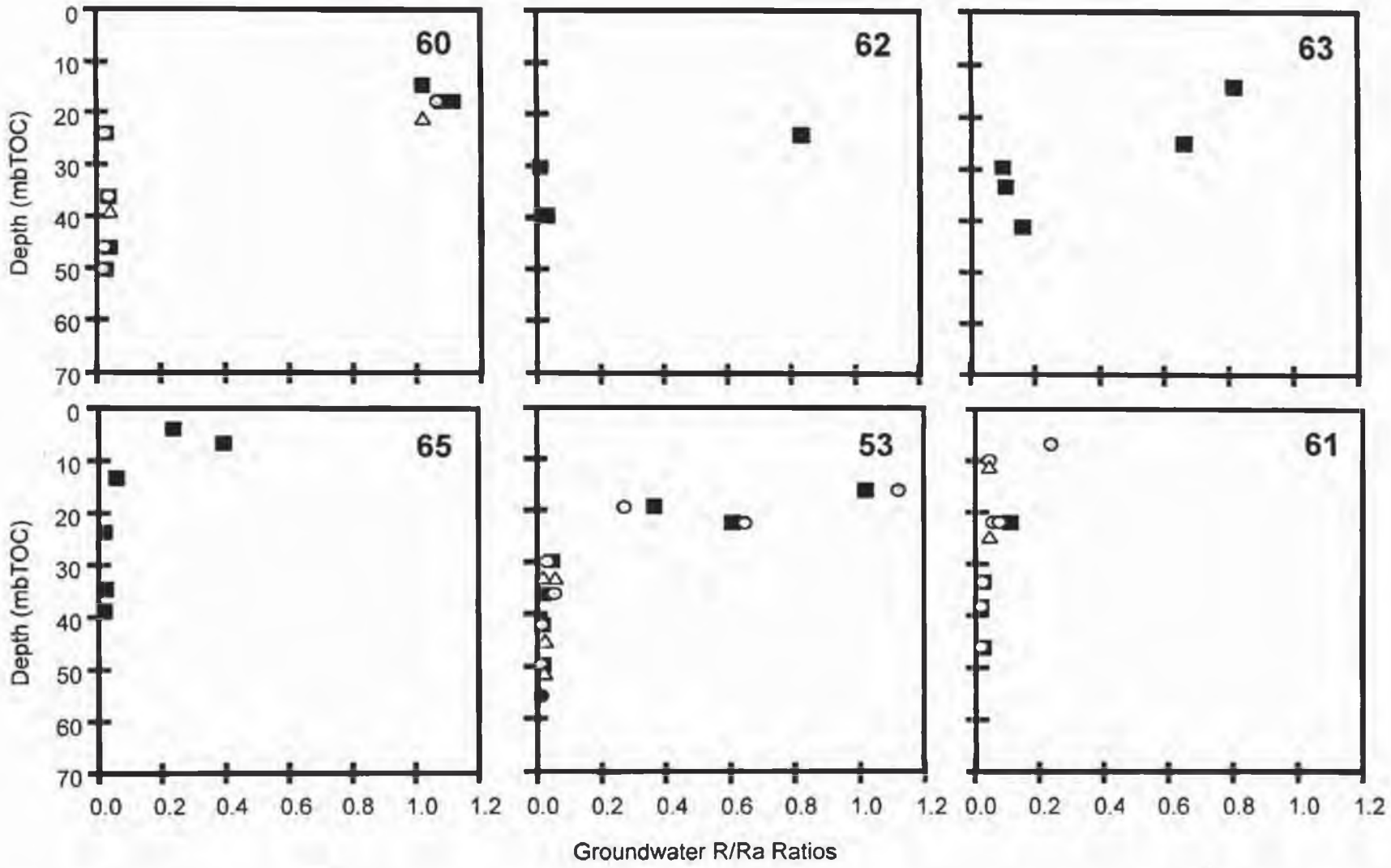

Figure 2.9. Groundwater R/Ra ratios with depth. Boreholes 60, 62, and 63 are located up-gradient. Boreholes 65, 53, and 61 are located down-gradient. Squares represent samples collected in 1997, circles 1998, open triangles the 1998 pumping port samples.

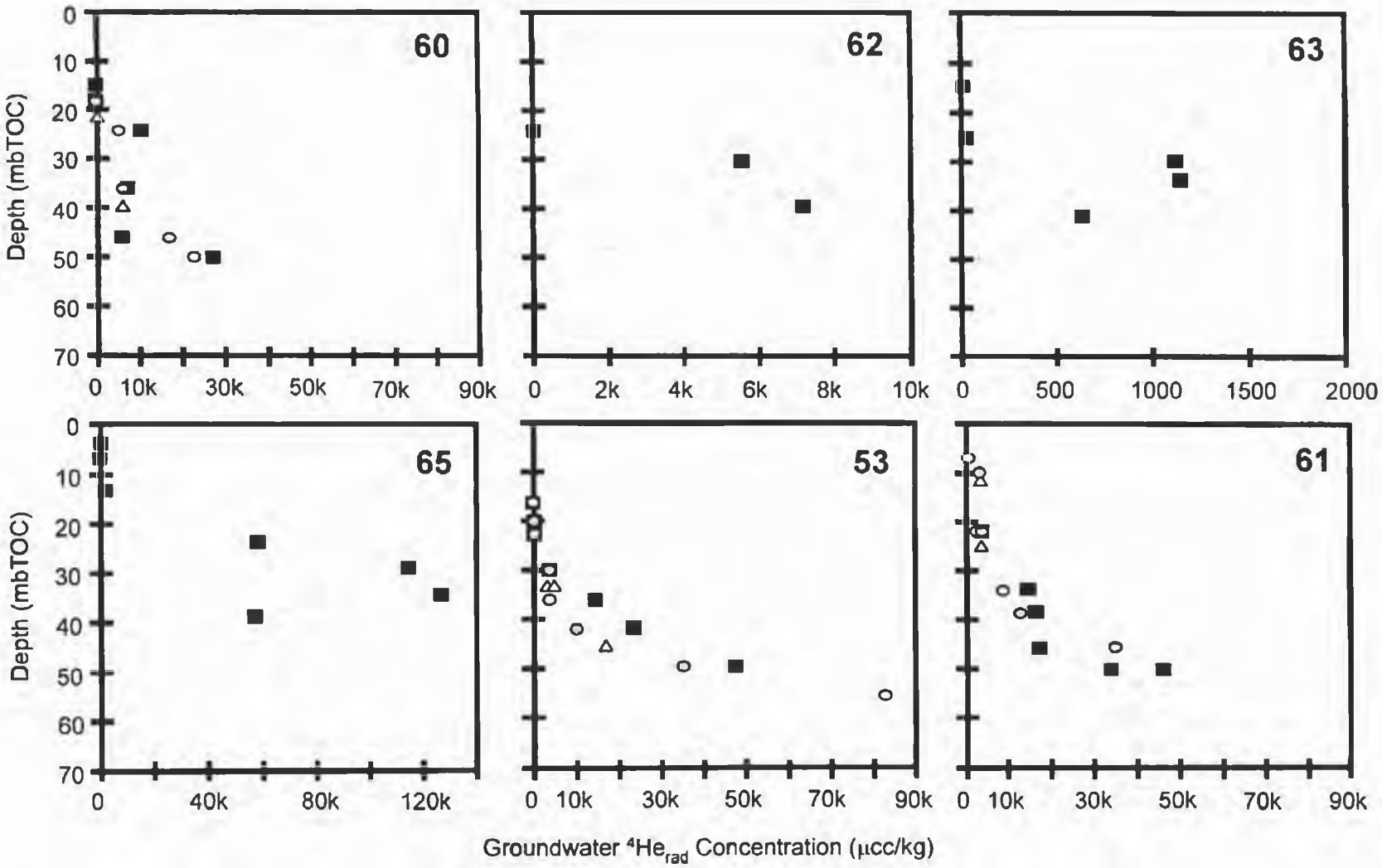

Figure 2.10. Groundwater $^4He_{rad}$ concentrations with depth. Note that the $^4He_{rad}$ scale varies for boreholes 62, 63, and 65. Boreholes 60, 62, and 63 are located up-gradient. Boreholes 65, 53, and 61 are located down-gradient. Squares represent samples collected in 1997, circles 1998.

according to Pearson and others (1991) as

$$G = \rho N_L \left\{ 8 \left[^{238}U\right] \left(\frac{\lambda_{238}}{M_{238}}\right) + 7 \left[^{235}U\right] \left(\frac{\lambda_{235}}{M_{235}}\right) + 6 \left[^{232}Th\right] \left(\frac{\lambda_{232}}{M_{232}}\right) \right\} \quad (2.5)$$

where

G	^{4}He release rate per unit volume of solids per unit time
ρ	density of solids
N_L	Avagadro's Number
λ_i	decay constants for radioactive isotopes, *i*, of U and Th
M_i	molecular weights of radioactive isotopes, *i*, of U and Th
[i]	decimal fraction of radioactive isotopes, *i*, of U and Th in solids.

Assuming dolostone U and Th concentrations (2 and 7 ppm, respectively), the maximum $^4He_{rad}$ production rate would be roughly 1 µcc/m^3/yr. Dividing the observed groundwater $^4He_{rad}$ concentration by this production rate yields the apparent groundwater age. The conservative estimate of groundwater age determined by this method would range over 4 orders of magnitude at the Smithville site (Figure 2.11). At depth, the $^4He_{rad}$ concentration indicates a groundwater age approaching 10 million years. These ages contradict the CFC, tritium, stable isotope and general chemistry results (Novakowski et al, 2000; Zanini et al., 2000) which indicate the presence of much younger water.

To evaluate this apparent conflict, a simple groundwater-mixing model was employed. The model assumed that mixing occurs between a deep source of high $^4He_{rad}$ water and shallow fresh groundwater having a $^4He_{rad}$ concentration near atmospheric solubility. Assuming a deep groundwater concentration similar to that observed (500 to 50,000 µcc/kg), the fraction of shallow water required to generate the observed range in R/Ra ratios was determined (Figure 2.12). For large R/Ra (>0.5), fresh water accounts for at least 90% of the observed concentration of ^{4}He, regardless of the deep water $^4He_{rad}$ concentration. The model indicates for large $^4He_{rad}$ concentrations (5000 to 50,000 µcc/kg), a substantial fraction of the mixture (≥60%) is shallow water. It is important to stress that the hydrologic framework at this site is not

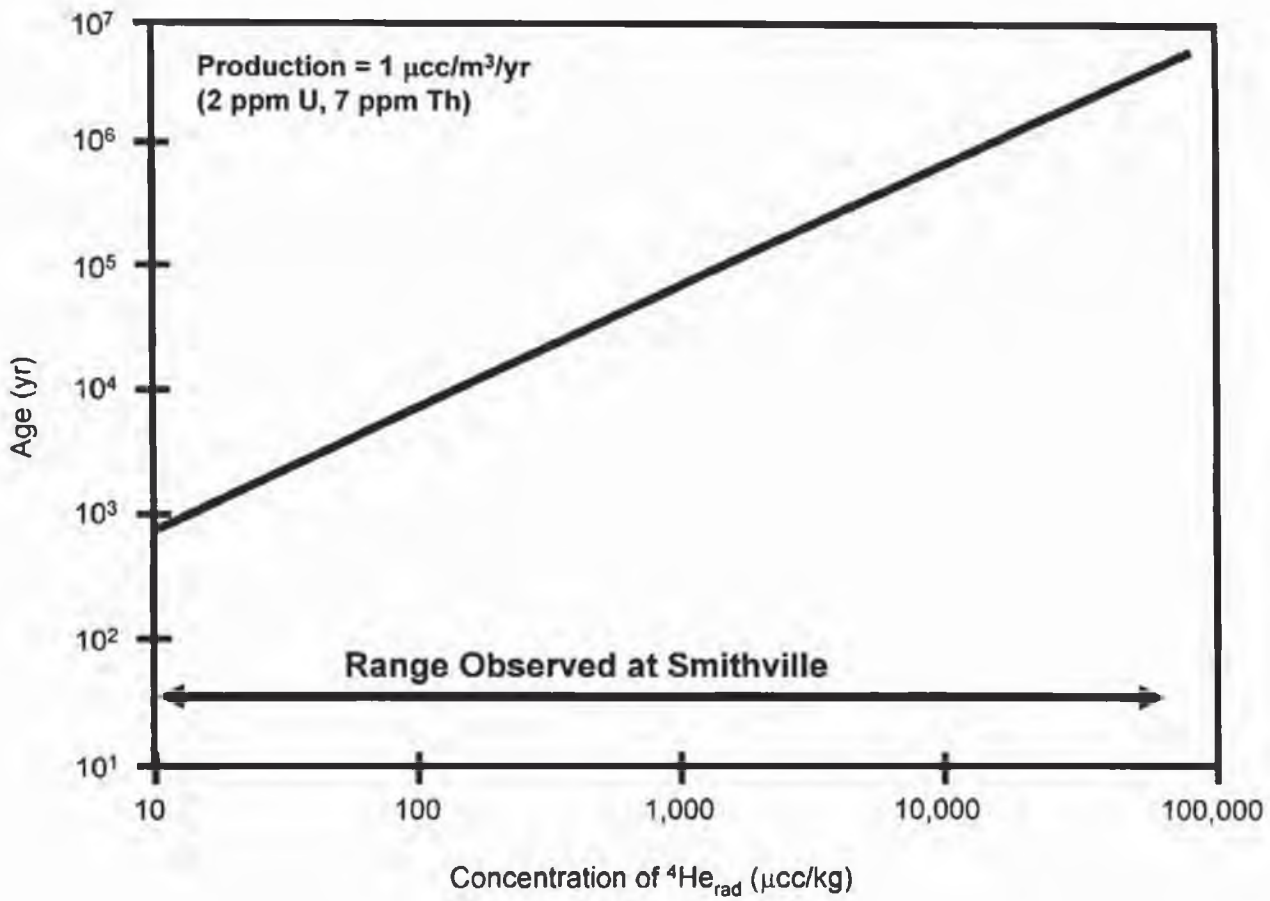

Figure 2.11. Groundwater ages determined by the decay of U/Th-series elements to $^4He_{rad}$. The Groundwater ages observed at the study site range over 4 orders of magnitude.

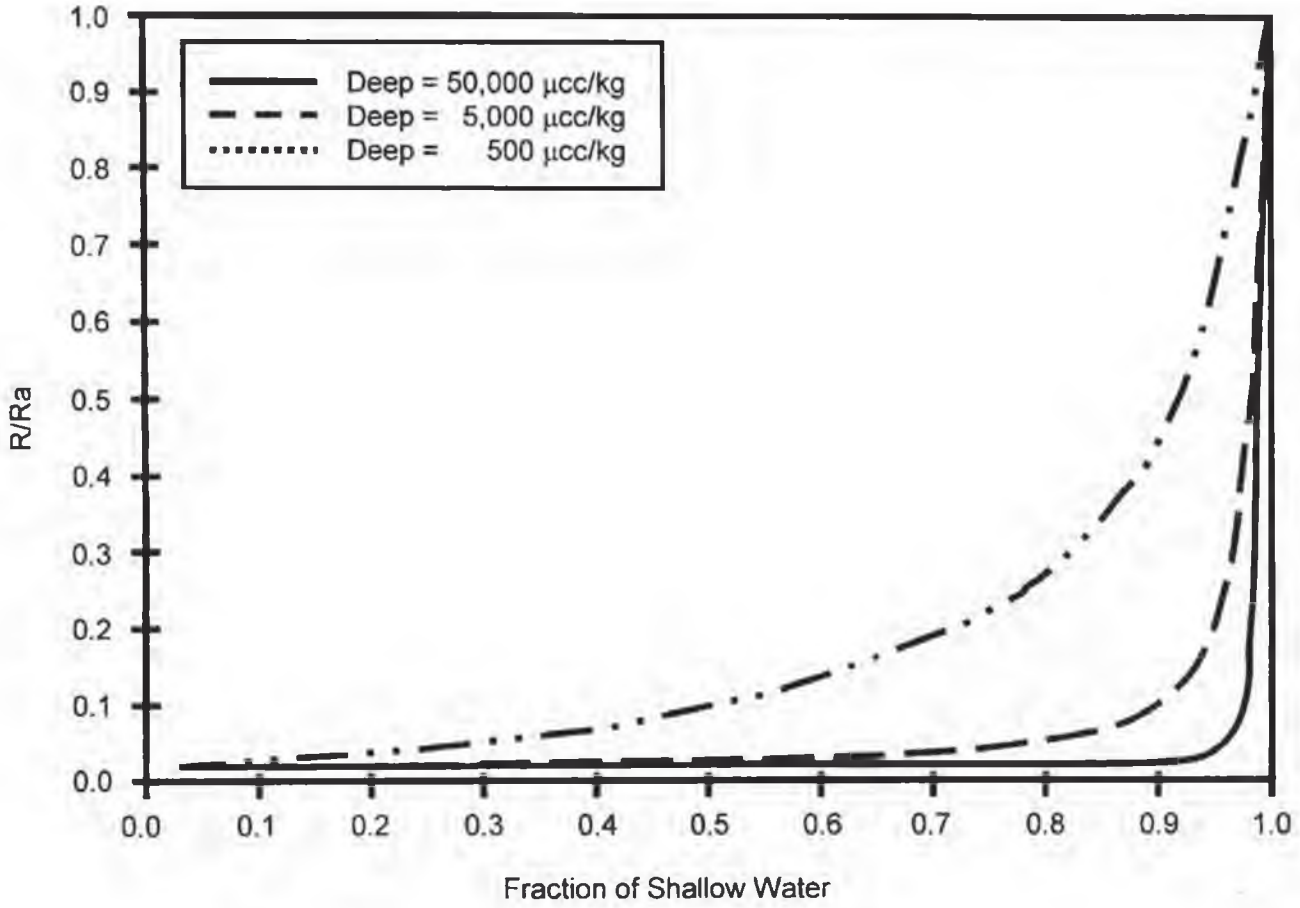

Figure 2.12. Groundwater mass mixing model. The fraction of shallow water mixed with deep groundwater to produce a given R/Ra ratio is determined assuming a range of deep groundwater concentrations.

supportive of a well-mixed groundwater scenario. Rather, the implication from this model is that the high $^4He_{rad}$ concentrations observed at depth might result from a very small contribution of mass from a high concentration source.

The CFC, tritium, and helium data suggest the source of helium is external to the groundwater flow regime. First, CFC and tritium data suggest young water occurring throughout the Lockport Formation. Second, the $^4He_{rad}$ concentration profiles at depth (near the Rochester Shale) indicate a common concentration gradient, suggesting a diffusive flux of helium from depth (external to the Lockport). Finally, very large ^4He concentrations are known to exist within the Rochester Shale (high ^4He source). The combination of tritium and dissolved gases argues against the internal production of $^4He_{rad}$ being a significant source at the site.

2.6.1 Mass Balance Box Model

A mass balance model was performed to evaluate the effective ^4He diffusion coefficient through the dolostones and the resulting high $^4He_{rad}$ concentrations observed in groundwater that may be younger than suggested by U/Th→He dating. The model is a simple box model that incorporates ^4He diffusion from below (the underlying Rochester Shale), and the flushing of ^4He through horizontal fractures. The internal production of ^4He was assumed negligible based on the evidence provided above and the measured production rates (<0.1 $\mu cc/kg_s/yr$) from similar lithologic units in western New York (Hunt and Poreda, pers. commun., 2001).

The model domain was designed to represent the regional groundwater system at the site. The domain length was 5000 m (Figure 2.13), representing the lateral distance between the poorly understood recharge and discharge areas. 20 Mile Creek (1 km south of the site; Figure 2.3) is believed to be a local discharge area with significant underflow and thus is not the downgradient model boundary. The domain height of 20 m represents the average distance from high ^4He concentrations at depth to the lower ^4He concentrations typically found in the Eramosa Member of the Lockport Formation. To calculate a mass balance from a two dimensional groundwater flow and solute transport model, the third dimension was set at 1 unit width.

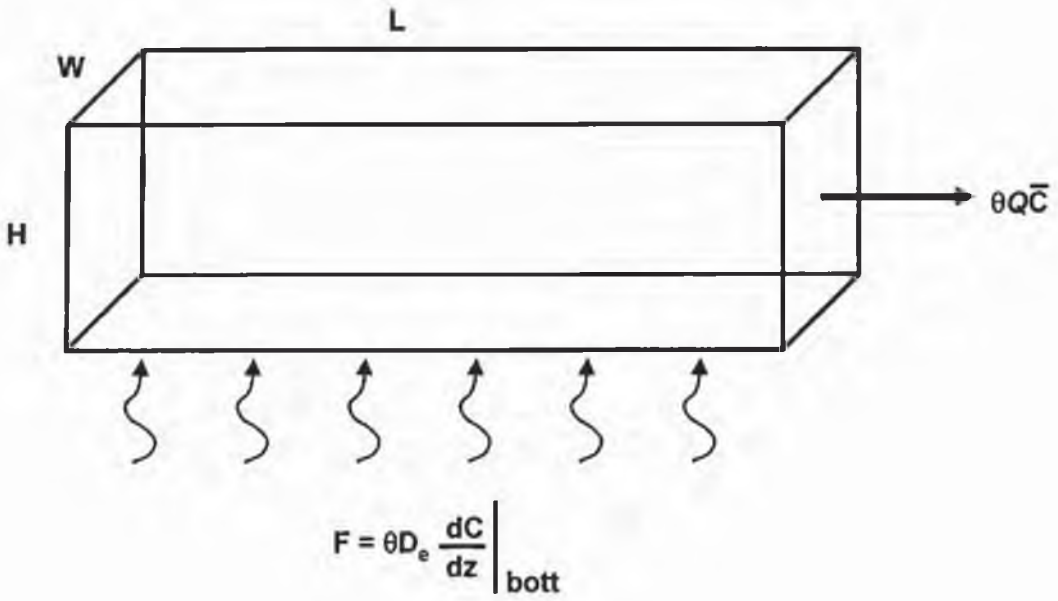

Figure 2.13. Simple ^{4}He mass balance model.

The simple mass balance model can be described as

$$q\theta\bar{C}WH = D_e WL\theta \frac{\partial C}{\partial Z}_{bott} \qquad (2.6)$$

where

q specific discharge [L/T]

θ porosity [L^3/L^3]

$\bar{C}$ average ^{4}He concentration [L^3/M]

D_e effective ^{4}He diffusion coefficient [L^2/T]

$\frac{\partial C}{\partial Z}_{bott}$ ^{4}He gradient at the lower boundary [L^3/M L]

L domain length [L]

H domain height [L]

W domain width [L].

The average groundwater $^4He_{rad}$ concentration ($\bar{C}$) and concentration gradient were determined based on measured data (1000 μcc/kg and 5000 μcc/kg m, respectively). Applying a specific discharge (q) of 1.6 x 10^{-3} m/d (Golder Associates, 1995), the model was solved for the effective ^{4}He diffusion coefficient (D_e).

The specific discharge (1.6 x 10^{-3} m/d) is consistent with a fracture fluid velocity on the order of 10^0 to 10^1 m/day, if all fluid flow is assumed to occur through fractures with a fracture porosity of 200 x 10^{-6} (Novakowski, personal communication, 1998). This velocity range agrees with other estimates made for the Eramosa Member at the site (Golder Associates, 1995; Lapcevic et al., 1996). Both the horizontal flux (q) and fracture velocity necessary to predict observed ^{4}He concentrations are reasonable for this system.

The model results suggest an effective ^{4}He diffusion coefficient of approximately 1.5 x 10^{-7} cm^2/s (4.7 x 10^{-4} m^2/yr) is necessary to predict the observed groundwater He concentrations. This effective diffusion coefficient describes the diffusion of helium from the

Rochester Shale. It is roughly 50 times smaller than the free solution diffusion coefficient of helium in water (D_o = 6.3 x 10^{-5} cm^2/s at 15°C, 5.1 x 10^{-5} cm^2/s at 5°C; Jähne et al., 1987).

With the effective diffusion coefficient determined, the approximation of $D_e \approx \theta^2 D_o$ can be evaluated at this site. Assuming a D_o of (5.1 - 6.3) x 10^{-5} cm^2/s, the matrix porosity of the Rochester Shale would be ~0.05. The actual matrix porosity of the unit is 0.061 (Novakowski et al., 2000). Thus the approximation of $D_e \approx \theta^2 D_o$ is an adequate estimation of the effective diffusion coefficient in the Rochester Shale.

The mass balance box model is a simple method to evaluate the effective ^{4}He diffusion coefficient through the system and the contribution of helium from the underlying Rochester Shale. Although the model is beneficial, it is limited in its ability to describe the observed helium concentration profiles as a function of depth within the Lockport Formation. A more complete numerical model is required to predict the observed helium concentrations.

The occurrence of methane provides an opportunity to evaluate whether diffusion is the primary means of He mass transport from the Rochester Shale. Assuming steady state conditions exist, the diffusive flux of He and CH_4 out of the Rochester Shale must equal the advective flux of these gases through the Lockport Formation (equation 2.6). Thus, the simple mass balance model can be used to determine if the diffusion of He is analogous to that of CH_4. Since the effective diffusion coefficient for methane is not known, free solution diffusion coefficients can be used for both He (Jähne et al., 1987) and CH_4 (Einstein, 1905) for the purpose of this evaluation. Equation 2.6 can then be written for both He and CH_4

$$q\theta\overline{He}\,WH = \theta^2 D_0^{He} WL \left.\frac{\partial He}{\partial Z}\right|_{bott} \qquad q\theta\overline{CH_4}WH = \theta^2 D_0^{CH_4} WL \left.\frac{\partial CH_4}{\partial Z}\right|_{bott} \qquad (2.7, 2.8)$$

where

$\overline{He}$, $\overline{CH_4}$ — average ^{4}He and CH_4 concentrations [L^3/M]

D_0^{He,CH_4} — free solution ^{4}He and CH_4 diffusion coefficients [L^2/T]

$\left.\frac{\partial C}{\partial Z}\right|_{bott}$ ^{4}He or CH_4 gradient at the lower boundary [L^3/M L].

Re-arranging equations 2.7 and 2.8 to solve for q results in the following relationship.

$$\left.\frac{D_0^{He}}{He}\frac{\partial He}{\partial Z}\right|_{bott} = \left.\frac{D_0^{CH_4}}{CH_4}\frac{\partial CH_4}{\partial Z}\right|_{bott} \quad (2.9)$$

The average groundwater ^{4}He and CH_4 concentrations and concentration gradients were determined based on measured data (Table 2.2). The solution to equation 2.9 indicates a general agreement (He: 9.94×10^{-1} m/yr; CH_4: 7.79×10^{-2} m/yr) for the range of He and CH_4 concentrations observed. Thus, diffusion is the primary means of mass transport in the Rochester Shale.

Similar to helium, the mass balance model (equation 2.6) can be used to determine the effective diffusion coefficient of CH_4 in the Rochester Shale. Applying the average groundwater CH_4 concentration and CH_4 concentration gradient (Table 2.2), the resulting effective diffusion coefficient for CH_4 is 3.7×10^{-8} cm^2/s (1.2×10^{-4} m^2/yr) in the Rochester Shale.

2.6.2 Numerical Modeling

Groundwater ^{4}He concentrations were modeled using FRAC3DVS (Therrien and Sudicky, 1996). A simple two dimensional model (3460 m x 44 m) was created to represent the

Table 2.2. Diffusion coefficients and He and CH_4 data within the Lockport Fm. Included are the concentration gradients from the underlying Rochester Shale.

	Helium	Methane	Units
D_o (at 15°C)	1.98×10^{-1}	3.98×10^{-2}	(m^2/yr)
Ave. Conc.	1000	100	(μccSTP/kg_w)
Conc. Gradient	5000	2000	(μccSTP/kg_w/m)

conceptualized cross-section of the site (Figure 2.4). The horizontal scale (3460 m) was defined to represent the distance from the swale located to the north of the site where recharge is most likely occurring, to borehole 61. The vertical dimension was chosen to extend into the Rochester Shale. The domain was discritized to avoid numerical error. Four hydrostratigraphic units were identified based on the hydraulic, isotope, and general chemistry data that outline the site conceptual model (Novakowski et al., 2000; Zanini et al., 2000). All of the units were modeled as horizontal layers of constant thickness, equivalent to their respective average thickness at the site.

The observed groundwater ^{4}He concentrations were simulated using both an equivalent porous media (EPM) model and a discrete fracture (DF) model. The results of hydraulic testing (Zanini et al., 2000) were used to define the transmissivity of each unit. Equivalent horizontal transmissivities were determined for the EPM model, while matrix and fracture transmissivities were used in the DF model (Table 2.3). The number, location, and aperature of bedding-plane fractures were in agreement with the current conceptual model of the site (Novakowski et al., 2000). Measured head values at the three boreholes (60, 53 and 61) were used to constrain the left and right boundary constant-head values (Figure 2.14a,b), creating a dominantly horizontal

Table 2.3. Parameter values applied to the equivalent porous media (EPM) and discrete fracture (DF) models to represent the hydrostratigraphic units at the site.

		EPM	DF	
Hydrostratigraphic Unit: Major Lithologic Component	Thickness (m)	T (m^2/s)	T (m^2/s)	no. of 100 μm fractures
1: Eramosa/Vinemount	16	10^{-5}	10^{-6}	4
2: Goat Island	10	10^{-8}	10^{-8}	0
3: Gasport/Decew	8	10^{-6}	10^{-8}	2
4: Rochester Shale	10	10^{-10}	10^{-10}	0

groundwater flow direction (Figure 2.14c,d). A downward gradient was required along the left boundary in the recharge area. The upper and lower boundaries were assumed to be no-flow.

The diffusion of helium from the underlying Rochester Shale was simulated using a constant ^{4}He concentration along the lower boundary (100,000 μcc/kg; Figure 2.14a,b). This concentration was constrained by the measured ^{4}He concentrations within the Rochester Shale and the measured concentration gradient near the Rochester Shale. A fixed concentration was defined for the upper boundary (48 μcc/kg; Figure 2.14a,b), representing groundwater in equilibrium with the atmosphere. Although the transient models were run towards steady-state solutions, the groundwater system was evaluated after 15,000 years, the time elapsed since the last glacial event in the area. Prior to glaciation and the deposition of the low-permeability surface tills, the groundwater system may have been significantly different from what is observed today.

Both the EPM and DF models successfully simulated the ^{4}He concentrations observed at the site (Figure 2.14e,f). The groundwater head distribution generated with the EPM model indicates a minimal vertical gradient in the vicinity of borehole 60 (Figure 2.14c), while the DF model better represents the observed gradient at this location (Figure 2.14d). The steeper vertical gradient (DF model) resulted in lower ^{4}He concentrations within the uppermost units in the vicinity of the recharge area (Figure 2.14f). In general, the results of the two models were otherwise similar and adequately describe the observed helium concentrations. Both models approached a steady-state solution after 20,000 years.

The agreement between these models suggests that over the time scale of He transport in this system, equilibrium between fracture and matrix water is nearly complete. This is a significant condition in contrast to tracers that have been in the system for less time, because the need to quantify and sample water in discrete fractures is minimized when using He as a tracer in this and similar systems.

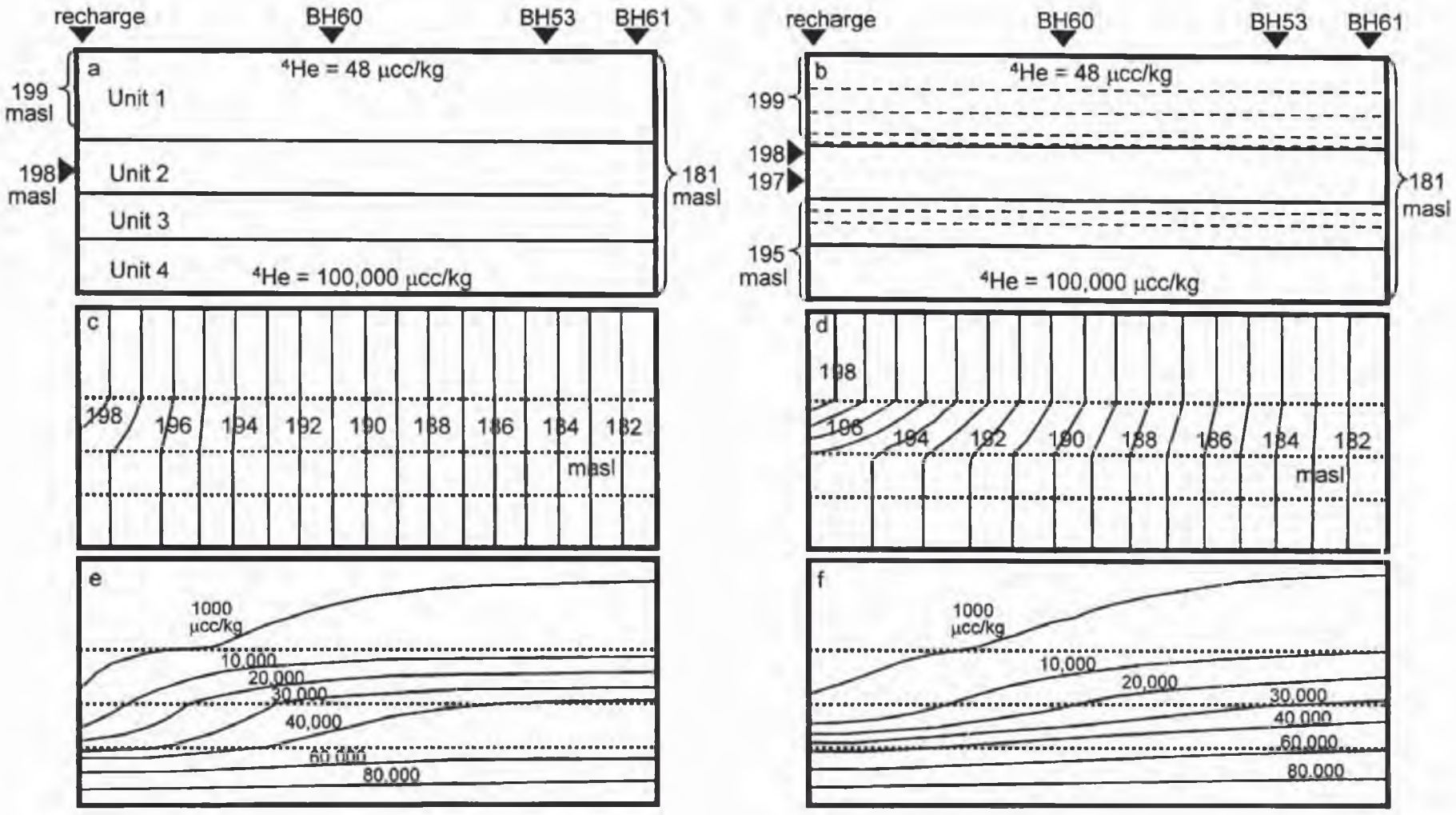

Figure 2.14. Numerical simulations. Numerical model boundary conditions (a, b), modeled hydraulic head distributions (c, d), and ^{4}He concentrations (e, f) as a function of depth using an equivalent porous media (EPM) approach (a, c, e) and a discrete fracture model approach (b, d, f). Fractures are illustrated as dashed lines.

2.7 Crustal Degassing

The groundwater ^{4}He data provide an opportunity to determine the current degassing flux from the Rochester Shale and compare it to the crustal radiogenic helium fluxes in the literature. The ^{4}He flux out of the Rochester Shale was determined according to Fick's 1st law of diffusion:

$$F = -\theta D_e \left.\frac{\partial C}{\partial z}\right|_{z=0} \qquad (2.10)$$

where θ is the porosity, D_e is the effective diffusion coefficient, and $\partial C/\partial Z$ is the ^{4}He gradient at the base of the Lockport. Applying the porosity of the Rochester Shale (0.061) and the effective ^{4}He diffusion coefficient of 4.68 x 10^{-4} m^2/yr (1.48 x 10^{-8} cm^2/s) determined by the mass balance model, the flux of ^{4}He from the Rochester Shale was determined (Appendix E). The ^{4}He gradient at the base of the Lockport (5000 - 7000 μccSTP/kg_w/m_{aq}) was determined using the helium concentration gradients measured in boreholes 65 and 53. The resulting ^{4}He degassing flux is (1.22 - 1.70) x 10^9 atoms/m^2_{aq}/s and is ultimately lost at the discharge point.

The degassing flux determined for the Rochester Shale can be compared to continental degassing fluxes determined for the Great Hungarian Plain (GHP), the Paris Basin, and the Great Artesian Basin (GAB). The flux is multiplied by 30% Earth land surface area to compare it to the crustal degassing fluxes, which range from 0.2 to 9.2 x 10^9 ^{4}He atoms/m^2_e/s (Table 2.4). The corresponding crustal degassing flux determined for the Rochester Shale is (3.7 – 5.1) x 10^7 ^{4}He atoms/m^2_e/s. This flux is two orders of magnitude less than the crustal degassing flux determined for the Earth (O'Nions and Oxburgh, 1983), and comparable to the flux determined for the Saijo Basin (Table 2.4).

The crustal degassing fluxes determined for the large-scale aquifer systems require advective He transport (Torgersen and Clarke, 1985; Torgersen, 1989). A hydrodynamic dispersion coefficient of 2 x 10^{-5} cm^2/s has been used to describe the transport of helium in the upper crust (Torgersen, 1989). This value has been used to calculate the helium degassing flux in several sedimentary basins. It is two orders of magnitude greater than the effective He

Table 2.4. Estimated continental helium fluxes. All crustal fluxes are referred to the entire surface area of the Earth (30% continental).

Site	Crustal Flux $\left(x10^9 \frac{^4He\ atoms}{m_e^2 s}\right)$	Reference
Continents	8.4	O'Nions and Oxburgh, 1983
Auob Sandstone, Namibia	7.8	Torgersen and Ivey, 1985;
Kanto Plain, Japan	2.7 – 3.0	Sano, 1986
Chinasui gas field, Taiwan	5.1 – 7.2	Sano and others, 1986
GAB, Australia	9.3	Torgersen and Clarke, 1987
Continents	8.1	Torgersen, 1989
GHP, Hungary	24	Martel and others, 1989
GHP, Hungary	0.2 – 1.4	Stute and others, 1992
PB, France	1.4	Marty and others, 1993
GHP, Hungary	4.4	Cserepes and Lenkey, 1999
Saijo Basin, Japan	0.09	Takahata and Sano, 2000
Nigashi-Niigata, Japan	2.5	Takahata and Sano, 2000
Smithville, Ontario	0.04 – 0.05	This study

diffusion coefficient determined in this study. Thus, the application of this dispersion coefficient would increase the degassing flux from the Rochester Shale by two orders of magnitude, causing it to be equivalent to the crustal degassing fluxes (Table 2.4).

According to Andrews (1985), the ^{4}He degassing flux is related to the internal helium production rate by

$$F = Gb \tag{2.11}$$

where F is the ^{4}He degassing flux, G is the ^{4}He production rate, and b is the thickness of the unit generating a steady-state loss of helium. Applying the ^{4}He degassing flux determined in this study (1.22 - 1.70 x 10^8 atoms/m^2_{aq}/s) and the internal production rate (0.1 μcc/kg_s/yr) from similar units in western New York (Hunt, 2000), the thickness of the layer producing the observed helium loss was determined to be less than 1 m. Thus, the thickness of the Rochester

shale at the site (17 m) is sufficient to generate the observed ^{4}He degassing flux. Furthermore, under steady-state conditions, the flux of helium can be further defined as

$$F = G2\sqrt{\frac{D_e t}{\pi}} \tag{2.12}$$

where D_e is the effective ^{4}He diffusion coefficient through the shale and t represents time (Andrews, 1985). Assuming a constant internal ^{4}He production rate similar to present conditions, the time elapsed since helium loss began can be estimated by

$$t = \frac{b^2 \pi}{4 D_e}. \tag{2.13}$$

According to this model, the loss of helium began between 420 to 1,076 years ago. Applying a free solution diffusion coefficient or the hydrodynamic dispersion coefficient of 2 x 10^{-5} cm^2/s (Torgersen, 1989) rather than the effective diffusion coefficient determined in this study would result in an apparent onset of ^{4}He degassing less than 10 years ago. The thickness of the Rochester Shale that is contributing to the measured ^{4}He flux and time since helium loss began both suggest that the system has not reached steady-state.

The length of time required to degas the Rochester Shale can be roughly estimated using the degassing flux and the total mass of helium within the Rochester Shale, assuming no internal ^{4}He production and a constant ^{4}He flux comparable to the present flux. The distribution of He within the Rochester Shale has not been determined. Therefore, a dissolved He concentration equivalent to the maximum measured value (~100,000 μccSTP/kg$_w$) was assumed throughout the thickness of the unit (17 m). The resulting conservative estimate of the mass of helium present would be 2.79 x 10^{21} atoms per unit area (m^2). The mass of He divided by the He degassing flux yields an estimate of the length of time required to degas the unit, assuming no significant production of helium within the unit over the duration of time required to degas it. Applying the degassing flux range of (1.22 - 1.70) x 10^8 atoms/m$^2_{aq}$/s, the length of time required to degas the Rochester Shale would be ~520,000 to 725,000 years. Alternatively, the

mass of helium within the Rochester Shale can be estimated by extrapolating the concentration gradient to the base of the unit to determine the helium concentration with depth. Based on this assumption, the helium concentration at the base of the Rochester Shale should be ~185,000 $\mu ccSTP/kg_w$, resulting in a total mass of helium within the unit of 3.98×10^{21} atoms per unit area (m^2). The length of time required to degas the Rochester Shale would therefore be ~740,000 - 1 million years. This is significantly less then the age of the rock unit (~450 million years).

2.8 Discussion

The results of tritium, CFC-12, and ^4He analyses agree with the conceptual model for the site. CFC-12 ages are supported by tritium data, which suggest younger water occurring at depth. Frequently, higher CFC-12 concentrations (younger apparent recharge year) coincide with elevated tritium and hydraulically active flow zones outlined in the site conceptual model (Figure 2.15). Younger water (high CFC-12 concentrations) at shallow depths in boreholes 61 and 65 might reflect the influence of the adjacent 20 Mile Creek and/or local vertical fractures extending to the surface (Figure 2.15). The R/Ra ratios ≥ 1.0 occurring at shallow depths, particularly upgradient, are consistent with the conceptual model of the site (Novakowski et al., 2000; Zanini et al., 2000), which would explain younger water occurring upgradient and within the Eramosa Member.

The presence of young water at depth can be explained by the relatively rapid transport of fresh water through horizontal fractures at depth. Locally, vertical fractures may assist in the transport of fresh water to depth. However, the vertical extent and interconnectivity of these fractures with horizontal fractures are believed to be limited (Golder Associates, 1995; Zanini et al., 2000). Vertical fractures within the recharge area (where the till is thin) may have a significant role in transporting recharge to the conductive zones.

The CFC-12 results of this study have provided an independent and direct method to identify the spatial location and extent of recharge to the fractured hydrologic system. The CFC-12 results suggest that spatially uniform recharge through the till does not occur at this site with the majority of recharge occurring at spatially discrete regions. The primary recharge zone

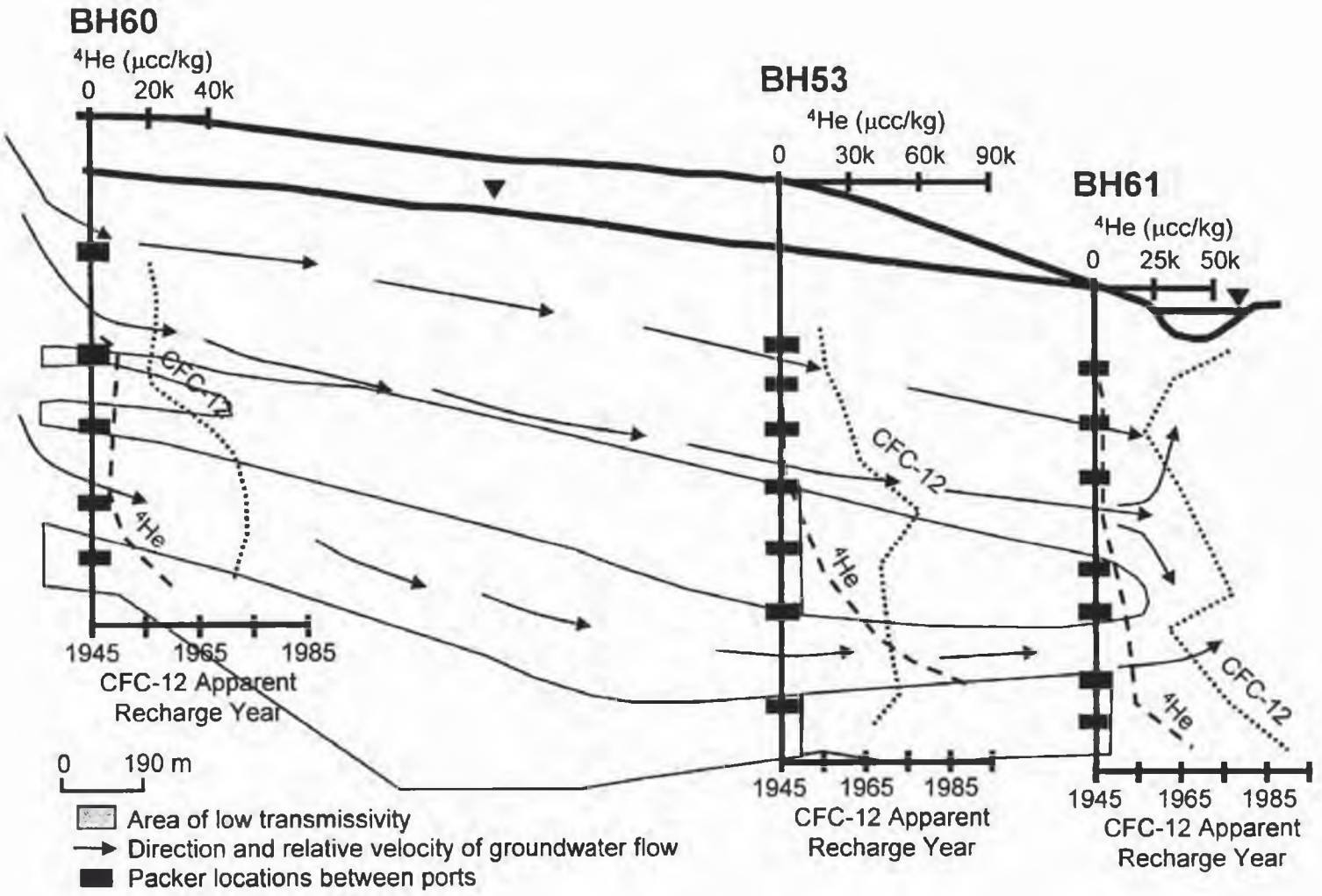

Figure 2.15. Site conpetual model including helium and CFC results. Groundwater ⁴He concentrations are marked With open symbols, CFC-12 apparent recharge years with closed symbols. Squares represent samples collected in 1997, circles in 1998.

probably exists upgradient from well 60, with secondary recharge possible in areas where the till is thin and near the stream through vertical fractures extending to the surface. Identifying capture zones for the site was one of the main original objectives for the combined research of the many investigators working at the site. Identifying the spatial location and extent of recharge is critical to delineating capture zones, particularly in a fractured system in which "old" water is underlain by "young" water. Although the CFC-12 data have indicated the spatial distribution of recharge, no boreholes exist in the discrete recharge area to allow the direct determination of the recharge flux.

Conceptually, the Rochester Shale may act as a cap rock to groundwater containing extremely high ^{4}He concentrations. The high ^{4}He concentrations may be a result of the natural production of methane at depth (Sanford et al., 1985). Methane bubbles, as they migrate, can strip groundwater of its dissolved gases (e.g., ^{4}He). Natural gas pockets below or within the Rochester Shale may thereby act to accumulate ^{4}He. Gas bubbles that manage to migrate upward into the Lockport Formation could have helium concentrations sufficiently high to contribute helium to the lower concentrated groundwater. Since CFCs are not produced in the subsurface, this process would only affect the CFC concentrations within the Lockport Formation (Novakowski et al., 2000) if gas bubbles exist within the Lockport. In this case, the gas bubbles would act to strip CFCs from the surrounding groundwater, resulting in apparently longer groundwater residence times.

The value of the effective ^{4}He diffusion coefficient determined by the mass balance model is appropriate for the geologic media studied. The results of three independent models (mass balance, numerical, and degassing flux) suggest that the effective diffusion coefficient accurately describes helium diffusion in fractured bedrock and can be estimated by $D_e \approx \theta^2 D_o$.

The simple mass balance model is a powerful method to quantify either the effective ^{4}He diffusion coefficient or the bulk groundwater flux through a system. With the diffusion of $^4He_{rad}$ from below, the groundwater $^4He_{rad}$ concentration within the Lockport is a direct result of the effective ^{4}He diffusion coefficient and the bulk groundwater flux (of meteoric water) through the system. A large fluid flux would flush ^{4}He from the system, resulting in a lower $^4He_{rad}$

groundwater concentration. A small bulk fluid flux would result in higher groundwater concentrations. Conceivably, the diffusive flux of helium from the underlying Rochester Shale has been occurring over the last ~15,000 years. If the bulk meteoric groundwater flux were small, the ^4He mass would not be flushed out of the system. The resulting groundwater $^4He_{rad}$ concentration profile would resemble a straight line, ranging from the extremely high concentration at depth to no $^4He_{rad}$ occurring at the water table. Thus, this tracer mass balance is extremely useful to evaluate the bulk fluid flux through groundwater systems if the tracer diffusion coefficient is known or can be accurately calculated. The results of this study suggest that the effective diffusion coefficient can be accurately determined by the relationship $D_e \approx \theta^2 D_o$. The simplicity of this box model, however, does not allow the simulation of the ^4He concentration profiles observed in individual boreholes.

The results of numerical modeling indicate the observed ^4He concentrations can be predicted using measured aquifer parameters and an equivalent porous media approach. The modeling results verify a) a source of ^4He external to the Lockport Formation, and b) groundwater helium concentrations are significantly affected by the flushing of groundwater through high transmissivity units. Thus, helium is a useful tracer of groundwater flux. Although groundwater flow is occurring within bedding-plane fractures, modeling at the spatial scale of fractures over a large time scale (15,000 years) was not necessary.

The assumptions of the numerical model result in slight differences between the modeled and observed helium concentrations. Reasons for potential differences include: a) non-uniform unit thickness; b) fractures modeled as laterally continuous across the model domain; c) horizontal variability in transmissivity; d) location, extent, and interconnection of both horizontal and vertical fractures; e) location and flux of groundwater recharge; and f) temporal variability in groundwater flux and head distribution. Although the models are not exact representations of the complex nature of the fractured system, they adequately serve the modeling purpose.

The numerical models applied in this study are limited in their application to the DNAPL contaminants at the site. The spatial and temporal scales of helium and the DNAPL contaminants are significantly different. Unlike helium, the DNAPL contaminants were recently

introduced to the system (e.g., 20 years versus 15,000 years). Thus, the fracture spatial-scale would be more significant in determining the fate and transport of contaminants over shorter time scales (10^0 to 10^2 years).

The internal ^{4}He production rate and degassing flux suggest that the onset of helium loss from the Rochester Shale does not correspond to the time of emplacement of the unit. It can be assumed that degassing of the Rochester Shale under the present conditions began with the onset of the current groundwater flow system, 15,000 years ago and He within the Rochester Shale may degas for at least another 520,000 to one million years. However, the total mass of He in the Rochester Shale is likely to be greater than estimated, particularly if methane bubbles are present. Thus, the length of time required to degas the unit should be considered a minimum. If the onset of helium loss began at the time of emplacement, however, the unit should have reached a steady-state flux equivalent to the mass transfer of helium resulting from in situ U/Th production. The model assumptions of a steady-state flux and steady-state internal production throughout the thickness of the unit are not valid at the site.

The onset of helium loss and remaining time required to degas the Rochester Shale have important implications for the understanding of crustal degassing. The results suggest that prior to deglaciation, helium produced by U/Th decay was primarily stored within grains of the Rochester Shale until the removal of overlying bedrock increased the porosity of the unit by expansion. The increase in porosity facilitated degassing of the unit by the mass transfer of helium into groundwater. Thus, unlike crustal degassing models that assume the transport (degassing) of helium through the entire thickness of the crust, the results of this study indicate that only the uppermost rock units are likely to be degassing and storage of helium occurs in deeper units.

2.9 Conclusion

The CFC-12 results indicate that groundwater at the site is datable using CFC-12 and strongly suggest recharge is occurring in spatially discrete locations. Groundwater ages ranged from roughly 8 to over 40 years, with older water occurring at shallower depths than younger water. The CFC-12 profiles strongly suggest, and point to, spatially discrete recharge areas,

most likely where the till is thin (possibly at the swale north of the site), and locally where vertical fractures are interconnected with horizontal fractures at depth.

The results of three independent models (mass balance, numerical, and degassing flux) substantiate the importance of applying an effective diffusion coefficient to describe the diffusive transport of dissolved gases in geologic media. Furthermore, the effective diffusion coefficient can be accurately estimated by the relationship $D_e \approx \theta^2 D_o$ in fractured bedrock.

Large amounts of $^4He_{rad}$ are entering the groundwater system from below, providing a powerful tracer of the effective ^4He diffusion coefficient through the system. With a diffusive mass flux from below, the groundwater ^4He concentration is a direct function of the effective ^4He diffusion coefficient and the flux of meteoric water through the system. Thus, the ^4He mass balance is an extremely useful method of evaluating either the bulk fluid flux through groundwater systems or the effective diffusion coefficient, if one or the other is known. With the ability to accurately estimate the effective diffusion coefficient, the mass balance model provides a relatively inexpensive alternative to conventional methods of estimating bulk fluid flux.

The results of the ^4He degassing model suggest indicate that the Rochester Shale is sufficiently thick to generate the observed ^4He flux. This flux is roughly 10^{-2} times less then the crustal degassing flux. A minimum of an additional 520,000 years time is required to degas the Rochester Shale.

CHAPTER 3

EVALUATION OF IN SITU DIFFUSION SAMPLERS FOR MEASUREMENTS OF DISSOLVED NOBLE GASES IN GROUNDWATER

3.1 Abstract

A new passive diffusion sampler is evaluated for the purpose of measuring dissolved noble gases in groundwater. The samplers consist of 3/16 inch (OD) copper refrigeration tubing, 3/16 inch (OD) silicon tubing, and 3/16 inch brass rod. The size of the samplers and minimal sampling equipment required minimizes the bulk typical of sampling equipment and makes them easily transportable. In addition, their size allows sampling of small diameter wells (1 cm). The results of field and laboratory experiments indicate that the samplers equilibrate in approximately 8 hours when placed in advection-dominated systems, and within 2 weeks in a controlled diffusion-dominated system. They can be deployed in low permeability zones which otherwise cannot be sampled because purging is minimized. Additional experiments indicate no measurable loss of gas occurs if the samplers are sealed within 2 - 5 minutes after being removed from a well, depending on the total dissolved gas pressure in the groundwater. Samples analyzed after 13 months in storage indicate no loss or contamination of gases compared to samples analyzed immediately after being obtained. Dissolved gas concentrations can be calculated when a total dissolved gas probe measurement is obtained, or modeled by simulating measured gas mole fractions determined by mass spectrometry. The samplers allow for high quality samples with minimal effort, time, and expense and can be readily deployed by untrained personnel. Furthermore, the samplers eliminate the issues of sample loss and contamination common to other methods of obtaining dissolved noble gas samples.

3.2 Introduction

Numerous sampling devices have been introduced within the last 20 years to simplify groundwater sampling efforts for solutes, volatile organic compounds (VOCs) and dissolved gases. Generally, traditional sampling methods require purging multiple well volumes followed by the collection of representative groundwater samples. In the case of VOCs and dissolved gases, the collection of representative groundwater samples is complicated by atmospheric contamination and the loss of sample due to low gas solubilities. This paper will focus on a new method of sampling for dissolved gases that eliminates many of the requirements and complications inherent to other sampling methods.

Generally, dissolved gas sampling methods can be categorized as extraction and/or re-equilibration techniques (Capasso and Inguaggiato, 1998). Extraction techniques require the collection of a groundwater sample from which dissolved gases are later extracted. Common extraction sampling methods include reservoir samplers or bailers (Johnson et al., 1987; Solomon, 1992; Sherwood Lollar et al., 1994), gas-tight syringes (Rudd and Hamilton, 1975; Sugisaki and Taki, 1987), and vacuum flasks (Carter et al., 1959; Heaton and Vogel, 1981). Re-equilibration techniques involve the equilibration of dissolved gases with a host, typically a gas. In some cases, a combination of techniques are used. Rudd and Hamilton (1975) collected dissolved gas samples by the equilibration of lake water with water inside tygon tubing. The re-equilibrated host water was then extracted into air-tight syringes. Most recently, Capasso and Inguaggiato (1998) described a method combining the use of water collection in vacuum flasks followed by the re-equilibration with a host gas in the laboratory.

Recent years have seen the introduction of numerous passive in situ re-equilibration sampling methods. Ping-pong balls and gas-filled latex tubing have been used to sample dissolved gases, particularly helium, in lake water and sediment (Dyck and Da Silva, 1981; Gascoyne and Sheppard, 1993; Stephenson et al., 1994). Sanford and others (1996) introduced a sampler constructed of an automotive tire stem and a removable shrader valve, and copper and latex tubing to sample helium and neon concentrations in groundwater. Dialysis tubing and

sorbent materials have been used for sampling VOCs and solutes (Karp, 1993; Harper et al., 1997).

The dissolved gas sampling methods listed above range in simplicity and elegance, even including a motorized down-hole bailer (Sherwood Lollar et al., 1994). There are benefits and draw-backs for each method. While some methods are rather simple to perform, others involve cumbersome field equipment, time, expense, and training. Some methods require the immediate (within 48 hours) analysis of samples (i.e., ping-pong balls, latex tubing, shrader-valve samplers), which may require establishing a portable field laboratory. Other methods involve multiple stages: water collection followed by dissolved gas extraction in the laboratory (i.e., bailers). If sampled correctly, most methods produce high-quality samples. Generally, however, the reproducibility, storage capacity, and sample size vary according to the method chosen. The purpose of this paper is to introduce a new sampler designed to provide high quality samples with minimal effort, time, and expense.

3.3 Sampler Criteria

Since there are existing methods of producing viable dissolved gas samples, new sampler designs need to address some of the current limitations and/or complexities of obtaining dissolved gas samples. Some of the criteria that a new dissolved gas sampler must meet to be considered for wide spread application include the following.

- The samplers should be simple and inexpensive to make and deploy.
- The samplers should be nontechnical such that untrained personnel can utilize them without risk of sample contamination or loss.
- The sampling method should be designed to reduce, if not eliminate, any loss of dissolved gases during collection.
- The sampling method should be designed to reduce, if not eliminate, trapped air bubbles or entrained evolved gas bubbles problematic to reservoir samples.
- The sampling method should be applicable to a variety of well types and surface water bodies.

- Down-hole samplers should be designed to fit within the screened interval, regardless of depth.
- If the method involves host-gas equilibration, the sampler should require minimal time to reach equilibration.
- The sampling method should minimize well purging.
- The samplers should prevent any sample degradation during transport and storage.
- The sampling method should permit samples to be stored for long periods of time.
- The sampling method should provide reproducible, high-quality dissolved gas samples.
- The sampling method should provide a dissolved gas sample in one simple process thereby eliminating the laboratory gas extraction step required of water samples.
- The sampling method should eliminate any possible cross-contamination.

It is important to recognize the increasing frequency of small diameter wells/peizometers being installed and used for groundwater studies. In keeping with this trend, new sampling methods are beneficial if they are applicable to these as well as larger wells, and surface water bodies.

The dissolved gas sampler introduced in this paper was designed for the collection of reproducible dissolved gas samples for noble gas isotope analysis. The sampler design is a modification of the sampler design of Sanford and others (1996). Unlike their sampler, this sampler can withstand a longer duration for storage and is suitable for noble gas analysis by mass spectrometry. This paper will present the sampler and critique its ability to meet the listed criteria.

3.4 Sampler Design and Use

A passive, in situ diffusion sampler has been designed to minimize purging, fit down small diameter wells (1 cm), and produce high-quality reproducible dissolved gas samples. The samplers consist of a headspace volume and a thin-walled semipermeable membrane. The semi-permeable membrane allows gases to diffuse through it, thereby allowing the headspace to equilibrate with dissolved gases in the surrounding water. The samplers are simple and inexpensive to construct and use. In fact, the samplers can be made from materials common to

many laboratories. Samplers constructed of Si-tubing can be used to collect any gas capable of diffusing through silicone. These gases include Ar, CH_4, H_2, He, Kr, N_2, Ne, O_2, and SF_6.

The sampler consists of 3/16 inch (OD) copper refrigeration tubing, 3/16 inch (OD) silicon tubing, and 3/16 inch brass rod (Figure 3.1). The copper tubing is initially annealed at 600°F in an Ar atmosphere. The copper tubing is cold-welded at one end to form a leak-tight seal (Figure 3.1). Over the open end is placed a length of thin-walled (1/32 inch) Si-tubing plugged at its distal end. Although brass rod was used, the plug can be constructed of other materials. A hole drilled through the plug allows the samplers to hang in wells/peizometers by string, fishing line, or cable (Figure 3.1). Copper wire inserted in the Si tubing reduces the internal volume and decreases the time required for equilibration.

The Cu wire insert also provides structural support to the membrane. This support prevents the membrane from collapsing under hydrostatic pressure. Even under pressure, the void space within the membrane remains a conduit for gas diffusion. Other materials, such as sand or glass beads and wool, may be used. However, strands of wool used to keep the glass beads within the membrane may interfere with crimping causing the samplers to leak. In addition, a strand of wool within the sampler may become problematic for valve seals if introduced to a mass spectrometry clean-up line.

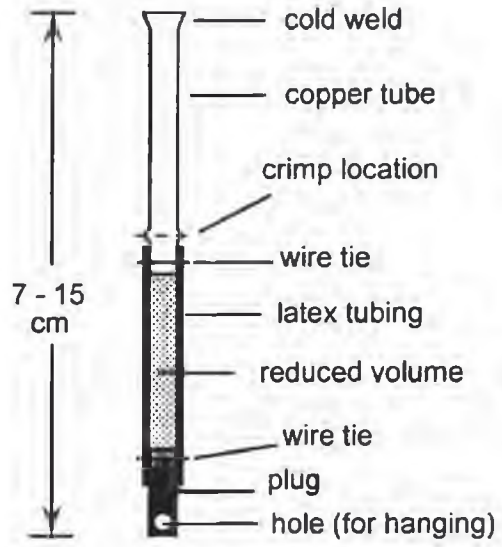

Figure 3.1. In-situ dissolved-gas headspace sampler.

The sampler can be constructed of 1/4 inch or 3/16 inch tubing of varying lengths to provide a particular volume of gas. The 3/16 inch tubing provides the small gas volume necessary for analysis by mass spectrometry in a sampler of reasonable dimensions. A 2 inch (5 cm) length of 3/16 inch Cu tubing, crimped at one end, will provide roughly 0.3 cm^3 of gas after sealing. The length of the membrane (Si-tubing) and total internal volume significantly affect the duration of time required to obtain equilibration. The length of the membrane can be optimized using the equilibration model of Sanford and others (1996).

Under conditions in which the pressure within the sampler (P_s) may be significantly greater than the atmospheric pressure (P_{atm}), the Si membrane may require reinforcement onto the Cu tube and plug. In a recent study, the expansion of gas within the membrane due to $P_s > P_{atm}$ caused the membrane unit to pop off the samplers during crimping. The in situ total dissolved gas pressure measured ranged up to 1.61 atmospheres in the wells which resulted in explosive samplers. To prevent the potential loss of sample, wire ties were used to secure the tubing in place (Figure 3.1). O-ring gaskets can also be used. The wire ties or o-ring gaskets are placed over the Si membrane in a groove rounded into the Cu tube sampler. A simple rounding wheel on a pipe cutter can be used to form the groove.

After equilibration, the samplers are pulled from the wells and the open end of the copper tubing is immediately sealed (Figure 3.1). Sealing of the Cu tube is accomplished by crimping with a cold-weld tool. The Si-tubing can then either be disposed of or re-used. The gas sample, ready for analysis, is contained within the small disposable Cu tube chamber. The cold-welded ends of the sampler can be protected from dents during transport by wrapping them in black tape or sliding plastic caps or small pieces of flexible tubing over them. A cracking device installed on the inlet port of a mass spectrometer clean-up line allows the gas to be directly introduced to the system for analysis (Figure 3.2).

3.5 Sampler Equilibration

Analytical models exist to determine the duration of time required to achieve equilibration of diffusion samplers with dissolved gases in water. Sanford and others (1996) provide an analytical solution to determine the equilibration time of He and Ne for samplers

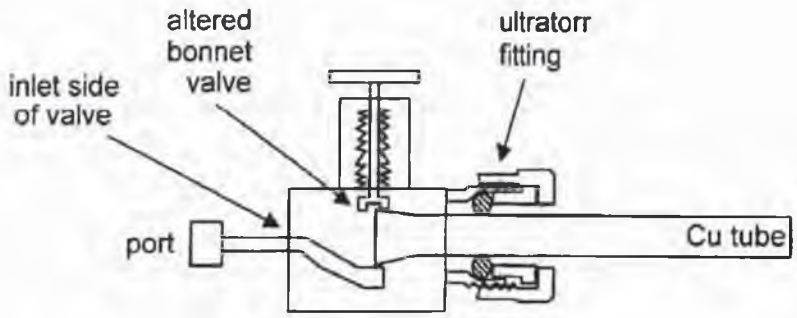

Figure 3.2. Cracking device. The device is installed on the inlet port of a mass spectrometer clean-up line.

placed in a well-mixed solution having a constant dissolved gas concentration. Harrington and others (2000) modeled the equilibration time for diffusion samplers placed in diffusion-dominated groundwater systems. The models assume samplers are placed either in open boreholes or within adequately screened intervals. Both models are theoretically based and in the case of Sanford and others (1996), laboratory tested.

The equilibration time determined by either the Sanford or Harrington methods (Sanford et al., 1996; Harrington et al., 2000) should be considered an estimate of the actual length of time required to obtain equilibrium. Neither solution was verified by field-based calibrations. Natural variability in most groundwater systems and poorly defined effective gas diffusion coefficients would indicate that the actual equilibration time might fall somewhere between the two models, depending on the nature of the system.

The equilibration model proposed by Sanford and others (1996) is suitable for wells screened in highly transmissive zones in which advection provides a constant source concentration in the groundwater surrounding the sampler. The effective gas diffusion coefficient within the membrane, membrane thickness, sampler volume, and membrane surface area exposed to solution become the limiting factors determining the equilibration time required. The membrane thickness and surface area can be measured and the internal volume estimated. Values of the required effective diffusion coefficients, however, have not been experimentally determined for all dissolved gases (i.e. Kr). Thus, the equilibration time determined should be

considered a minimum length of time required to obtain equilibrium of all gases present but may be suitable for the more abundant gases with known membrane diffusion coefficients (Table 3.1).

Although the model of Harrington and others (2000) provides an estimate of the equilibration time in zero advection (i.e., strictly diffusion-dominated) systems, the modeled equilibration time might be an under-estimation. The model assumes that samplers can be installed within the screened interval. This is not always possible due to the small diameter of many new wells/peizometers. Since the length over which diffusion must occur significantly influences the equilibration time in diffusion-dominated systems, samplers not installed within the well screen will require longer equilibration times. The effectiveness of the semi-permeable membrane may decrease through time and use. Particles such as sediment or precipitates and microbial films adhered to the membrane might reduce the membrane surface area and/or decrease its permeability. The result of either case is an increase in the equilibration time required. Thus, in strictly diffusion-dominated systems the model of Harrington and others (2000) should be considered a first approximation of the equilibration time.

The equilibration of a sampler installed in a diffusion-dominated system can be hastened by removing some of the well volume, thereby inducing at least some groundwater flow into the well casing and past the sampler. Unlike advection-dominated systems, estimating the equilibration time must incorporate the well recovery rate. In such a case, the equilibration time can be estimated using a "cell" model (Appendix A). The model assumes that the gas within the sampler exchanges with the dissolved gases in the "cell" of water immediately surrounding the sampler membrane (Figure 3.3). As the water level in the well slowly recovers from pumping, additional cells of water exchange with the sampler headspace volume. Final equilibration occurs when the headspace gas has a concentration that differs from the dissolved gas concentration by the Henry's Law constants for each gas at the in situ temperature.

3.6 Determining Dissolved Gas Concentrations

Dissolved gas concentrations can be determined by two methods when in situ diffusion samplers are used. According to Henry's Law, the solubility of a particular gas within the sampler

Table 3.1. Gas diffusion coefficients through sillicone tubing.

	O_2	CO_2	N_2	^4He	Ne	units
Silastic* (Galletti et al., 1966)	2.02×10^{-3}	1.05×10^{-2}	1.00×10^{-3}	1.22×10^{-3}		$cm^3STP/s/cm^2/atm/mm$ thickness
silicone (Sanford et al., 1996)				4×10^{-7}	4×10^{-7}	cm2/s

* Silastic is a registered trademark of Dow Corning Corporation.

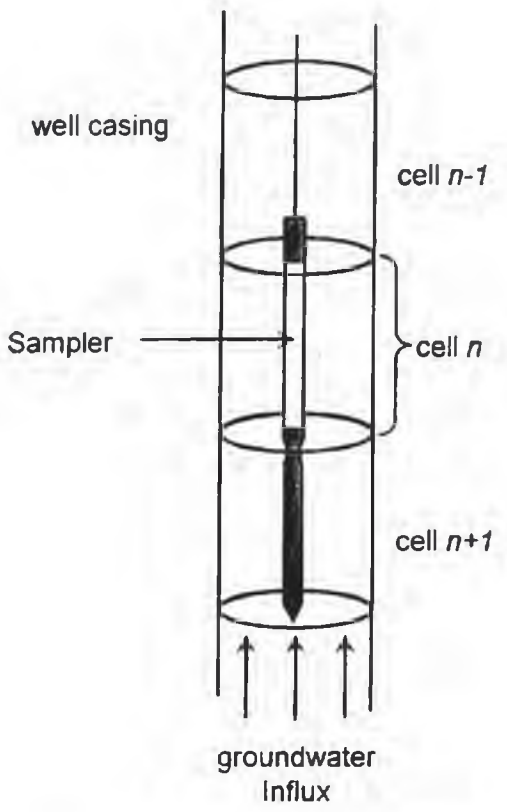

Figure 3.3. Sampler equilibration model. Gas within the sampler equilibrates with the dissolved gas within the surrounding "cell" of water. The sampler volume progressively approaches final equilibration through a step-wise process involving subsequent cells of groundwater.

volume is given by

$$p_i = k_i X_i \quad (3.1)$$

where p_i is the gas partial pressure, X_i is the mole fraction of dissolved species *i*, and k_i is the Henry's Law constant that describes the gas partitioning between the aqueous and gas phases at a given temperature and pressure. The Henry's coefficient can be readily determined using the empirical data of Benson and Krause (1976) and Wilson (1986). Andrews (1992) and Solomon and others (1998) report these data and the relationship to determine the dissolved gas solubility concentrations.

In order to determine the dissolved gas concentration, or partial pressure, the gas phase concentration must first be determined. Rare-gas instruments can readily determine the mole fractions of dried gas. The calculation of the gas phase concentration must include the water vapor phase present at the in-situ temperature and the total dissolved gas pressure. Partial pressures can therefore be determined by

$$p_i = x_i (P_t - p_{H2O}) \quad (3.2)$$

where x_i is the dry gas mole fraction of gas species *i* (measured), P_t is the total dissolved gas pressure, and p_{H2O} is the water vapor pressure. This relationship is similar to that of Warner and Weiss (1985) that describes the partial pressure of gas in air. The vapor pressure can be calculated by

$$\ln(p_{H2O}) = 24.4543-67.4509(100/T)-4.8489\ln(T/100)-0.000544S \quad (3.3)$$

where S is the water salinity (Weiss and Price, 1980).

The total dissolved gas pressure, however, is not necessarily equal to the gas pressure within the sampler after it has been removed. The in situ pressure may not be maintained during sample collection for several reasons. If the membrane is flexible, the total volume of the sampler will change as it is removed from a well. For example, if a sampler is located 10 m below the water surface in a well, the hydrostatic pressure outside the sampler will be about 1

atm greater than the atmospheric pressure at the site. If the water is saturated with gas at atmospheric pressure (which is commonly the case), then the pressure inside the sampler will be the same as the atmosphere. As the sampler is removed from the well, the pressure outside of the membrane will decline to the atmospheric value. As a result, the volume of the flexible sampler will increase and this in turn will cause the pressure inside the sampler to decline. Also, the change in volume caused by crimping the sampler causes a slight increase in the gas pressure within the sampler. Thus, the in-situ partial pressures of dissolved gases cannot be directly determined through gas analyses of diffusion samplers without a measurement of the total dissolved gas pressure. However, ballooning of the silicone membrane does not result in the fractionation of gases (Poreda, pers. commun.,1999), and thus the measured gas mole fractions are representative of the gas proportions in-situ.

In situ dissolved gas pressure measurements can be obtained in groundwater wells using a probe (Manning et al., 2000). The probe consists of a pressure-transducer with a semi-permeable membrane attachment (Figure 3.4). The attachment provides a minimal internal volume and maximum semipermeable surface area for rapid equilibration of dissolved gases (roughly 10 minutes). This probe is similar to models designed for surface water applications (D'Aoust and Clark, 1980; Anderson and Johnson, 1992; Carignan, 1998; Watten et al., 1997), but with a significantly smaller diameter for groundwater applications.

Although the total dissolved gas pressure can be measured directly (Manning et al., 2000), a direct measurement may not be possible in all field cases. The probe's diameter (1.9 inches) prohibits its use in small diameter wells. Also, probes for use in wells are relatively new and, therefore, may not be available in all cases.

An alternative method to determining dissolved gas concentrations exists since the composition of the gas within the sampler is a function of the recharge temperature, pressure (recharge elevation), and excess air (Figure 3.5). If a suite of gases is analyzed, an over-determined system of equations can be solved to arrive at the in situ partial pressures of each gas. The model must include the recharge temperature and pressure to generate groundwater with solubility concentrations of atmospheric gases (Andrews, 1992; Solomon et al., 1998). The

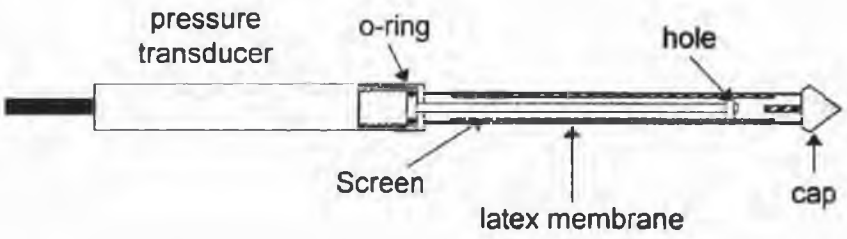

Figure 3.4. Total dissolved-gas pressure probe. The internal volume of the probe equilibrates with dissolved gases in groundwater through a semipermeable membrane. A hole connects the internal volume to the external surface. The external surface of the probe attachment is covered with a screen to increase the surface area over which exchange occurs. Thin-walled latex tubing placed over the screen provides the semipermeable membrane.

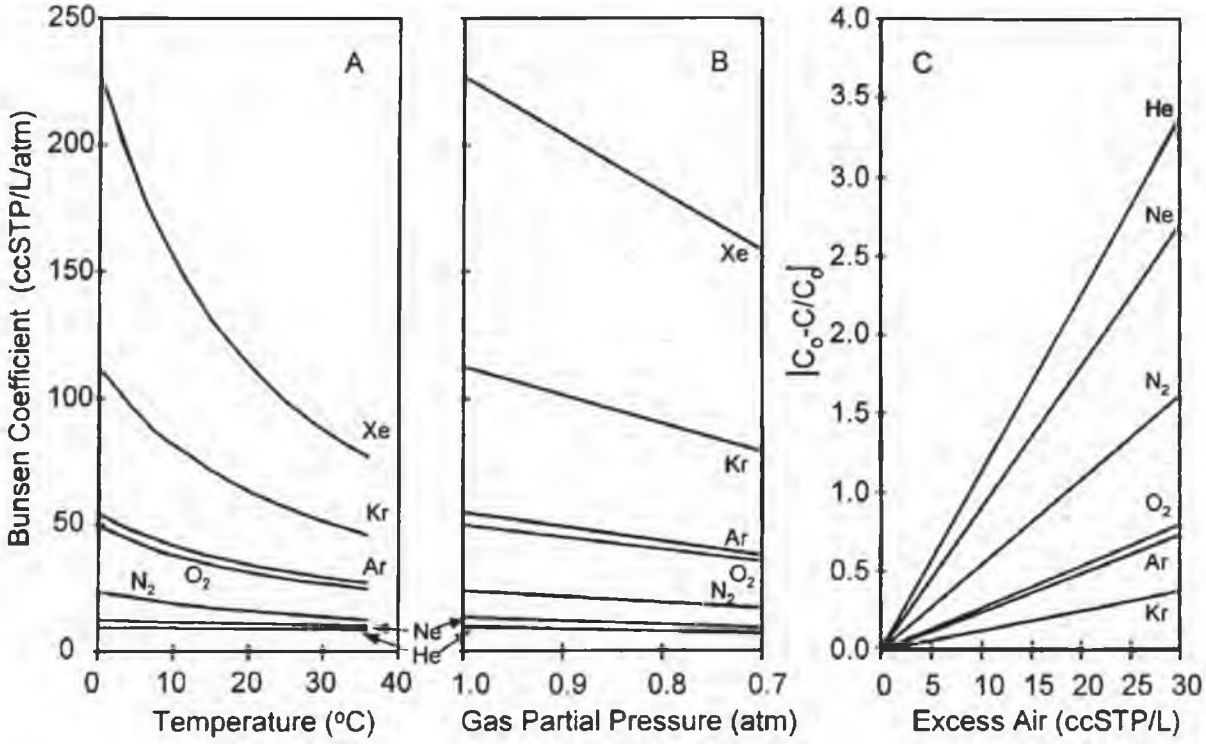

Figure 3.5. Solubility of dissolved gases. Variables include a.) recharge temperature, b.) pressure (0°C), and c.) excess air. The Bunsen Coefficient is the gas solubility when the gas partial pressure is 1 atm. C_o is considered at 10°C and 0 cm^3/kg_{water} excess air.

model should also allow for the possibility of excess air caused by the inclusion of trapped air bubbles near the water table. Excess air can be modeled by forcing into solution a given volume of air. Since oxygen is frequently consumed in the unsaturated zone, the consumption of oxygen should also be included. When dissolved oxygen measurements can be obtained, the model can incorporate the measured concentrations. The production and consumption of other gases, such as CO_2 and CH_4, may need to be considered if they are major components of the gas composition. Finally, the in situ groundwater temperature must be included to convert dissolved concentrations to gas partial pressures. Water vapor can be ignored since the dry-gas mole fractions are desired. The dry-gas mole fractions (x_i) can then be determined by

$$x_i = p_i / P_t \tag{3.4}$$

where the total dissolved gas pressure (P_t) is the sum of the gas partial pressures (p_i). The modeled dry-gas mole fractions are compared to measured values until agreement is obtained.

Although there may be several variables in the model (recharge temperature and pressure, excess air, oxygen consumption, other gas production), the model can be solved using optimization methods that, for example, minimize the sum of residuals squared. The above procedure is similar to that described by Hall and Ballentine (1996) and Ballentine and Hall (1999), except that dry mole fractions are used instead of dissolved concentrations. In other words, conventional approaches (Ballentine and Hall, 1999) employ a suite of dissolved gas concentrations to estimate the recharge temperature, recharge pressure, and excess air by making use of the fact that dissolved concentrations for a suite of gases have a unique response to the unknown values. Like dissolved concentrations, the dry mole fractions of gases inside a diffusion sampler are also unique functions of the recharge temperature, recharge pressure, and excess air. However, the sensitivity of dry mole fractions to recharge temperature, pressure, and excess air is substantially less than the sensitivity of dissolved gas concentrations to the same parameters. For example, the dissolved concentration of Kr at 0°C is approximately 36% greater than at 10°C. However, the mole fraction of Kr at 0°C is only 7% different than at 10°C. In contrast, if the total dissolved gas pressure is measured, the dissolved concentrations

can be computed directly and these results can be used in existing models to estimate recharge temperature, pressure, and excess air. When the total dissolved gas pressure is used, the sensitivity to recharge temperature, pressure and excess air is the same as if dissolved gas concentrations were measured directly.

3.7 Sampler Testing: Field and Lab

The samplers have been field tested to determine the duration of time required for equilibration of numerous dissolved gases. In addition, the samplers have been field and laboratory tested to determine the length of time during which the samplers must be sealed after removal from water before a significant loss of gas occurs ("sealing window"). The sample storage time has also been investigated. The dissolved gases N_2, Ar, O_2, He, Ne and Kr have been evaluated.

The samplers used in each of the following tests were designed to equilibrate within ~7 hours according to the equilibration model of Sanford and others (1996). The samplers had the following dimensions. The Cu tube measured 2 inches (5 cm) from crimped end to open end. The Si-tubing measured 6 inches (15 cm). It separated two Cu-tube samplers rather then a sampler and plug. These doubled samplers were used in all cases to provide sample replicates. Since samplers having a shorter length of membrane (~5 cm) are more commonly used, a set of smaller samplers was applied in a field equilibration test to provide a comparison.

3.7.1 Equilibration Tests

Three tests were performed to evaluate the time required to obtain equilibrium between the sampler volume and dissolved gases in groundwater. The first and most rigorous test was performed in a shallow unconfined aquifer well located in the Salt Lake Valley, northern Utah. The well was chosen for its depth and dissolved gas composition. The shallow well depth allowed the samplers to be removed from the well rapidly. Water samples collected indicate that the dissolved gas composition is different from that of air, which was the initial composition of the samplers. The second test was performed in well-mixed lab-air equilibrated water at the University of Utah. Samplers were first filled with nitrogen before being placed in the water in

order to evaluate the equilibration time of all gases, particularly Ar and Kr. The third test was performed in a stagnant column of de-oxygenated lab-air equilibrated water to evaluate the equilibration time by diffusion alone.

The field-based test consisted of hanging multiple samplers in a shallow well and removing the samplers after different lengths of time had elapsed. The well has a total depth of 11 m and is screened from 7.8 to 10.8 m in gravel. The water level was 6.19 m below land surface. During the first 12 hours of the test, water was pumped from just below the water level at a rate of 200 cm^3/min. The total dissolved gas pressure, water temperature, and dissolved oxygen content were independently measured using probes (Table 3.2). Water samples were also obtained using copper tubing for comparison.

The results of the field-based equilibration test indicate that the sampler required a minimum of 8 hours to reach equilibration for all gases present (Table 3.2). An immediate decrease in the oxygen and argon content and increase in dissolved nitrogen were observed. Oxygen and nitrogen equilibrated within ~6 hours with Ar requiring slightly more time (~8 hours, Figure 3.6). The ^3He to ^4He ratio of the gas sample (R_g) compared to the helium isotope ratio in air (R_a) indicates that helium also required roughly 8 hours to reach equilibrium (Figure 3.6; Table 3.1). An equilibration time could not be determined for Ne and Kr because their initial concentrations within the air-filled sampler and final equilibrium partial pressures were similar. Nearly all variations in the Ne and Kr data fell within the analytical error.

Some variability in the equilibrium dissolved-gas concentrations (after 8 hours) is possible due to the potential spatial and temporal variability of the groundwater composition. The samplers were hung at different depths in the well on one length of string. It is conceivable that spatial variability in the groundwater composition is possible along the screen length. Temporal changes (i.e. resulting from storm events) are even more likely. Considering only those samplers that had reached equilibrium, the average deviation from the mean for each gas concentration measured agrees with the analytical error, with few exceptions (O_2). Therefore, no conclusions can be drawn regarding spatial variability or temporal fluctuations with the data given.

Table 3.2 Sampler *Equilibration Time* field test results. Gas concentrations are in units of ccSTP/kgwater. The atmospheric pressure was 0.847 atm. The total dissolved gas pressure was 1.062 atm. The groundwater temperature was 12.9°C and the dissolved oxygen content was 1.49 ppm.

Time (hrs)	XN2	N2	XO2	O2	XAr	Ar	XKr ($\times 10^{-7}$)	Kr ($\times 10^{-5}$)	XNe ($\times 10^{-5}$)	Ne ($\times 10^{-5}$)	X4He ($\times 10^{-6}$)	4He ($\times 10^{-5}$)	Rg/Ra	R/Ra
15 cm														
2	0.883	16.43	0.104	3.89	0.0091	0.37	10.8	8.48	1.80	20.9	5.51	5.18	1.81	
4	0.911	17.10	0.076	2.56	0.0089	0.37	10.9	9.20	1.77	21.5	5.41	5.21	2.16	
4	0.919	16.96	0.068	2.84	0.0090	0.37	11.7	8.57	1.85	20.6	5.54	5.09	2.13	
6	0.953	17.73	0.034	1.28	0.0087	0.36	10.8	8.46	1.78	20.6	5.36	5.04	2.46	
8	0.963	17.88	0.025	1.01	0.0085	0.37	10.6	8.13	1.76	20.7	5.43	5.27	2.70	
8	0.961	17.91	0.027	0.94	0.0090	0.35	10.4	9.36	1.79	20.4	5.60	5.11	2.53	
10	0.943	17.54	0.043	1.59	0.0084	0.35	9.1	7.16	1.75	20.4	5.44	5.11	2.72	
12	0.962	17.89	0.027	1.00	0.0085	0.35	9.1	7.11	1.78	20.7	5.46	5.14	2.67	
14	0.954	17.74	0.033	1.25	0.0086	0.35	9.4	7.39	1.76	20.5	5.59	5.25	2.70	
16	0.951	18.06	0.037	0.64	0.0085	0.34	9.3	7.68	1.76	20.6	5.46	5.12	2.66	
16	0.971	17.69	0.017	1.37	0.0083	0.35	9.8	7.28	1.77	20.5	5.45	5.14	2.78	
20	0.959	17.39	0.028	2.00	0.0084	0.34	10.1	7.29	1.79	20.4	5.41	5.06	2.74	
20	0.935	17.84	0.053	1.06	0.0083	0.34	9.3	7.94	1.76	20.8	5.39	5.09	2.47	
24	0.966	17.79	0.022	1.23	0.0085	0.36	10.2	7.66	1.79	23.6	5.44	5.09	2.68	
24	0.956	17.97	0.033	0.83	0.0088	0.35	9.8	8.02	2.03	20.8	5.41	5.12	2.62	
28	0.947	17.84	0.041	1.14	0.0084	0.36	11.1	7.03	1.81	20.7	5.39	5.07	2.61	
28	0.959	17.61	0.030	1.54	0.0087	0.34	9.0	8.69	1.79	21.0	5.39	5.04	2.65	
32	0.976	18.15	0.013	0.47	0.0082	0.33	11.4	8.94	1.87	21.7	5.54	5.21	2.87	

Table 3.2 Continued.

Time (hrs)	XN2	N2	XO2	O2	XAr	Ar	XKr ($\times 10^{-7}$)	Kr ($\times 10^{-5}$)	XNe ($\times 10^{-5}$)	Ne ($\times 10^{-5}$)	X4He ($\times 10^{-6}$)	4He ($\times 10^{-5}$)	Rg/Ra	R/Ra
10 cm														
3.8	0.919	17.10	0.068	2.56	0.0090	0.37	11.7	9.20	1.85	21.5	5.54	5.21	2.13	
16.0	0.971	18.06	0.017	0.64	0.0083	0.34	9.8	7.68	1.78	20.6	5.45	5.12	2.78	
20.0	0.935	17.39	0.053	1.99	0.0083	0.34	9.3	7.28	1.76	20.5	5.38	5.06	2.47	
25.3	0.956	17.79	0.033	1.23	0.0088	0.36	9.8	7.67	2.03	23.6	5.41	5.09	2.62	
28.0	0.959	17.84	0.030	1.14	0.0087	0.36	9.0	7.03	1.79	20.7	5.39	5.07	2.65	
28.0	0.947	17.61	0.041	1.54	0.0084	0.34	11.1	8.69	1.81	21.0	5.36	5.04	2.61	
Water samples														
(months apart)		12.36				0.22				13.6		3.41	2.97*	2.94
field test day		20.59				0.41				22.7		5.52	2.39*	2.36

* values calculated using the He water-gas phase fractionation factor at 12.9 °C.

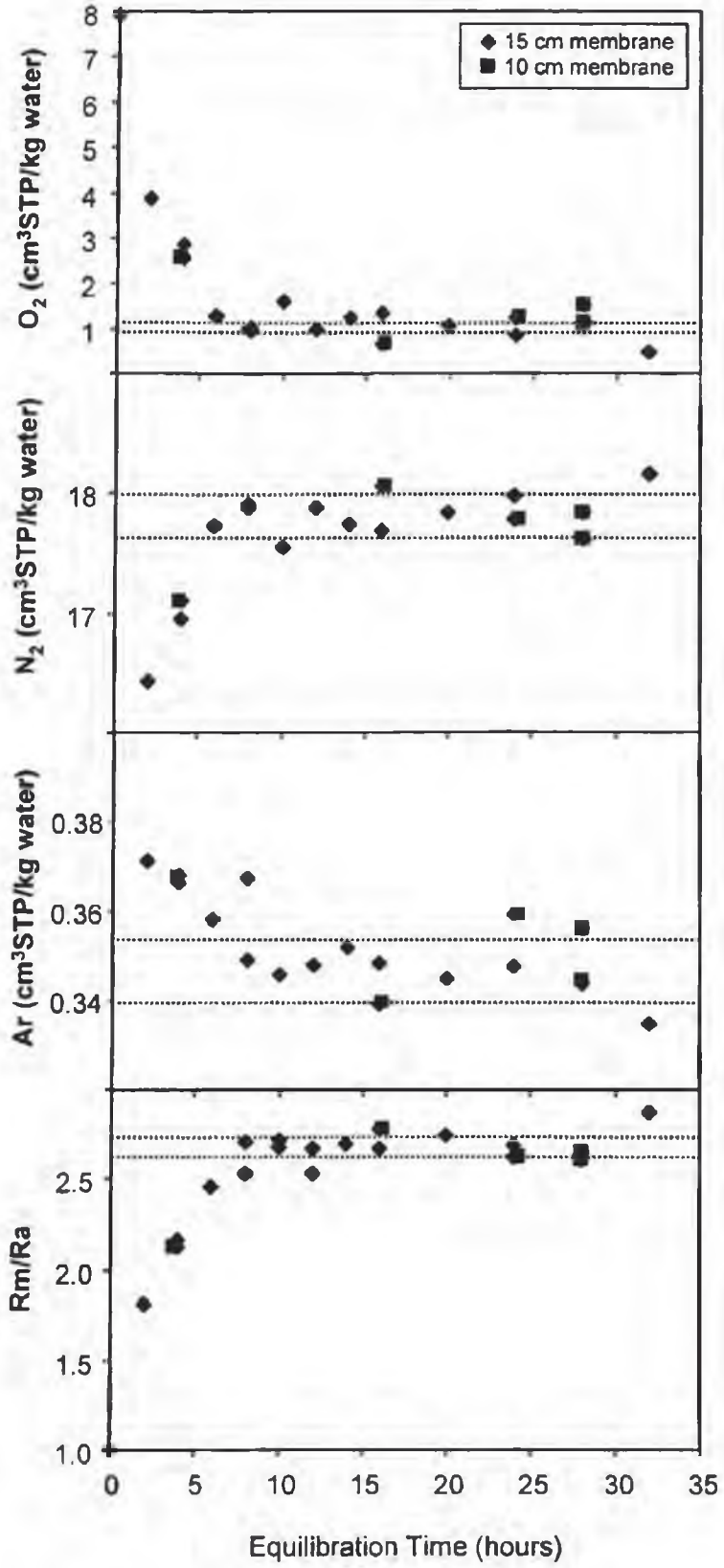

Figure 3.6. Field equilibration of diffusion samplers in a shallow aquifer well. Error bounds for O_2 (± 10%), N_2 (± 1%), Ar (± 2%) and R/Ra (± 2%) are depicted by dashed lines.

The measured oxygen concentration varied significantly during the field test. Potential causes for the varying oxygen concentration include small air bubbles adhered to the outside of the sampler membrane, oxygen diffusing into the sampler before crimping, oxygen reacting with the Cu tubing in the presence of water, analytical error, and leakage through the crimp. The range of oxygen observed (1-3% mole fraction) is significantly less than that of air (~21%). Small air bubbles adhered to the membrane exterior would dissolve under hydrostatic pressure, causing an increase in concentration of atmospheric gases. If we assume an equilibrium oxygen mole fraction of 0.02, roughly 2 ccSTP/kg of "excess" air would be required to raise the mole fraction to 0.03. In the process, the mole fractions of He, Ne and N_2 would increase by as much as 18%, 15%, and 10%, respectively. The lack of such large variations in the mole fractions of He, Ne, or N_2 indicates that the dissolution of air bubbles adhered to the sampling equipment is not the source of oxygen variability. Furthermore, groundwater flushes through the well screen. The measured oxygen concentrations are most likely the result of oxygen reacting with the copper tubing in the presence of water. The possibility of oxygen diffusing into the sampler before sealing or leakage through the crimp will be addressed in the *Sealing Window Tests* and *Sample Storage* sections, respectively. The analytical error will be addressed at the end of this section.

The diffusion samplers yielded slightly different results compared to the water samples obtained in copper tubing (Table 3.2). Dissolved oxygen measurements are not obtained from water samples since the oxygen reacts with the copper tubing. Stripping of the water during sampling could have resulted in obtaining lower apparent gas concentrations, whereas the capture of a gas bubble would result in higher apparent gas concentrations. Since the total dissolved gas pressure (1.062 atm) was greater than atmospheric (0.847 atm), degassing of the water during sampling could have occurred by bubble formation.

The second test was performed in the laboratory. The objective of this test was to verify that Ne and Kr, in particular, can diffuse through the Si-membrane. The field test was inconclusive regarding these gases. Several samplers were initially filled with N_2. One set of double samplers was crimped immediately to verify the initial sampler gas composition (N_2). The

other samplers were submerged in well-mixed lab-air equilibrated water at 22.5 °C. The stirring mechanism, however, temporarily failed during the first day. Thus, the actual equilibration time should be slightly less than the test predicts. The total dissolved gas pressure was measured (0.844 atm) and samplers were removed after 1, 2, and 3 days.

The test results indicate that all gases are in equilibrium within a day (Figure 3.7, Table 3.3). The mole fractions of all gases increased immediately from trace amounts to equilibrium concentrations as the proportion of nitrogen decreased from near unity. Minor variations between days sampled may be the result of temperature and/or pressure fluctuations, but no definitive statement can be made since the variations generally fall within the analytical error. The test verifies that Kr can diffuse through the Si-membrane and reach equilibrium with the surrounding dissolved concentration within a reasonable sampler deployment time.

A final equilibration test was performed to evaluate the equilibration time required for samplers installed in wells located in diffusion-dominated groundwater systems. Lab-air equilibrated water was generated and then de-oxygenated by the addition of ~3 g Na_2SO_3 per liter of water. Both a dissolved gas probe and a dissolved oxygen probe were used to verify the removal of oxygen. The water was transferred to a laboratory well constructed of 2 inch diameter clear PVC pipe (10 m length). The well was slowly gravity filled via a port located at its base to prevent any mixing with air. Lab-air filled samplers were installed along a length of string weighted at the bottom. A sampler was removed each week for 5 consecutive weeks.

The initial gas concentrations within the samplers (except O_2) should differ from their dissolved concentrations by their respective Henry's constants, assuming there was no change in the ambient air temperature between the time the lab-air equilibrated water was made and the samplers were installed (~1 week). Changes in the ambient air temperature and atmospheric pressure are likely to have been minor. Therefore, the equilibration of each gas primarily depends on the rate at which oxygen diffuses out of the sampler and water vapor diffuses into it.

The result of the diffusion test indicates that most gases equilibrated within two weeks (Table 3.3, Figure 3.8). The mole fraction of oxygen within the samplers decreased as a result of the exchange with the de-oxygenated water. Simultaneously, a proportional increase in the mole

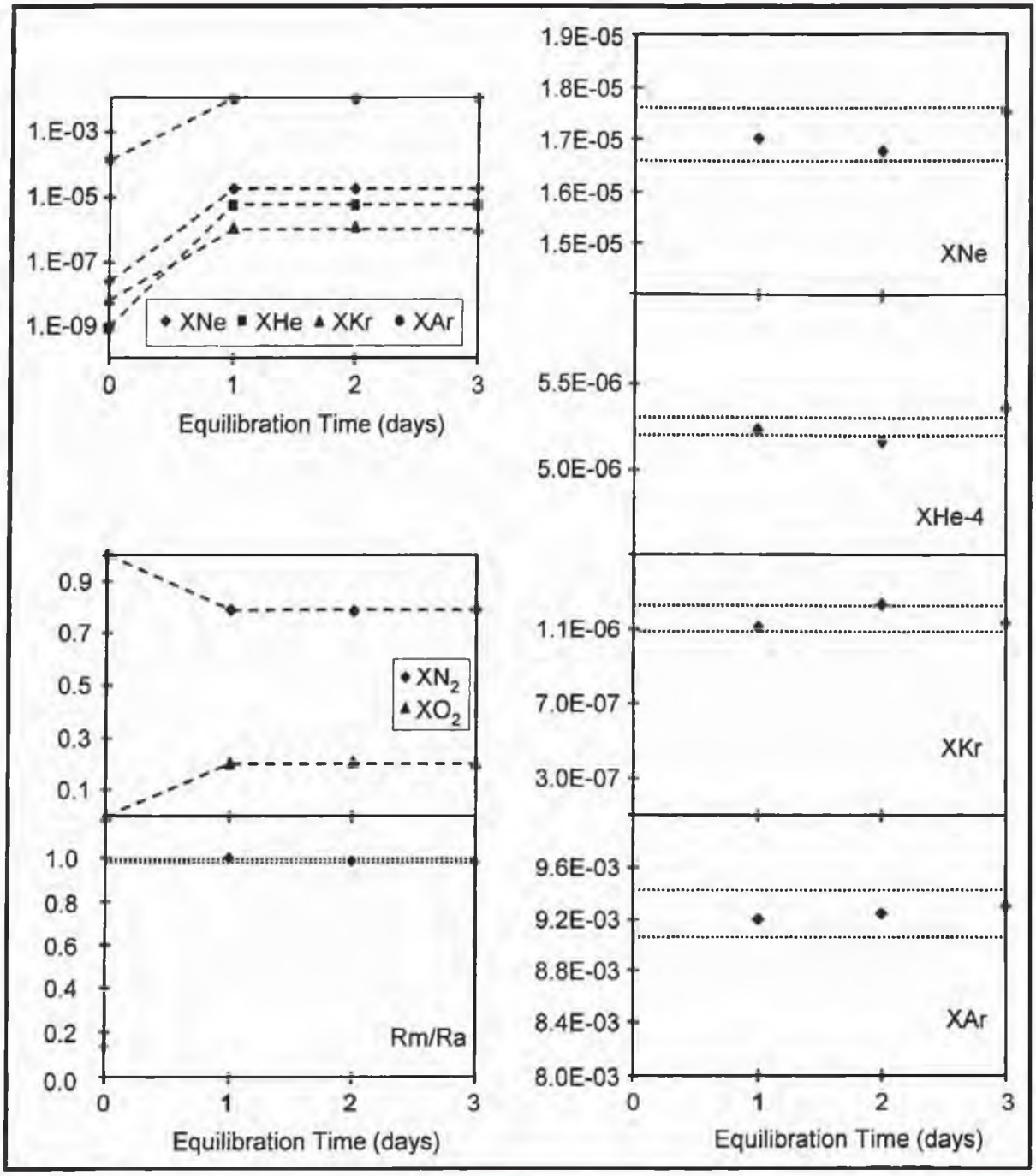

Figure 3.7. Laboratory equilibration of diffusion samplers initially filled with nitrogen. The samplers were submerged in lab-air equilibrated, well-mixed water. Error bounds for N_2 (± 1%), Ar (± 2%), 4He (± 1%), R/Ra (± 1%), Ne (± 3%), and Kr (± 6%) are depicted by dashed lines. The O_2 data fall within ± 3%.

Table 3.3. Sampler *Equilibration Time* laboratory test results. Gas concentrations are in units of ccSTP/kgwater. The total dissolved gas pressure in the carboy initially filled with nitrogen was 0.844 atm.

	Sampled Time	XN2	XO2	XAr	XKr	XNe	X4He	Rg/Ra
Laboratory Test Using Samplers Initially Filled With Nitrogen								
	Day 0	1.000	8.39E-06	0.0001	6.81E-09	2.30E-08	8.13E-10	0.13
	Day 1	0.790	0.201	0.0092	1.11E-06	1.70E-05	5.23E-06	1.00
	Day 2	0.785	0.206	0.0092	1.23E-06	1.68E-05	5.16E-06	0.99
	Day 3	0.787	0.204	0.0093	1.13E-06	1.75E-05	5.36E-06	0.98
Laboratory Well Test Using De-oxygenated Water								
	Week 0	0.781	0.209	0.0093	6.48E-07	1.65E-05	5.24E-06	1.00
	Week 1	0.989	1.88E-06	0.0127	1.62E-06	2.23E-05	6.24E-06	1.00
	Week 2	0.988	1.60E-05	0.0116	1.34E-06	2.25E-05	6.32E-06	0.99
	Week 3	0.989	1.54E-05	0.0112	1.24E-06	2.27E-05	6.26E-06	0.99
	Week 4	0.988	1.05E-06	0.0114	1.24E-06	2.24E-05	6.51E-06	0.99
	Week 5	0.988	1.35E-05	0.0114	1.28E-06	2.20E-05	6.22E-06	0.97

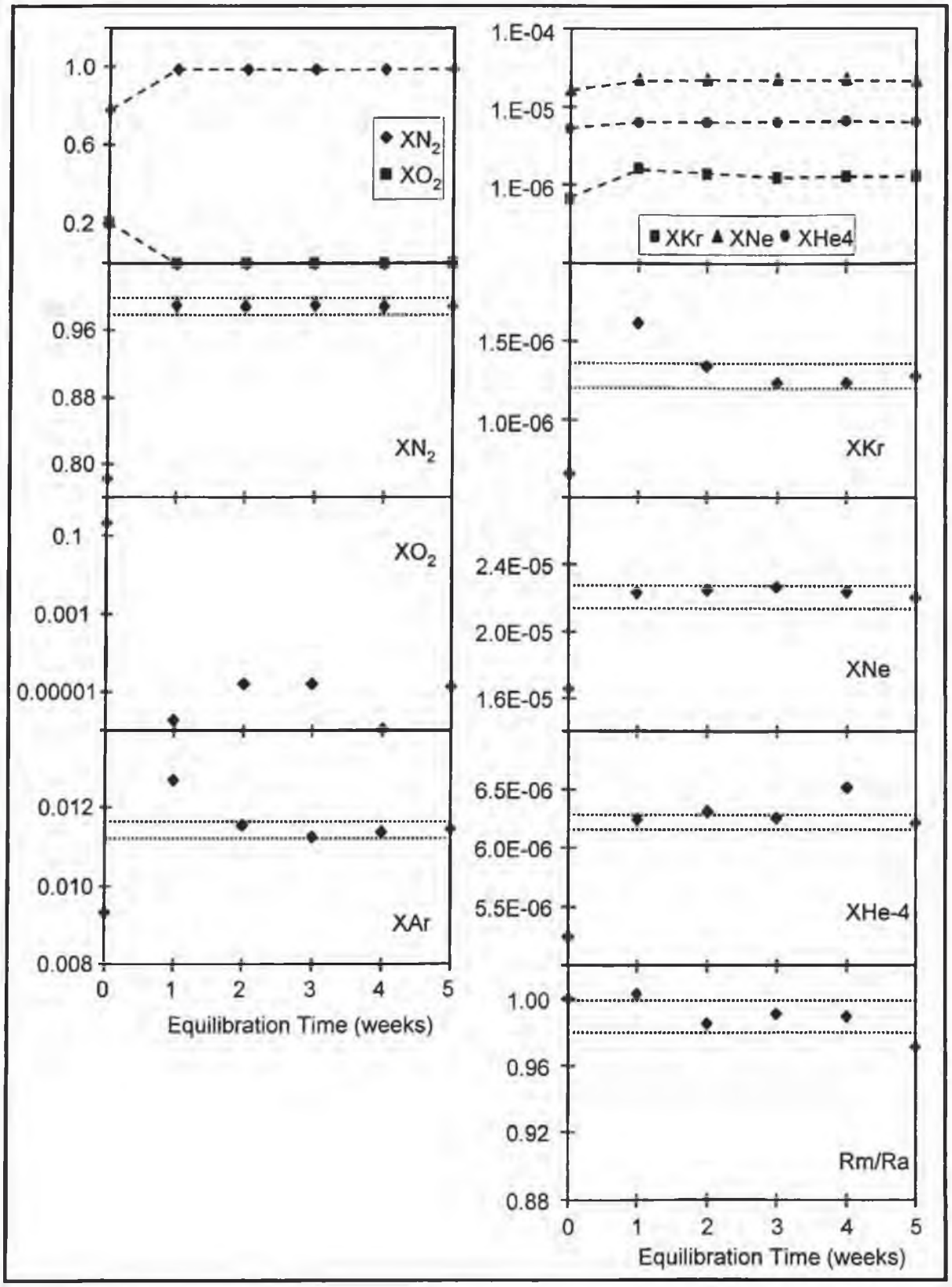

Figure 3.8. Laboratory equilibration of diffusion samplers placed in a stagnant column of de-oxygenated water. Error bounds for N_2 (± 1%), Ar (± 2%), 4He (± 1%), R/Ra (± 1%), Ne (± 3%), and Kr (± 6%) are depicted by dashed lines.

fraction of N_2 was observed, as were minor increases in the amount of Kr, Ne and He. Other than the initial decrease in the mole fraction of oxygen within the sampler, the subsequent variations in oxygen most likely reflect the limitation of analysis.

3.7.2 Sealing Window Tests

Two tests were performed to evaluate the length of time during which the samplers must be sealed after being removed from a well before loss of gas occurs ("sealing window"). The first test was performed in a cold room. The cold room test eliminated the duration of time that elapses while samplers are removed from a well, thereby representing an ideal sampling scenario. The second test involved the shallow well described above in which the total dissolved gas pressure in the groundwater was greater than atmospheric. This over-pressurization provided an opportunity to determine if a pressure gradient increases the rate of diffusion through the membrane.

The laboratory test was performed to compare the field test to a more idealized situation in which no time is lost removing the samplers from a well. A 5-gallon glass carboy was partially filled with water and placed in a cold room set at 7 ± 0.5 °C. The water was continuously stirred for a week to insure a well-mixed and thermally equilibrated solution. Samplers filled with lab-air (22.5 °C) were then submerged in the water. After 3 days the samplers were removed. The first two samplers were sealed immediately inside the cold room. The other samplers were removed from the refrigerator to the laboratory (~23 °C) and sealed after differing lengths of time had elapsed.

The samplers were removed to the laboratory for the purpose of comfort and to examine whether a change in temperature might cause a separation of gases within the sampler. When sampling in the field, the groundwater and ambient air temperatures are rarely equal. Evaporative-cooling or warming would affect the Cu and Si tubing differently, allowing a thermal gradient to develop within the sampler. It is conceivable that a thermal gradient could cause a fractionation of the gases within the sampler due to the gases having differing free-air diffusion coefficients. Simply removing the samplers into the laboratory is not a rigorous test of

the possible fractionation of gases caused by a thermal gradient. It should, however, provide an indication.

The results of the cold room test indicate no change in the mole fractions of gases within the samplers from 0 to 5 minutes time elapsed before the samplers were sealed (Table 3.4; Figure 3.9). The Rg/Ra values for the diffusion samplers were equivalent to that of the laboratory air. The results indicate that at least a 5-minute sealing window is possible under idealized conditions. These conditions include the ability to rapidly remove the samplers from depth and a total dissolved gas pressure similar to atmospheric. The upper limit of the sealing window was not determined by the test performed. No thermal affects were detected, although the samplers underwent a ~15 °C temperature increase between the cold room and the laboratory.

A second carboy of water was used for the purpose of obtaining water samples. Several diffusion samplers were installed in this carboy for comparison. The Rg/Ra measurements obtained from the diffusion samplers were slightly greater than the results obtained from water samples even with the He fractionation between water and gas phases considered (Table 3.4). All Rg/Ra results from the second carboy, however, were significantly less than the results from the first carboy listed above (Table 3.4). The low Rg/Ra values obtained from the second carboy of water indicate an additional source of ^{4}He. The likely source of helium is diffusion from the glass carboy itself. Several prior experiments were performed in which helium was injected into water filled carboys. It is likely that this carboy might have been used in one of those experiments and was continuing to degas the ^{4}He that diffused into the glass during those experiments.

The second test was performed to determine the sealing window under field conditions. Several double samplers were installed in the shallow unconfined aquifer well and allowed to reach equilibrium. After 5 days in the well, the samplers were simultaneously removed and sealed after different lengths of elapsed time. The groundwater temperature, total dissolved gas pressure and dissolved oxygen composition were measured (Table 3.5).

Table 3.4 Sampler *Sealing Window* laboratory test results. Gas concentrations are in units of ccSTP/kgwater. The atmospheric pressure was 0.847 atm. The total dissolved gas pressure was 0.837 atm. The water temperature was 7 °C.

Time (min)	XN2	N2	XO2	O2	XAr	Ar	XKr (x 10^{-6})	Kr	XKr (x 10^{-5})	Ne	X4He (x 10^{-6})	4He	Rg/Ra	R/Ra
Diffusion samplers from carboy #1.														
0.1	0.780		0.211		0.0092		1.16		1.79		5.26		1.00	
0.5	0.779		0.211		0.0094		1.15		1.77		5.26		0.98	
0.7	0.771		0.219		0.0092		1.08		1.78		5.27		0.99	
1.7	0.776		0.215		0.0091		1.00		1.76		5.22		1.00	
1.9	0.780		0.210		0.0093		1.15		1.78		5.25		0.99	
3.0	0.780		0.211		0.0092		1.34		1.77		5.20		0.99	
4.0	0.781		0.210		0.0091		1.11		1.77		5.26		0.99	
5.0	0.777		0.213		0.0092		1.31		1.77		5.24		0.99	
Lab Air														
	0.779		0.211		0.0092		1.08		1.73		5.30		0.99	
Diffusion samplers from carboy #2.														
	0.789	13.27	0.202	6.92	0.0093	0.35	1.02	7.62E-05	1.75	1.72E-04	6.58	5.06E-05	0.79	
	0.788	13.25	0.203	6.98	0.0092	0.34	1.21	9.02E-05	1.72	1.69E-04	7.24	5.56E-05	0.75	
Water samples collected in Cu tubes from carboy #2.														
		15.00				0.43				1.95E-04		6.15E-05	0.71*	0.71
		15.23				0.43				1.97E-04		6.20E-05	0.74*	0.73

* values calculated using the He water-gas phase fractionation factor at 7 °C.

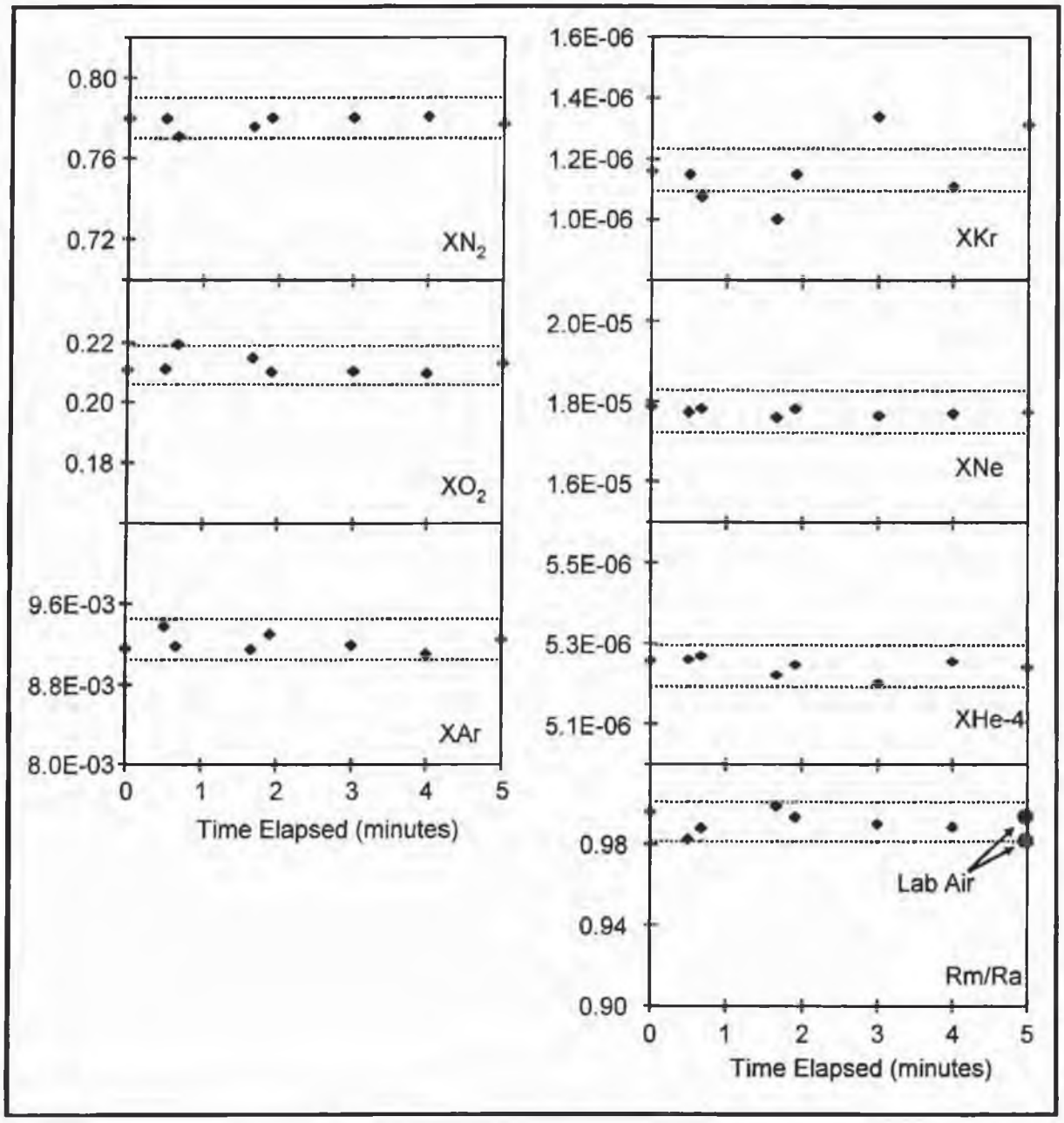

Figure 3.9. Sealing window test of samplers removed from lab-air equilibrated water. The water was well-mixed and refrigerated. The samplers were sealed after different lengths of time had elapsed. Error bounds for N_2 (± 1%), Ar (± 2%), 4He (± 1%), Rm/Ra (± 1%), Ne (± 3%), and Kr (± 6%) are depicted by dashed lines. The O_2 data fall within ± 3%. Rm/Ra values of laboratory air are indicated by labeled circles.

Table 3.5 Sampler *Sealing Window* field test results. Gas concentrations are in units of ccSTP/kgwater. The atmospheric pressure was 0.847 atm. The total dissolved gas pressure was 1.062 atm. The water temperature was 12.9 °C and the dissolved oxygen content was 1.49 ppm.

Time Sampled	XN2	XO2	XAr	XKr	XNe	X4He	Rg/Ra
Field Test							
0.22 min.	0.986	0.002	0.0078	9.85E-07	1.64E-05	5.29E-06	2.97
0.55 min.	0.987	0.002	0.0079	8.68E-07	1.73E-05	5.34E-06	2.92
0.97 min.	0.989	3.00E-04	0.0078	8.97E-07	1.63E-05	5.01E-06	2.98
1.15 min.	0.989	8.73E-05	0.0076	9.41E-07	1.63E-05	5.05E-06	2.99
2.03 min.	0.988	1.00E-04	0.0082	1.03E-06	1.79E-05	5.35E-06	2.84
4.08 min.	0.975	0.014	0.0079	1.05E-06	1.68E-05	5.23E-06	2.77
6.30 min.	0.965	0.025	0.0078	9.58E-07	1.68E-05	5.31E-06	2.65
7.98 min.	0.957	0.034	0.0081	9.99E-07	1.75E-05	5.22E-06	2.62
10.0 min.	0.934	0.056	0.0077	9.66E-07	1.67E-05	5.19E-06	2.48
15.0 min.	0.923	0.068	0.0080	9.53E-07	1.75E-05	5.19E-06	2.20

The measured total dissolved gas pressure indicates that the groundwater is over-saturated with dissolved gases. The pressure measured was ~3.0 psi above atmospheric. This corresponds to ~3.8 ccSTP/kg_{water} of excess air in the water sampled. This volume of excess air is a fair representation of the volume of excess air typical of many other groundwater sites (0 - 6 ccSTP/kg_{water}, Wilson and McNeill, 1997). The well test provides an opportunity to evaluate whether a pressure gradient increases the rate of exchange across the membrane. Since samplers installed in groundwater containing excess air will likely be pressurized relative to the atmospheric pressure, an increase in the exchange rate caused by such a pressure gradient would decrease the sealing window. Thus, the test should determine the sealing window in typical field scenarios.

The results of the field test indicate that the samplers should be sealed within 2 minutes of being removed from the well to prevent the loss of gas. Appreciable change was detected in the mole fractions of O_2 and N_2, and the Rg/Ra ratio (Table 3.5, Figure 3.10). After 2 minutes, the mole fraction of N_2 and the Rg/Ra ratio decreased linearly as the O_2 mole fraction increased. The O_2 mole fraction increased at a rate of ~0.5% per minute. Therefore, a similar ~0.5% per minute decrease in the N_2 mole fraction was observed. The relative change in the mole fraction of N_2 after 2 minutes was <1%, 2% after 6 minutes, and ~5% after 10 minutes. A slight decrease in the mole fraction of ^4He and increase in the Ne mole fraction were also apparent. The relative change in the mole fractions of ^4He and Ne, however, were less than 3% in 10 minutes. The Rg/Ra ratio, however, declined at a rate of ~5% per minute. Initially, the Rg/Ra value was similar to that determined for a water sample obtained in copper tubing (Table 3.5). Differences in the dissolved gas concentrations between the water and diffusion samples are explained in the *Equilibrium Tests* section.

The optimal sealing window for the dissolved gases measured in this study is 2 minutes. If selected gases are targeted for sampling rather than the entire suite, then the sealing window will vary. Generally, however, no significant loss (<1%) of any gas was detected within 2 minutes. Appreciable changes in the major gases present (i.e. N_2) and gases that have been produced (i.e., He) or consumed (i.e. O_2) should be anticipated after 2 minutes if the dissolved

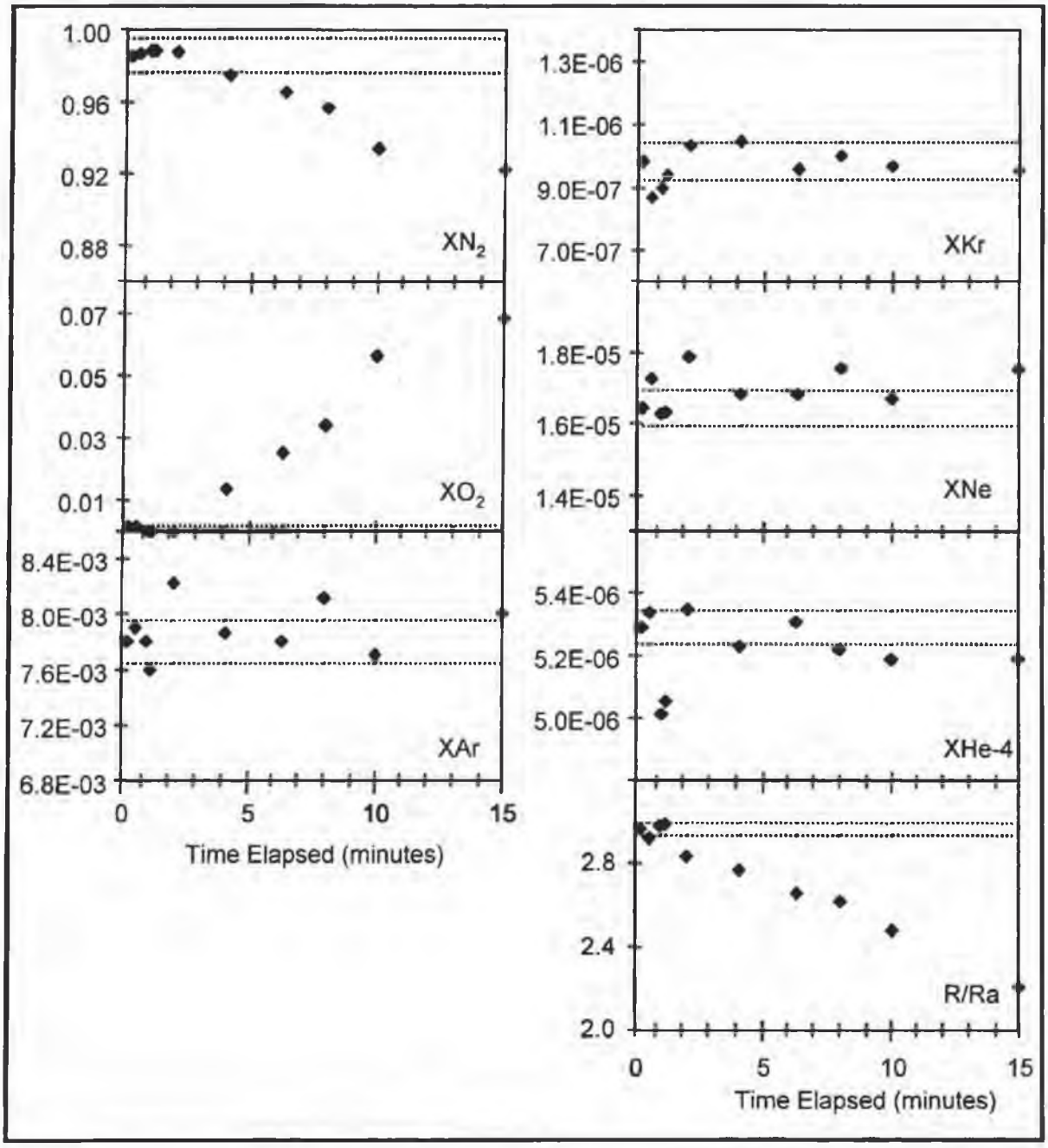

Figure 3.10. Sampler sealing window test performed in a shallow aquifer well. The groundwater was over-saturated with dissolved gases. Error bounds for N_2 (± 1%), Ar (± 2%), 4He (± 1%), R/Ra (±1%), Ne (± 3%), and Kr (± 6%) are depicted by dashed lines. A 5% change from the initial mole fraction of oxygen falls within the dashed line thickness.

gas concentration differs from that of air. Under conditions in which the gas pressure gradient between the sampler and air is greater, the sealing window may be less. The application of the diffusion samplers in numerous wells suggests that the samplers can be easily removed and sealed within 2 minutes.

The results of the sealing window tests indicate that oxygen diffusion through the Si-tubing prior to crimping was not the likely cause of variation in the O_2 concentration observed during the field equilibration test (Table 3.2, Figure 3.6). The samplers deployed in that test were sealed within a minute of being removed from the well. Furthermore, the results of nearly 50 well tests indicate that the dissolved O_2 concentrations determined using a probe are consistently greater (10-20%) than sampler O_2 concentrations (Manning, pers. commun. 2001), regardless of the O_2 gradient between the atmosphere and the sampler. Since oxygen is commonly below solubility in groundwater, the diffusion of O_2 into samplers upon removal from wells would be expected, resulting in an apparently higher O_2 concentration. The well tests, however, indicate that this is not the case (Manning, pers. commun., 2001).

3.7.3 Sample Storage

The sample storage time for the diffusion samplers is significantly greater than that of ping-pong balls or latex tubing because the gas sample is contained within the Cu tube. Sample duplicates stored up to 13 months agreed with samples analyzed immediately, indicating no measurable loss of gas or change to the gas composition (Table 3.6). Therefore, leakage through the crimp is not a concern if the crimped ends are protected during storage. The variability in the mole fraction of oxygen was on the same order (10^{-2}) as that observed during the field equilibration test. This is likely the result of O_2 reacting with the Cu tubing in the presence of a small amount of water within the sampler.

3.8 Conclusion

In situ headspace samplers allow sampling of tight zones which otherwise cannot be sampled because purging is minimized. When the samplers are placed in aquifer well screens, pumping is not required at all. Samplers are easily deployed in both groundwater wells and

Table 3.6. *Sample Storage* test results.

Sample ID	Storage Time (days)	(months)	XO/XN2	XN2	XO2	XAr	XKr	XNe	X4He	Rg/Ra
DC-S-2.1A	19	0.62	0.146	0.865	0.126	0.0095	6.27E-07	1.78E-05	6.93E-06	1.18
DC-S-2.1B	443	14.55	0.138	0.868	0.120	0.0090	6.34E-07	2.10E-05	7.23E-06	1.16
DC-S-1.4E	13	0.43	0.131	0.875	0.115	0.0086	5.82E-07	1.90E-05	7.14E-06	1.04
DC-S-1.4D	390	12.81	0.134	0.868	0.116	0.0096	6.93E-07	1.80E-05	7.22E-06	0.99
Big Cottonwood Creek	1	0.03	0.260	0.784	0.204	0.0096	3.04E-07	1.71E-05	5.33E-06	1.02
Big Cottonwood Creek	207	6.80	0.254	0.789	0.201	0.0093	6.55E-07	1.66E-05	5.17E-06	1.00
Big Cottonwood Creek	315	10.35	0.205	0.822	0.169	0.0097	6.76E-07	1.56E-05	5.27E-06	1.00

surface water bodies. The length of time required to obtain gas equilibration can be reasonably estimated.

The samplers eliminate the issues of sample loss and contamination common to other methods of dissolved gas sampling. Due to the samplers re-equilibration technique, they eliminate the possibility of collecting trapped air bubbles or evolved gas bubbles. In addition, the possibility of sample loss during collection can be prevented if the samplers are sealed within the recommended "sealing window." Two minutes is more than enough time to remove a sampler from most wells and seal them. For these reasons, the dissolved gas samplers greatly increase sampling confidence.

Although dissolved gas concentrations cannot be directly determined, they can be calculated when a total dissolved gas probe measurement is obtained. Alternatively, dissolved gas concentrations can be modeled by simulating measured gas mole fractions.

APPENDIX A

DISSOLVED GAS SAMPLING

Sampling for dissolved gases traditionally involves purging multiple well volumes, followed by obtaining groundwater samples in copper tubes. Down-hole samples are obtained by lowering Cu tubing (typically 3/8 inch) into the screened interval. A bottle in-line and above the Cu tubing assures adequate flushing. A one-way valve placed below the Cu tubing maintains the sample integrity until refrigeration clamps can be installed at the surface. Samples obtained at the surface are acquired in Cu tubing (using refrigeration clamps) that is in-line with a WaTerra pump of similar diameter. In either case, multiple well volumes (3) are purged before sampling. Due to the tight nature of the clays and the peizometer diameters (typically < 0.8 in), acquiring samples using traditional methods was impractical at the sites studied.

In-situ diffusion sampling devices provide an alternative sampling method. Diffusion samplers have been used in a variety of designs and for various applications. Samplers constructed of dialysis tubing have been developed and used to collect general chemistry samples (Ronen et al., 1987; Harper et al., 1997; Webster et al., 1998). Gascoyne and Sheppard (1993) used ping-pong balls to identify sources of groundwater discharge by measuring helium gradients. Ping-pong balls and latex tubing have been deployed to sample helium concentrations within lake sediment (Dyck and Da Silva, 1981; Stephenson et al., 1994). Sanford and others (1996) developed a diffusion sampler consisting of copper and latex tubing to collect noble gas samples from groundwater. Contrary to water samples diffusion samplers do not require well purging prior to sampling. This presents an immediate advantage for applications in aquitards. In addition, diffusion samplers eliminate the possibility of either stripping dissolved gases in water samples during collection or collecting trapped air bubbles.

An in-situ diffusion or headspace sampler was designed to minimize purging and mechanically fit down small diameter (1 cm) peizometers at the site (Figure A.1). The samplers consist of a headspace volume and a thin-walled semipermeable membrane similar to the sampler used by Sanford and others (1996). The semipermeable membrane allows gases to diffuse through it, thereby allowing the headspace to equilibrate with dissolved gases in the surrounding groundwater. Samplers were constructed of copper tubing to a volume of 0.3 cc. The sampler design was optimized based on the diffusion model of Sanford and others (1996). See Appendix A.1 Sampler Design for details.

At each site, samplers were installed in multiple peizometers open to various depths within the clay and underlying aquifer. Samplers were placed immediately above or within screened sections, under a minimum of 0.2 m water. Each peizometer was purged slightly to induce groundwater flow into the casing and past the sampler. After several months equilibration time (see Appendix A.2), the samplers were removed. Immediately upon being pulled from the wells, the "open" end of the Cu tubing was sealed using a cold-welding tool, trapping the gas inside. Multiple suites of samples were obtained from each site between 1996 and 1999.

A measurement of the total dissolved gas pressure was required to determine the individual gas partial pressures and groundwater concentrations. To obtain in-situ dissolved gas pressure measurements, a specially designed probe was employed (Manning, 2000). The probe consists of a pressure-transducer with a semipermeable membrane attachment (Figure A.2). The attachment was designed with a minimal internal volume and maximum semipermeable surface area for rapid equilibration of dissolved gases. Laboratory studies indicate the probe design requires roughly 1 hour for equilibration. The probe was used to determine total dissolved-gas pressure measurements of groundwater within the aquifer at both sites. Due to the probe width, it was not possible to take measurements in the aquitard peizometers. Attempts to develop a small diameter probe that would fit in micro-wells were unsuccessful.

Although some variability occurred between replicate samples, the diffusion samplers allowed for the collection of dissolved gas samples from micro-wells within an aquitard. Traditional sampling methods prevent obtaining dissolved gas samples from micro-wells and

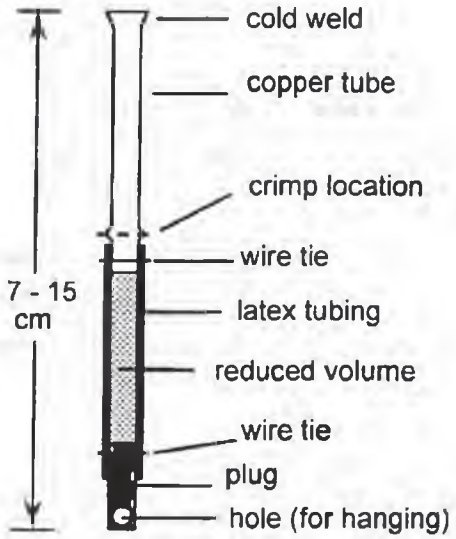

Figure A.1. In-situ dissolved-gas headspace sampler.

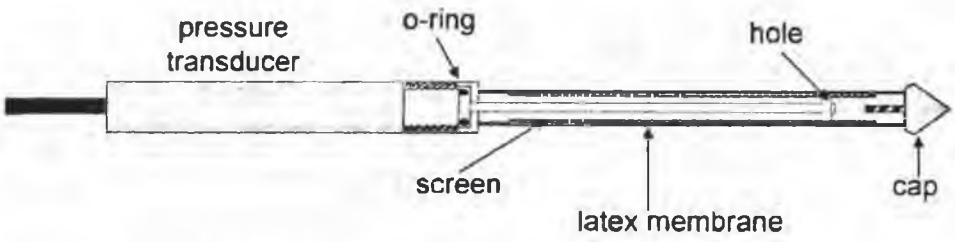

Figure A.2. Total dissolved-gas pressure probe. The internal volume of the probe equilibrates with dissolved gases in groundwater through a semi-permeable membrane. A hole connects the internal volume to the external surface. The external surface of the probe attachment is covered with a screen to increase the surface area over which exchange occurs. Thin-walled latex tubing placed over the screen provides the semipermeable membrane.

aquitards. Total dissolved-gas probe measurements in conjunction with diffusion samplers provide a direct means of determining in-situ dissolved gas concentrations, even under pressurized conditions.

A.1 Sampler Design

Samplers were designed according to the headspace sampler equilibration model of Sanford and others (1996).

$$C_g = H_{cc} C_w \left(1 - \exp\left[\frac{-DAt}{\forall L}\right]\right) \qquad (A.1)$$

where

C_g gas phase ^4He concentration in the sampler [$M\ L^{-3}$];

H_{cc} dimensionless Henry's constant;

C_w dissolved ^4He concentration [$M\ L^{-3}$];

D efective gas diffusion coefficient in the membrane [$L^2\ T^{-1}$];

A area of membrane exposed to the aqueous solution [L^2];

t time [T];

$\forall$ internal volume of the sampler [L^3];

L membrane thickness [L].

The model was designed to describe the equilibration of headspace samplers with well-mixed groundwater having a constant dissolved-gas concentration. H_{cc} represents the partitioning of gases between the aqueous phase, membrane, and gas phase.

In the study presented, the above model was used to determine the sampler membrane length required to equilibrate the samplers in a short duration of time. The samplers were designed to yield a final gas volume of ~0.3 cc for analysis by mass spectrometry. The time required to obtain 95% equilibration was used to optimize the membrane length. Since the groundwater at the sites is not well-mixed, the actual sampler equilibration time was greater than this model predicted. See Appendix A.2 Sampler Equilibration Model for the sampler equilibration model used in this study.

A.2 Sampler Equilibration Model

A step-equilibration model was used to estimate the equilibration time for sampler installed at Brander Park and Warwick. The model requires a continuous influx of groundwater into the peizometer/well casing and past the sampler (Figure A.3). The model assumes that this influx occurs at a rate slow enough to allow the sampler to fully exchange gases with the "cell" of water in its immediate vicinity. Since there is not an infinite volume of water in the cell, subsequent cells are required for the sampler to reach full equilibration with the groundwater. A derivation of the model follows.

The concentration of a gas species (C_i) in the aqueous (aq) or gas (g) phase is defined as the moles of gas (M_i) per unit volume of water (w) or gas (g). Thus,

$$C_{i,g} = \frac{M_{i,g}}{V_s} \tag{A.2}$$

$$C_{i,aq} = \frac{M_{i,aq}}{V_w} \tag{A.3}$$

According to Henry's Law,

$$C_{i,g} = \frac{C_{i,aq}}{H} \tag{A.4}$$

where H is a dimensionless Henry's constant. Substituting equation A.3 into equation A.4 yields

$$C_{i,g} = \frac{M_{i,aq}}{HV_w} \tag{A.5}$$

The solution to $M_{i,g}$ can then be determined through the combination of equations A.2 and A.5.

$$M_{i,g} = \frac{M_{i,aq}V_s}{HV_w} \tag{A.6}$$

Balancing the number of moles of gas species *i* while cell *n* is adjacent to the sampler yields:

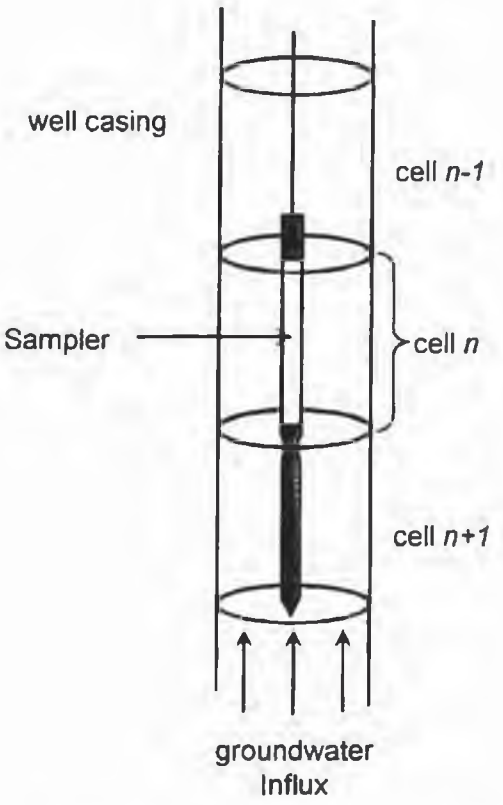

Figure A.3. Sampler equilibration model. Gas within the sampler equilibrates with the dissolved gas within the surrounding "cell" of water. The sampler volume progressively approaches final equilibration through a step-wise process involving subsequent cells of groundwater.

$$M_{i,g}^{n} + M_{i,aq}^{n} = M_{i,g}^{n-1} + M_{i,aq}^{n+1} \quad \text{(A.7)}$$

where $M_{i,g}^{n=0}$ represents the initial amount (in moles) of gas species *i* in the sampler. While the sampler is exchanging gases with groundwater in cell *n*, equations A.3 through A.6 can be re-written as:

$$C_{i,aq}^{n} = \frac{M_{i,aq}^{n}}{V_w} \quad \text{(A.8)}$$

$$C_{i,g}^{n} = \frac{C_{i,aq}^{n}}{H} \quad \text{(A.9)}$$

$$C_{i,g}^{n} = \frac{M_{i,aq}^{n}}{HV_w} \quad \text{(A.10)}$$

$$M_{i,g}^{n} = \frac{M_{i,aq}^{n} V_s}{HV_w} \quad \text{(A.11)}$$

Substituting equation A.11 into equation A.7 yields:

$$\frac{M_{i,aq}^{n} V_s}{HV_w} + M_{i,aq}^{n} = M_{i,g}^{n-1} + M_{i,aq}^{n+1} \quad \text{(A.12)}$$

Re-arranging to solve for $M_{i,aq}^{n}$

$$M_{i,aq}^{n} = \frac{M_{i,g}^{n-1} + M_{i,aq}^{n+1}}{1 + \frac{V_s}{HV_w}} \quad \text{(A.13)}$$

The concentration of gas species *i* in the gas and aqueous phases can then be determined. Equations A.8 and A.10 can be solved using equation A.13 and the volumes of the sampler and surrounding cell of groundwater.

$$C_{i,aq}^{n} = \frac{M_{i,g}^{n-1} + M_{i,aq}^{n+1}}{V_w + \frac{V_s}{H}} \tag{A.14}$$

$$C_{i,g}^{n} = \frac{M_{i,g}^{n-1} + M_{i,aq}^{n+1}}{HV_w + V_s} \tag{A.15}$$

Equations A.14 and A.15 can be solved for every subsequent cell of groundwater. Equation A.9 can be used in place of either equation A.14 or A.15 to solve for either the gas or aqueous phase concentration. Since equation A.9 relates the gas and aqueous phase concentrations according to Henry's Law, it can also be used to verify that the code has been written properly. Final equilibration is reached when

$$C_{i,g}^{n} = \frac{C_{i,aq}^{n+1}}{H}. \tag{A.16}$$

A.3 Sample Analysis

The samples were extracted and analyzed on magnetic sector-field mass spectrometers at the University of Rochester and the University of Utah.

Radiogenic ^4He concentrations were determined by several methods. First, $^4He_{rad}$ concentrations were determined using measured He and Ne concentrations and He and Ne solubility data (Schlosser et al., 1989).

$$^4He_{rad} = {}^4He_{aq} - {}^4He_{sol} - R_{He-Ne}\left[Ne_{aq} - Ne_{sol}\right] \tag{A.17}$$

where

$^4He_{rad}$ radiogenic component of ^4He

$^4He_{aq}$ aqueous ^4He concentration

$^4He_{sol}$ solubility ^4He concentration

Ne_{aq} aqueous Ne concentration

Ne_{sol} solubility Ne concentration

R_{He-Ne} atmospheric He/Ne ratio.

A recharge temperature of 5°C was used to calculate $^4He_{sol}$ and Ne_{sol} using the solubility data of Weiss (1971). The measured in-situ temperatures of 12°C (Warwick) and 13°C (Brander Park) were used to determine the aqueous concentrations of ^4He and Ne from Henry's Law.

$$^4He_{aq} = {}^4He_m \times H_{He} \qquad Ne_{aq} = Ne_m \times H_{Ne} \qquad \text{(A.18 - A.19)}$$

where

^4He_m measured ^4He concentration in the gas sampler

Ne_m measured Ne concentration in the gas sampler

H Henry's law constant relating aqueous to gas phase concentrations

The Ne-based approach to determining the in-situ $^4He_{rad}$ concentrations did not agree with the dissolved gas concentrations determined using alternative methods (description to follow). The dissolved-gas pressure at many sampled depths was greater than atmospheric due to the presence of methane, which caused the membrane to balloon when the sampler reached the surface. The increase in sampler volume caused by ballooning decreased the volume of gases collected. Thus, the mole fractions of individual gases are representative but the ^4He_m and Ne_m represent only a portion of the total concentrations present in-situ. Ne-based corrections were valid for groundwater sampled at shallow depths where methane is minimal.

Helium concentrations were next determined using a mixing model that utilizes the $^3He/^4He$ ratio observed (R_m) along with the $^3He/^4He$ ratio of atmospheric and radiogenic helium as the two end-members. The observed ratio is a function of the fraction of each end-member present.

$$\alpha R_m = \frac{{}^3He_{sol} + {}^3He_{nuc} + {}^3He_{ea} + {}^3He_{trit}}{{}^4He_{sol} + {}^4He_{rad} + {}^4He_{ea}} \qquad \text{(A.20)}$$

where

$^3He_{sol}$ solubility ^3He concentration

$^3He_{nuc}$ nucleogenic ^3He concentration

$^3He_{ea}$ excess air ^3He concentration

$^3He_{trit}$ tritiogenic ^3He concentration

$^4He_{sol}$ solubility ^4He concentration

$^4He_{rad}$ radiogenic ^4He concentration

$^4He_{ea}$ excess air ^4He concentration

α water-gas fractionation factor.

The measured $^3He/^4He$ ratio of the gas sample (R_m) must be converted to a dissolved concentration ratio by the water-gas fractionation factor (α). The water-gas fractionation factor is 0.988 ± 0.002 at 0^oC and increases by $-0.0001/^oC$ (Weiss, 1970).

The solution to equation A.20 can be found using $^3He/^4He$ ratios resulting from: a.) the solubility equilibrium of groundwater with the atmosphere, R_{sol}; b.) the production of nucleogenic and radiogenic helium within groundwater, R_{rad}; and c.) excess air, R_a. Nucleogenic ^3He is produced by the fission of ^6Li neutrons produced during U/Th series decay. Excess air is air that is trapped and dissolved in groundwater through a rise in the water table or capillary fringe. Tritiogenic ^3He was assumed to be negligible due to the presence of Pleistocene aged groundwater within the clay at these sites. Using these R values, equation A.20 becomes

$$\alpha R_m = \frac{R_{sol}\,{}^4He_{sol} + R_{rad}\,{}^4He_{rad} + R_a\,{}^4He_{ea}}{{}^4He_{sol} + {}^4He_{rad} + {}^4He_{ea}} \qquad \text{(A.21)}$$

where

$$^3He_{sol} = R_{sol}\,{}^4He_{sol}$$

$$^3He_{nuc} = R_{rad}\,{}^4He_{rad}$$

$$^3He_{ea} = R_a\,{}^4He_{ea}$$

$^4He_{ea}$ can be estimated by applying a reasonable range to the volume of excess air present.

$$^4He_{ea} = {}^4He_{air} \times \textit{excess air} \qquad \text{(A.22)}$$

where *excess air* refers to the volume (in cm^3) of excess air and $^4He_{air}$ represents the atmospheric ^4He concentration. Although excess air in groundwater may be as high as 30

cm^3/L, 0 - 5 cm^3/L is more common (Wilson and McNeill, 1997). A range of 0 - 3 cm^3/L was assumed in this case. Substituting equation A.22 in equation A.21:

$$\alpha R_m = \frac{R_{sol}\,{}^4He_{sol} + R_{rad}\,{}^4He_{rad} + R_a\,{}^4He_{air}(excess\ air)}{{}^4He_{sol} + {}^4He_{rad} + {}^4He_{air}(excess\ air)} \qquad (A.23)$$

The solution to equation A.23 is then determined for $^4He_{rad}$

$$^4He_{rad} = \frac{{}^4He_{sol}(R_{sol} - \alpha R_m) + {}^4He_{air}(excess\ air)(R_a - \alpha R_m)}{(\alpha R_m - R_{rad})} \qquad (A.24)$$

An R_{sol} of 1.36×10^{-6} representing water in equilibrium with the atmosphere at 5°C was applied. A $^3He/^4He$ ratio of crustal helium ($R_{rad} = 1 \times 10^{-8}$; Mamyrin and Tolstikhin, 1984) was used and R_a was defined as 1.384×10^{-8} (Clarke et al., 1976). Water-air fractionation factors (α) of 0.9868 and 0.9867 were used to describe the fractionation of helium isotopes at the in-situ groundwater temperatures of 12°C (Warwick) and 13°C (Brander Park), respectively.

Although the above R-based correction is less precise than the Ne-based correction, it may be useful for groundwater having R/R_a values near 1.0. The R-based $^4He_{rad}$ determinations proved to be useful for groundwater samples that had R/R_a values greater than 0.20. As the R_{rad} end-member is approached ($R/Ra \leq 0.10$), however, the serror becomes large and the ^4He concentration becomes insensitive to R/Ra. Thus, this method was applicable only to shallow groundwater samples from the two field sites investigated.

Dissolved gas concentrations (C_i) of groundwater within the aquifer were determined using the mole fractions (X_i) and total dissolved gas pressures (P_t) measured

$$C_i = K_i X_i P_T \qquad (A.25)$$

where K_i is the Henry's Law constant. $^4He_{rad}$ was then determined using equation A.17. The dissolved gas concentrations of groundwater within the aquitard could not be determined by this direct method since total dissolved gas measurements could not be obtained from the small diameter peizometers.

Finally, an optimization routine was used to generate the measured dissolved gas mole fractions (Appendix A.4). Although the mole fractions of individual gases are not as sensitive to recharge temperature and excess air gas partial pressures, they are sufficiently sensitive to permit the determination of the in situ dissolved gas concentrations. The optimization routine simultaneously solves multiple equations that relate input parameters (recharge temperature, pressure, in situ temperature, excess air, production or consumption of gases including helium) to the mole fractions of measured dissolved gases. Unlike the R/R_a correction, the routine uses multiple dissolved gases to constrain the input parameters and the fraction of each end-member present. Initially, the routine generates solubility partial pressures of individual gases at a given recharge temperature and pressure. Excess air can then be added. The optimization routine also allows for the production of CO_2, CH_4, and $^4He_{rad}$, and the consumption of O_2. Total dissolved-gas pressure and individual gas concentrations at the in-situ temperature are determined simultaneously. Finally, an optimization code minimizes the difference between the measured and modeled dissolved-gas mole fractions by varying the input parameters within user-defined ranges. The model accuracy was verified by reproducing the dissolved gas mole fractions, concentrations, and total dissolved-gas pressures measured for the aquifer samples.

The optimization routine was useful for groundwater samples for which probe measurements were unattainable and the Ne- and R-based corrections were not reliable. It provided the only determination of dissolved gas concentrations for the majority of groundwater sampled within the clay till.

A.4 Dissolved Gas Concentrations

The use of in-situ diffusion samplers, under certain conditions, may require an alternative method for determining dissolved gas concentrations. For water samples, dissolved gas concentrations can be determined from measurements of gas partial pressures. Radiogenic helium concentrations can then be calculated using a recharge temperature and excess air correction. The concentration of dissolved gases can be determined from gas samples obtained using in-situ diffusion samplers if the total dissolved gas pressure or the sampler volume is known. Acquiring a total dissolved gas pressure measurement, however, is not always possible

in micro-wells due to the probe dimensions. Although the volume of gas within a sampler can be determined on a vacuum line, it might not represent the in-situ gas volume if "ballooning" of the sampler membrane occurs during sample collection due to over-pressurization. In this case, measured dissolved gas concentrations are not representative of the in-situ conditions. This was the case at the site presented in this paper. Thus, the dissolved concentrations could not be reliably determined from the partial pressures.

The measured gas mole fractions provide an alternative method to determine the dissolved gas concentrations since the mole fractions are not affected by membrane ballooning. Similar to partial pressures, the mole fractions of gases also depend on the recharge temperature and excess air (Figure A.4). Compared to the dissolved gas concentrations, however, the mole fractions are less sensitive to variations in either (Figure A.4). The absolute value of the difference in the mole fraction due to a 1 ^{o}C temperature decrease or addition of 1 cc excess air is less than the resulting difference in the dissolved concentration. Although the mole fractions of individual dissolved gases are not as sensitive to recharge temperature and excess air as dissolved concentrations (Figure A.4), they are sufficiently sensitive to permit the determination of the dissolved gas concentrations.

An optimization technique was used to determine $^{4}He_{rad}$ concentrations from the mole fractions of gases measured. This method allows for the correction of excess air and He solubility without the total dissolved gas pressure being known. It optimizes the excess air correction by evaluating N_2, Ar, and Ne, rather than the common method of using one of these elements alone (typically Ne). This model was designed to incorporate methane which was sufficient in the samples collected near Sarnia, Ontario, as to affect the mole fractions of N_2, Ar, Ne, and He. The model works by first creating solubility-controlled dissolved gas concentrations using a "recharge temperature" variable. Second, the model adds excess air using an "excess air" variable. Third, oxygen is removed from the system. For oxygenated waters, this step can be eliminated. Fourth, radiogenic helium is added using a "He generated" variable. Fifth, methane is added using a "methane added" variable. The mole fraction of each gas is determined and compared to that which was measured for a particular sample. Using the Solver routine in

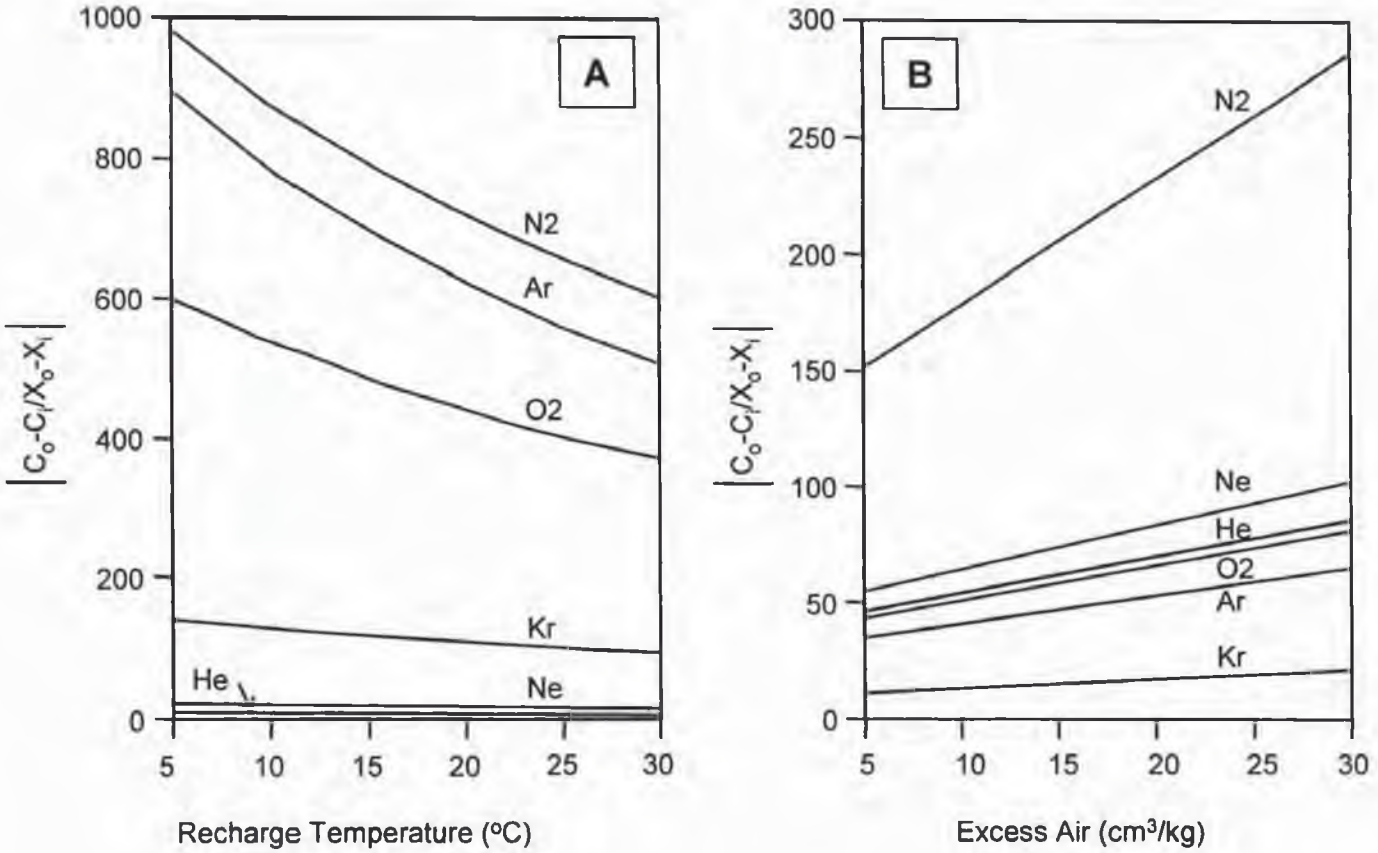

Figure A.4. Sensitivity of dissolved gas concentratons (C) and mole fractions (X) to changes in recharge temperature (A) and excess air (B). C_o is considered at 0°C and 0 cm^3/kg_{water} excess air. As the recharge temperature decreases and excess air increases, the volume of dissolved gases increases. In both cases, there is a greater change in the dissolved gas concentration compared to the gas mole fraction.

Microsoft Excel, the sum of the differences between modeled and measured dissolved-gas mole fractions is minimized. The Solver routine allows the user to specify variables to optimize. Limitations for each variable can be listed to restrict the solution to a reasonable solution. The following is an example of the routine.

Variables:

"Excess Air"	$\left[cm^3_{gas}/kg_{water}\right]$
"Recharge Temperature"	[°C]
"Oxygen"	$\left[cm^3_{oxy}/kg_{water}\right]$
"In-Situ Temperature"	[°C]
"CH_4 added"	$\left[cm^3_{methane}/kg_{water}\right]$
"He generated"	$\left[cm^3_{4He}/kg_{water}\right]$

STEP 1. Determine the solubility concentration of individual gases N_2, Ar, Ne, He, O_2 at the recharge temperature using empirical data (Weiss, 1971). The dissolved gas concentrations of individual gas species *i* will be referred to as C_i and are reported in units of cm^3_i/kg_{water}.

STEP 2. Add excess air. When the value of excess air is negative, the water is under-saturated with respect to atmospheric gases. When the value is positive, excess air has been entrained in groundwater. Therefore,

when "excess air" < 0; C_i (cm^3/kg) = $C_{i,step\ 1}$ + excess air*$C_{i,step\ 1}$

when "excess air" > 0; C_i (cm^3/kg) = $C_{i,step\ 1}$ + excess air*atmospheric concentration of *i*.

STEP 3. Remove O_2. The dissolved gas concentrations of N_2, Ar, Ne, and He remain the same, while the concentration of O_2 is reduced.

STEP 4. Add $^4He_{rad}$. The dissolved gas concentrations of N_2, Ar, Ne, and O_2 remain the same. The concentration of ^{4}He becomes:

^{4}He (cm^3/kg) = $^4He_{step\ 3}$ + He-generated.

STEP 5. Add methane. The dissolved gas concentrations of N_2, Ar, Ne, He, and O_2 remain the same. The concentration of methane becomes:

CH_4 (cm^3/kg) = CH_4 added.

STEP 6. Determine the total dissolved gas pressure (P_t), and the partial pressure (P_i) and mole fraction (X_i) of each gas at the in-situ water temperature.

$$P_i = \frac{C_i}{Hk_i} \qquad P_t = \sum P_i \qquad X_i = \frac{P_i}{P_t}$$

where Hk refers to the Henry's constant for gas species *i* at the in situ water temperature.

STEP 7. Run the solver routine. There are several options to running the optimization routine to obtain the dissolved gas concentrations. All involve minimizing the difference between the measured and modeled mole fractions of individual dissolved gases by changing the variables.

One option is to solve for all gas species by optimizing all of the variables simultaneously. (The in-situ temperature does not have to be a variable if it is known.) This method can be more difficult to solve since all variables are addressed simultaneously. Another option is to first evaluate the effects of excess air, recharge temperature, and oxygen by comparing only the modeled mole fractions of Ne, Ar, O, and N to those measured. Only excess air, recharge temperature and oxygen are considered variables in this step. After obtaining a solution from the first step, the differences between modeled and measured mole fractions of all gases can be minimized by varying the methane-added and He-generated variables, or by considering all of the variables. The model can be run repeatedly to achieve a solution through iteration. The number of iterations depends on how close the initial variables guesses are to the actual values, and whether the routine is solved by considering all variables simultaneously, or in steps.

APPENDIX B

MEASURED DATA

Table B.1. Measured data for Brander Park.

	Depth (m)	R/Ra	XN_2	XAr ($x10^{-3}$)	X4He ($x10^{-6}$)	XNe ($x10^{-6}$)	XO_2 ($x10^{-6}$)	XKr ($x10^{-6}$)	XCH4	Date/Place Analyzed*
Brander Park	2.98	1.254	0.978	10	8.50	19.9	167	0.94	0.012	Roch
	2.98	1.059	0.968	11	11.0	21.1	200	0.65	0.023	04269905
	2.98	0.927	0.936	9	9.36	22.3	27	0.52	0.044	09139907
	4.34	0.639	0.864	10	14.9	19.2	215	0.65	0.128	04269903
	4.34	0.628	0.826	11	10.6	19.2	92	0.84	0.163	04269916
	4.34	0.649	0.800	9	12.3	19.5	9	0.53	0.180	09139908
	6.02	0.380	0.673	10	14.7	17.1	46	0.75	0.320	04149915
	6.02	0.388	0.584	12	15.5	17.0	96	0.72	0.408	04269907
	6.02	0.378	0.581	8	14.0	16.5	11	0.44	0.407	09139910
	7.54	0.264	0.618	10	18.7	15.6	47	0.68	0.375	04149906
	7.54	0.243	0.568	9	17.9	14.7	51	0.63	0.426	04149907
	7.54	0.255	0.536	7	16.5	15.5	8	0.48	0.455	09139911
	8.83	1.182	0.913	11	8.98	22.3	102	1.15	0.074	Roch
	8.83	0.431	0.900	11	9.30	26.7	162	0.51	0.085	04209909
	11.85	0.450	0.902	10	19.4	19.3	153	1.57	0.088	Roch
	11.85	0.169	0.536	7	22.9	14.4	8	0.45	0.455	09149905
	15.88	0.160	0.778	8	34.2	14.5	215	1.11	0.205	Roch
	15.88	0.118	0.442	7	28.1	14.3	14	0.50	0.552	09149906
	21.34	0.145	0.568	6	23.4	8.03	46	0.77	0.424	Roch
	21.34	0.117	0.259	6	24.9	9.33	72	0.45	0.739	04149914
	21.34	0.118	0.270	8	23.2	8.40	101	0.54	0.727	04269906
	21.34	0.106	0.279	8	23.0	8.99	9	0.57	0.718	09149908
	33.51	0.065	0.196	5	36.5	6.04	75	0.35	0.801	04199903
	33.51	0.058	0.156	6	26.2	5.73	6	0.35	0.842	09149909
	39.83	0.058	0.451	5	69.8	12.4	69	0.97	0.535	Roch
	39.83	0.043	0.114	4	33.2	4.39	111	0.29	0.885	04199904
	43.66	0.095	0.336	4	40.9	8.32	88	0.67	0.656	Roch
	43.66	0.050	0.103	5	39.4	7.25	91	0.35	0.895	04199907
	43.66	0.044	0.060	3	19.2	3.53	5	0.18	0.939	09149912
	45.89	0.092	0.293	10	47.7	13.5	6160	0.59	0.700	04199908
	49.19	0.060	0.230	3	35.5	7.33	65	0.39	0.765	Roch

* Date/place analyzed records the sample number for samples analyzed at the University of Utah. For example, 04269905 was the 5th run of the day on April 26th, 1999.

Table B.2. Measured data for Warwick.

	Depth (m)	R/Ra	XN_2	XAr ($x10^{-3}$)	X4He ($x10^{-6}$)	XNe ($x10^{-6}$)	XO_2 ($x10^{-6}$)	XKr ($x10^{-6}$)	XCH4	Date/Place Analyzed*
Warwick	5.25	0.919	0.656	9	1.39	6.20	206	2.75	0.046	Roch
	5.25	0.957	0.853	9	9.86	21.9	18	0.48	0.138	09149916
	9.36	0.843	0.912	10	23.4	21.1	103	69.3	0.002	Roch
	9.36	0.224	0.977	6	13.5	11.8	60	0.41	0.013	04149911
	9.36	0.213	0.918	9	24.4	20.1	26	0.55	0.071	09149914
	14.39	0.148	0.966	8	31.4	14.6	78	0.56	0.023	04149913
	14.39	0.140	0.963	7	44.6	15.8	54	0.53	0.025	04149910
	16.97	0.199	0.983	10	46.3	23.2	270	1.52	0.006	Roch
	16.97	0.144	0.974	9	60.1	26.5	16	0.53	0.015	09149920
	22.76	0.129	0.972	11	100	23.6	393	1.39	0.017	Roch
	22.76	0.109	0.917	9	78.1	23.0	12	0.54	0.072	09149922
	28.25	0.126	0.627	7	57.7	15.2	124	0.82	0.365	Roch
	28.25	0.119	0.456	10	65.1	19.1	107	0.64	0.539	04199906
	28.25	0.118	0.392	7	58.8	16.9	6	0.45	0.603	09159901

* Date/place analyzed records the sample number for samples analyzed at the University of Utah. For example, 04269905 was the 5th run of the day on April 26th, 1999.

APPENDIX C

TRANSIENT NUMERICAL MODEL

The following is a Matlab code to solve the transient advection-dispersion equation with an internal production term.

$$\frac{\partial C}{\partial t} + V_z \frac{\partial C}{\partial z} = D_h \frac{\partial^2 C}{\partial z^2} + \frac{G^*}{\theta} \qquad (C.1)$$

```
function helium=helium(bound,release,stress,grainsize)

% Bound refers to the lower boundary condition. 0 = a constant conc of 0. 1 = a growing
% concentration. Bound > 1 is a constant conc >0. Release refers to the method of describing
% release. 0 = radial diff model with 1 ave grain size per z. 1 = rad diff w/multiple grain sizes
% per z. 2 = an eqn to describe release. This eqn must to entered where marked in the code.
% Stress refers to whether stress periods are desired. 1 = 1 run. 2 = more than 1 and it uses
% the last conc profile produced (from previous run) as the start conc. Grainsize refers to how
% the grain sizes/percentages are to be handled. 0 = NA, use with rel=0,2, 1= wtd ave mid-
% grain sizes are determined. 2 = even size increments are determined with correlating
% percentages. The model is designed such that z is + downwards.  MAKE CERTAIN UNITS
% ARE AS LISTED. Conversion equations are in the model as needed.
```

```
%   z   wtwtwtwtwtwtwt      numerous hydrologic/lithologic units
%   z   1              1    porosity for each unit
%   z   1111111111111       spatially variable release, grain size, gw 4He conc
%   z   2222222222222       The model is set for 3 units.
%   z   3333333333333       Unit 1 = till or unconsolidated w/release
%   z   3              3    Unit 2 = aquifer w/possible release
%   z   LLLLLLLLLLLLL       Unit 3 = bedrock w/ U/Th release rate
% MULTIPLE STRESS PERIODS CAN BE HANDLED. YOU MUST change to and tf and other
% variables (v). Make certain you change the name of output files before re-starting.
% OUTPUT: See "Files Saved" and "Figures". Un-comment files/figures desired.
format long


% ENTER VALUES WHERE THERE ARE ## SYMBOLS BELOW
dt= ##;          % time increment                                          yr
to= ##;          % initial time                                           yr
tf= ## ;         % total length of time                                   yr
tfig= ##;        % tfig*dt = interval wanted for plotting
dz= ##;          % spatial increment                                      m
wt= ##;          % upper boundary location (water table)                  m
L= ##;           % lower boundary location                                m
por1= 0.##;      % porosity of the upper unit (till)                      m3/m3
por2= 0.##;      % porosity of the middle unit (aquifer)                  m3/m3
por3= 0.##;      % porosity of the lower unit (bedrock)                   m3/m3
v= ##;           % average linear groundwater velocity  + downwards       m/yr
co= ##;          % initial groundwater 4He concentration                  ucc/kg(w)
Dh= ##;          % Hydrodynamic dispersion coefficient, Dh=dispersivity*v+De  m2/yr
Ds= ##;          %solid state diff coeff for He in grains                 cm2/yr
Kws=##;          % the water to solid partitioning coeff.                 unitless
```

```
% FILL IN THE FOLLOWING QUESTIONS, LIKE ABOVE
% How long were the grains releasing He before the gw system "started"?
Et= ##;                                                    %yrs

% List the depths of known data for units 1 (z1) and 2 (z2). Leave a space between entries as
% shown.
z1=[## ## ## ##] ;                                         %m
z2=[## ##];                                                %m

% For each z listed above, enter the corresponding grain diameters. d1 and d2 are for uniform
% size at each depth  (ie average grain size),  gd1, gd2, etc., are for multiple grain sizes at
% each depth, having also a percent passing (ppgd) of the total grains.
d1=[## ## ## ##];                                          %mm
d2=[## ##];                                                %mm

% the number of gd#s MUST equal the number of z depths
gd1=[## ## ## ## ## ##];                                   %mm
gd2=[## ## ## ## ## ##];                                   %mm
gd3=[## ## ## ## ## ##];                                   %mm
gd4=[## ## ## ## ## ##];                                   %mm

% Percent passing of each gd entry (in percent). The number of ppgd#s MUST equal the
% number of gd#s.
ppgd1=[##.## ##.## ##.## ##.## ##.## ##.##];
ppgd2=[##.## ##.## ##.## ##.## ##.## ##.##];
ppgd3=[##.## ##.## ##.## ##.## ##.## ##.##];
ppgd4=[##.## ##.## ##.## ##.## ##.## ##.##];
```

```
% complete these matrices so that all gd#s and ppgd#s are included in the vectors.
gd=[gd1; gd2; gd3; gd4];                                        %mm
ppgd=[ppgd1;ppgd2;ppgd3;ppgd4];

% For each z, enter the corresponding initial 4He concentration in the grains.
CO11=[## ## ## ##]*1000 ;                                       %ucc/kg(s)
CO22=[## ##]*1000 ;                                             %ucc/kg(s)

% List the measured release rates for each z. See comment above.
GG1=[## ## ## ##];                                              %ucc/kg(s)/yr
GG2=[## ##];                                                    %ucc/kg(s)/yr

% Below, list the measured gw 4He conc (CC) for given depths zz (all units).
zz=[## ##] ;                                                    %m
CC=[## ##];                                                     %ucc/kg

% For unit 3, He release may be like above or directly related to U/Th decay.
z3=[z2(length(z2))+1 L] ;
% upper and lower (L) depths of unit 3. These must NOT equal any value in z2.
Ut=##;          % length of time rock has been releasing 4He prior to model start yr
U238=##;        % the 238U concentration                        ppm
U235=##;        % the 235U concentration                        ppm
Th=##;          % the 232Th concentration                       ppm
rho=##;         % unit 3 density                                g/m3

% All input is complete. Thank you!
```

```
% Determine the steady-state production of 4He from U/Th series decay
NL=6.02e+23  ; %Avogadro's number                                   atoms/mol
L238=4.92e-18 ; %decay constant for 238U                            1/sec
L235=3.12e-17 ; %decay constant for 235U                            1/sec
L232=1.57e-18 ; %decay constant for 232Th                           1/sec
M238=238     ; % molecular weight of 238U                           g/mol
M235=235     ; % molecular weight of 235U                           g/mol
M232=232     ; % molecular weight of 232Th                          g/mol
RG=rho*NL*(8*(U238*10^-6)*L238/M238+7*(U235*10^-6)*L235/M235+6*(Th*10^-
6)*L232/M232);                                                      %atoms/m3(no voids)/sec
RG=RG*3600*24*365.25/((1/por3)-1);                                  %atoms/m3(w)/yr
RG=RG*22414.689/6.02e+23*10^6 ;                                     %ucc/m3(w)/yr
co3=Ut*RG;                                                          %ucc/m3(w)

% CONVERSIONS
if grainsize == 0
  midgd=1; %this is prevent error message. It represents nothing.
elseif grainsize == 1
  [midpg,midgd]=mids(gd,ppgd);          %this is a separate program
elseif grainsize == 2
  [midpg,midgd]=interpgd(gd,ppgd);      %this is a separate program
else
  % define midgd and midpg
end
co=co*1000;                                                         %ucc/m3(w)
d1=d1/10;                                                           %cm
d2=d2/10;                                                           %cm
midgd=midgd/10;                                                     %cm
```

```
CO1=CO11*((2.65-por1*2.65)*1000);                          %ucc/m3(a)
CO2=CO22*((2.65-por2*2.65)*1000);                          %ucc/m3(a)
GG1=GG1*((2.65-por1*2.65)*1000);                           %ucc/m3(a)/yr
GG2=GG2*((2.65-por2*2.65)*1000);                           %ucc/m3(a)/yr
CC=CC*1000;                                                %ucc/m3(w)/yr
z=[z1 z2];                                                 %m
d=[d1 d2];                                                 %cm
CO=[CO1 CO2];              % initial 4He conc in grains     %ucc/m3(a)
CO12=[CO11 CO22];          % initial 4He conc in grains     %ucc/kg(a)
GG=[GG1 GG2];              % measured release rates         %ucc/m3(a)/yr

t=[to:dt:tf];
lt=length(t);
lz=length(z);
Z=[wt:dz:z(length(z))];
lZ=length(Z);
Z3=[z(length(z))+dz:dz:L];
zall=[Z Z3];
n=length(zall);
co=Z*0+co;
coZ3=Z3*0+co3;
coall=[co coZ3];
por=[z1*0+por1 z2*0+por2];
por12=por;
por=interp1(z,por,Z,'linear');
porall=[por 0*Z3+por3];
RG3=(Z3*0+RG)/por3;
if sign(v)<0
```

```
    p1=(1/dt)+(Dh/(dz^2));
    p2=(-Dh/(2*dz^2));
    p3=(-Dh/(2*dz^2));
    q1=(1/dt)+(v/dz)-(Dh/(dz^2));
    q2=(-v/dz)+(Dh/(2*dz^2));
    q3=(Dh/(2*dz^2));
  else
    p1=(1/dt)+(Dh/(dz^2));
    p2=(-Dh/(2*dz^2));
    p3=(-Dh/(2*dz^2));
    q1=(1/dt)-(v/dz)-(Dh/(dz^2));
    q2=(Dh/(2*dz^2));
    q3=(v/dz)+(Dh/(2*dz^2));
  end
  A=zeros(n,n);
  B=zeros(n,n);
  for i=2:n-1;
    A(i,i)=p1;
    A(i,i+1)=p2;
    A(i,i-1)=p3;
    B(i,i)=q1;
    B(i,i+1)=q2;
    B(i,i-1)=q3;
  end
  A(1,1)=p1;
  A(1,2)=p2;
  A(n,n)=p1;
  B(1,1)=q1;
```

```
B(1,2)=q2;
B(n,n)=q1;
if stress == 1
  c=coall';
elseif stress > 1
  load c
end
if release == 0
  r=d/2;
  lambda=Ds*(1./(r.^2));
else
  r=midgd/2;
  lambda=Ds*(1./(r.^2));
end
He(:,1)=coall';
areapert(1)=trapz(zall,coall.*porall);
topflux(1)=(coall(2)-coall(1))/dz*Dh*por1;
botflux(1)=(coall(length(coall)-1)-coall(length(coall)))/dz*Dh*por3;
masstop(1)=topflux(1)*1*1*dt;
massbot(1)=botflux(1)*1*1*dt;
CGRAIN=CO12';
for j=1:lt-1
 if release == 0                    %rad diffusion model with one average grain size
   clear N
   for i=1:length(z)
    clear w ww
    w(1)=exp((-lambda(i))*(j*dt+Et+to)*(pi^2));
    ww(1)=w(1);
```

```
    m=1;
    while w(m)>0.001
     m=m+1;
     w(m)=exp((-lambda(i))*(j*dt+Et+to)*(pi^2)*(m^2));
     ww(m)=(1/(m^2))*w(m);
    end
    N(i)=6*lambda(i)*(CO(i)-(c(i)*Kws))*sum(w);
    Herelm3(i,j+1)=N(i);
    CGRAIN(i,j+1)=6*CO12(i)*sum(ww)/(pi^2);
    PLOSS(i,j+1)=(CO12(i)-CGRAIN(i,j+1))/CO12(i)*100;
  end
  N=interp1(z,N,Z,'linear');
  massprod(j)=sum(N)*dz*1*1*dt+RG*(L-z2(length(z2)))*1*1*dt;
elseif release == 1                %rad diffusion model with multiple grain sizes
  clear N
  for k=1:length(midgd(:,1))
    for i=1:length(midgd(1,:))
      clear w ww
      w(1)=exp((-lambda(k,i))*(j*dt+Et+to)*(pi^2));
      ww(1)=w(1);
      m=1;
      while w(m)>0.001
        m=m+1;
        w(m)=exp((-lambda(k,i))*(j*dt+Et+to)*(pi^2)*(m^2));
        ww(m)=(1/(m^2))*w(m);
      end
      N(k,i)=6*lambda(k,i)*(CO(k)'-(c(k)*Kws))*sum(w);
      cgrains(k,i)=6*CO12(k)*sum(ww)/(pi^2);
```

```
    end
  end
  perN=N.*(midpg/100);
  percgrains=cgrains.*(midpg/100);
  clear N cgrains
  for i=1:length(perN(:,1))
    N(i)=sum(perN(i,:));
    Herelm3(i,j+1)=N(i);
    CGRAIN(i,j+1)=sum(percgrains(i,:));
    PLOSS(i,j+1)=(CO12(i)'-CGRAIN(i,j+1))/CO12(i)*100;
  end
  N=interp1(z,N,Z,'linear');
  massprod(j)=sum(N)*dz*1*1*dt+RG*(L-z2(length(z2)))*1*1*dt;
  clear perN percgrains

% ENTER BELOW THE EQUATION THAT DESCRIBES He RELEASE
else                        % solve G(t) for an equation given
  N=##; %ucc/m3(a)/yr
  %N=z*0+N;
% for production for UNITS 1 AND 2 if you want this you must change massprod
  N=z2*0+N;  % for UNIT 2 PRODUCTION ONLY
  massprod(j)=N(1)*(z2(length(z2))-z1(length(z1)))*1*1*dt+RG*(L-z2(length(z2)))*1*1*dt;
  for i=1:length(N)
    Herelm3(i,j+1)=N(i);
  end
  N=interp1(z,N,Z,'linear');
 end
 clear w S m
```

```
 G=N./por;
 G=[G RG3]';
 G(1)=0;
 if bound==0              % C(L,t) = 0
  G(n)=0;
  c(n)=0;
 elseif bound==1          % C(L,t) = increasing
  A(n,n)=1;
  B(n,n)=1;
 else                     % C(L,t) = Co
  G(n)=0;
  c(n)=bound;
  A(n,n)=1;
  B(n,n)=1;
  A(1,1)=0;
  A(1,2)=0;
  B(1,1)=0;
  B(1,2)=0;
 end
 Heprodm3(:,j+1)=G;
 h=(B*c)+G;
 a=[A h];
 l(1,1)=0;
 u(1,2)=0;
 s(1)=0;
 for i=2:n-1
  l(i,i-1)=a(i,i-1);
  l(i,i)=a(i,i)-l(i,i-1)*u(i-1,i);
```

```
    u(i,i+1)=a(i,i+1)/l(i,i);
    s(i)=(1/l(i,i))*(a(i,n+1)-l(i,i-1)*s(i-1));
  end
  l(n,n-1)=a(n,n-1);
  l(n,n)=a(n,n)-l(n,n-1)*u(n-1,n);
  s(n)=(1/l(n,n))*(a(n,n+1)-l(n,n-1)*s(n-1));
  c(n)=s(n);
  for i=n-1:-1:1;
    c(i)=s(i)-u(i,i+1)*c(i+1);
  end
  He(:,j+1)=c;    % This creates a matrix with colms = conc for each dt
  areapert(j+1)=trapz(zall,He(:,j+1).*porall')-trapz(zall,He(:,j).*porall');
  topflux(j+1)=(c(2)-c(1))/dz*Dh*por1;
  botflux(j+1)=(c(length(c)-1)-c(length(c)))/dz*Dh*por3;
  masstop(j+1)=topflux(j+1)*1*1*dt;
  massbot(j+1)=botflux(j+1)*1*1*dt;
end
Totprod=sum(massprod);
areaf=trapz(zall,c.*porall');
topsum=sum(masstop);
botsum=sum(massbot);
Cg=CO';
for i=1:length(CO)
  for j=1:length(Herelm3(1,:))-1
    Cg(i,j+1)=Cg(i,j)-(Herelm3(i,j+1)*dt);
  end
end
for i=1:length(Herelm3(1,:))
```

```
  Herelkg(:,i)=Herelm3(:,i)./((2.65-por12*2.65)'*1000);
End
t=[dt:dt:tf];
relm3t=Herelm3(:,2:length(Herelm3));
relkgt=Herelkg(:,2:length(Herelkg));

% Files Saved
%save c c -ascii                    % the last conc profile only
%save He He -ascii                  % all conc profiles through time
%save Heprodm3 Heprodm3 -ascii      % production rate w/depth through time
%save Cg Cg -ascii                  % conc in modeled grains through time
%save massprod massprod -ascii      % mass produced at each time step
%save Totprod Totprod -ascii        % total He produced
%save areapert areapert -ascii      % calc'd mass (area under curve*por) through time
%save areaf areaf -ascii            % cal'd final mass in gw (area under curve tf)
%save Herelm3 Herelm3 -ascii        % release (ucc/m3(a)/yr) with z through time
%save Herelkg Herelkg -ascii        % release (ucc/kg(s)/yr) with z through time
%save topflux topflux –ascii        % 4He flux across top boundary
%save botflux botflux –ascii        % 4He flux across lower boundary
%save masstop masstop –ascii        % mass of 4He through top boundary
%save massbot massbot –ascii        % mass of 4He through lower boundary
%save CGRAIN CGRAIN -ascii          %grain conc thru time, analytical soln
%save PLOSS PLOSS -ascii            %percent lost from grain through time

% FIGURES
%RELEASE (m3) VERSUS TIME
%figure
%hold on
```

```
%semilogy(t+Et,relm3t(1,:))
%hold on
%for i=2:length(relm3t(:,1))
%   semilogy(t+Et,relm3t(i,:))
%end
%grid on
%ylabel('4He release (ucc/m3(sed)/yr)')
%xlabel('time (yr)')
%title('Brander Park')

%RELEASE (kg) VERSUS TIME
%figure
%semilogy(t+Et,relkgt(1,:))
%hold on
%for i=2:length(relkgt(:,1))
%   semilogy(t+Et,relkgt(i,:))
%end
%grid on
%xmax=tf+Et;
%axis([0 xmax .01 100]);
%ylabel('4He release (ucc/kg(sed)/yr)')
%xlabel('time (yr)')
%title('Brander Park')

%FINAL 4He(gw) CONCENTRATION VERSUS DEPTH
%figure
%hold on
%plot(c,zall,'b');
```

```
%plot(CC,zz,'ro')
%plot(CCCC,zzzz,'k+')
%axis ij
%%title('Final 4He Concentration:  C(L,t) = ' num2str(bound)', G method = 'num2str(release))
%xlabel('concentration in ucc/m3(w)')
%ylabel('depth (mbgs)')
%title('Brander Park')

%CONTOURS OF 4He(gw) CONC THROUGH TIME WITH DEPTH
%figure
%hold on
%for i=tfig+1:tfig:length(He(1,:))
%   plot(He(:,i),zall)
%end
%plot(CC,zz,'ro')
%plot(CCCC,zzzz,'k+')
%axis ij
%title('He conc profiles every dt*tfig yrs, C(L,t) = ' num2str(bound)', release = '
num2str(release)')
%xlabel('concentration in ucc/m3(w)')
%ylabel('depth (mbgs)')
%title('Brander Park')

%GRAIN 4He CONCENTRATION THRU TIME
%tt=[to:dt:tf];
%figure
%xmax=tf;
%xmin=to;
```

```
%ymax=max(CGRAIN(1,:));
%ymin=10^3;
%semilogy(tt,CGRAIN(1,:))
%hold on
%for i=1:length(CGRAIN(:,1))
%   semilogy(tt,CGRAIN(i,:))
%end
%axis([xmin xmax ymin ymax])
%grid on
%ylabel('4He Grain Conc (ucc/kg)')
%xlabel('time (yrs)')
%title('Analytical Solution To Grain Concentration Through Time')

%PERCENT OF 4He LOST FROM GRAINS THROUGH TIME
%figure
%plot(tt,PLOSS(1,:))
%hold on
%for i=1:length(PLOSS(:,1))
%   plot(tt,PLOSS(i,:))
%end
%grid on
%ylabel('Percent 4He loss from grains')
%xlabel('time  (yrs)')
%title('Percent 4He Lost From Grains Through Time')

% SUB-PROGRAMS
mids
```

```
function [midpg,midgd]=mids(gd,ppgd)
midgd(:,1)=gd(:,1);
midpg(:,1)=100-ppgd(:,1);
for i=1:length(gd(:,1))
 for j=2:length(gd(1,:))
  midgd(i,j)=gd(i,j-1)-((gd(i,j-1)-gd(i,j))/2);
  midpg(i,j)=ppgd(i,j-1)-ppgd(i,j);
 end
end
midgd(:,length(gd(1,:)))=gd(:,length(gd(1,:))-1);

interpgd
function [midpg,midgd]=interpgd(gd,ppgd)
gdum=gd*1000; %convert gd from mm to um.
for i=1:length(gd(:,1))
  mingd(i)=min(gdum(i,:));
  maxgd(i)=max(gdum(i,:));
  minmingd=min(mingd);
  maxmaxgd=max(maxgd);
  incgd(i,:)=[minmingd:1:maxmaxgd]/1000;
  incpg(i,:)=interp1(gd(i,:),ppgd(i,:),incgd(i,:),'linear');
  for j=2:length(incgd(1,:))
    midgd(i,j-1)=(incgd(i,j)-incgd(i,j-1))/2+incgd(i,j-1);
    midpg(i,j-1)=incpg(i,j)-incpg(i,j-1);
  end
  totpg(i)=sum(incpg(i,:));
end
  midgd(:,length(midgd)+1)=incgd(:,length(incgd))+.5/1000;
```

```
  vect=midpg(:,1)*0;
  midpg=[midpg vect];
for i=1:length(midpg(:,1))
  midpg(i,length(midpg))=100-sum(midpg(i,:));
end
```

APPENDIX D

HE DEGASSING FLUX FOR THE CLAY TILL

The ^{4}He flux into the atmosphere was determined using Fick's 1st law of diffusion:

$$F = -\theta D_e \left.\frac{\partial C}{\partial z}\right|_{z=0} \tag{D.1}$$

where θ is the porosity, D_e is the effective diffusion coefficient, and $\partial C/\partial Z$ is the ^{4}He gradient at the water table. The till porosity of 0.40 and the model-determined effective ^{4}He diffusion coefficient of 0.02 m^2/yr were applied. The ^{4}He gradient at the till surface (40 μccSTP/kg_w/m_{aq}) was converted from groundwater concentration units according to the following relationships. Subscripts w, aq, and sed refer to water, aquifer, and sediment, respectfully.

$$\theta \left.\frac{\partial C}{\partial z}\right|_{z=0} = \left(\frac{40\mu ccSTP}{kg_w m_{aq}}\right) * \left(\frac{10^{-6} cc}{1\mu cc}\right) * \left(\frac{1000 kg_w}{1 m_w^3}\right) * \left(\theta = \frac{0.4 m_w^3}{1 m_{aq}^3}\right) \tag{D.2}$$

$$\theta \left.\frac{\partial C}{\partial z}\right|_{z=0} = \frac{1.6x10^{-2} ccSTP}{m_{aq}^4} \tag{D.3}$$

This gradient can be further defined in terms of atoms of helium using Avogadro's constant (6.022 x 10^{23} atoms/mole) and the molar volume of an ideal gas (22.4 L/mole at 0°C, 1 atm).

$$\theta \left.\frac{\partial C}{\partial z}\right|_{z=0} = \left(\frac{1.6x10^{-2} ccSTP}{m_{aq}^4}\right) * \left(\frac{1L}{1000cc}\right) * \left(\frac{1mole}{22.4L}\right) * \left(\frac{6.022x10^{23} atoms}{1mole}\right) \tag{D.4}$$

$$\theta \left.\frac{\partial C}{\partial z}\right|_{z=0} = \frac{4.30x10^{17} atoms}{m_{aq}^4} \tag{D.5}$$

Applying Fick's Law, the He flux was determined as follows.

$$F = \theta D \left.\frac{\partial C}{\partial z}\right|_{z=0} = \left(\frac{4.3x10^{17}\,atoms}{m_{aq}^4}\right) * \left(\frac{0.02m^2}{yr}\right) * \left(\frac{1yr}{3.15x10^7 s}\right) \quad (D.6)$$

$$F = \frac{2.73x10^8\,atoms}{m_{aq}^2 s} \quad (D.7)$$

The internal ^{4}He release rate was converted into atomic mass units, assuming an average release rate of 0.1 μcc/kg$_{sed}$/yr, Avogadro's constant (6.022 x 10^{23} atoms/mole) and the molar volume of an ideal gas (22.4 L/mole at 0°C, 1 atm).

$$G^* = \left(\frac{0.1\mu cc}{kg_{sed}yr}\right) * \left(\frac{10^{-9}L}{\mu cc}\right) * \left(\frac{1mole}{22.4L}\right) * \left(\frac{6.022x10^{23}\,atoms}{mole}\right) * \left(\frac{1yr}{3.15x10^7 s}\right) \quad (D.8)$$

$$G^* = \frac{8.52x10^4\,atoms}{kg_{sed}s} \quad (D.9)$$

The internal release rate is converted from mass units to units of length by the density of the unconsolidated till (ρ_{till}), which can be estimated by:

$$\rho_{till} = \rho_{rock} - \theta_{till}\rho_{rock} \quad (D.10)$$

where the average silica-rich rock density is 2.65 x 10^3 kg/m^3.

$$G^* = \left(\frac{8.52x10^4\,atoms}{kg_{sed}s}\right) * \left[\frac{(2.65 - 0.4 * 2.65)x10^3 kg_{sed}}{m_{aq}^3}\right] \quad (D.11)$$

$$G^* = \frac{1.36x10^8\,atoms}{m_{aq}^3 s} \quad (D.12)$$

The production rate is further multiplied by the average till thickness (~20 m) to determine the total ^{4}He being released from the till.

$$G^* = \frac{2.71x10^9\,atoms}{m_{aq}^2 s} \quad (D.13)$$

APPENDIX E

HE DEGASSING FLUX OF THE ROCHESTER SHALE

The ^{4}He flux into the atmosphere was determined using Fick's 1st Law of diffusion:

$$F = -\theta D_e \left.\frac{\partial C}{\partial z}\right|_{z=0} \tag{E.1}$$

where θ is the porosity, D_e is the effective diffusion coefficient, and $\partial C/\partial Z$ is the ^{4}He gradient at the base of the Lockport. The porosity of the Rochester Shale (0.061) and the model-determined ^{4}He effective diffusion coefficient of 6.3 x 10^{-3} m^2/yr (2 x 10^{-6} cm^2/s) were applied. The ^{4}He gradient (5000 - 7000 μccSTP/kg_w/$m_{aquifer}$) was converted from groundwater concentration units according to the following:

$$\theta \left.\frac{\partial C}{\partial z}\right|_{z=0} = \left(\frac{5000\mu ccSTP}{kg_w m_{aq}}\right) * \left(\frac{10^{-6} cc}{1\mu cc}\right) * \left(\frac{1000 kg_w}{1 m_w^3}\right) * \left(\frac{0.061 m_w^3}{1 m_{aq}^3}\right) \tag{E.2}$$

$$\theta \left.\frac{\partial C}{\partial z}\right|_{z=0} = \frac{3.05x10^{-1} ccSTP}{m_{aq}^4} \tag{E.3}$$

This gradient can be further defined in terms of helium atoms.

$$\theta \left.\frac{\partial C}{\partial z}\right|_{z=0} = \left(\frac{3.05x10^{-1} ccSTP}{m_{aq}^4}\right) * \left(\frac{1L}{1000cc}\right) * \left(\frac{1mole}{22.4L}\right) * \left(\frac{6.022x10^{23} atoms}{1mole}\right) \tag{E.4}$$

$$\theta \left.\frac{\partial C}{\partial z}\right|_{z=0} = \frac{8.20x10^{18} atoms}{m_{aq}^4} \tag{E.5}$$

Applying Fick's Law, the He flux was determined as follows.

$$F = \theta D \left.\frac{\partial C}{\partial z}\right|_{z=0} = \left(\frac{8.20x10^{18}\,atoms}{m_{aq}^4}\right) * \left(\frac{4.68x10^{-4}\,m^2}{yr}\right) * \left(\frac{1yr}{3.15x10^7\,\sec}\right) \quad \text{(E.6)}$$

$$F = \left(\frac{1.22x10^8\,atoms}{m_{aq}^2\,\sec}\right) \quad \text{(E.7)}$$

The mass of helium per unit area in the Rochester Shale was determined using the porosity (0.061) and unit thickness (17 m).

$$He_{RS} = \left(\frac{100{,}000\,\mu cc}{kg_w}\right) * \left(\frac{1000kg_w}{1m_w^3}\right) * \left(\frac{0.061m_w^3}{1m_{RS}^3}\right) * (17m) \quad \text{(E.8)}$$

$$He_{RS} = \frac{1.037x10^8\,\mu cc}{m_{RS}^2} \quad \text{(E.9)}$$

The mass was converted to atomic mass units using Avogadro's constant (6.022 x 10^{23} atoms/mole) and the molar volume of an ideal gas (22.4 L/mole at 0°C, 1 atm).

$$He_{RS} = \left(\frac{1.037x10^8\,\mu cc}{m_{RS}^2}\right) * \left(\frac{10^{-9}L}{\mu cc}\right) * \left(\frac{1mole}{22.4L}\right) * \left(\frac{6.022x10^{23}\,atoms}{mole}\right) \quad \text{(E.10)}$$

$$He_{RS} = \frac{2.79x10^{21}\,atoms}{m_{RS}^2} \quad \text{(E.11)}$$

REFERENCES

AFEAS, Production, sales, and atmospheric release of fluorocarbons through 1995. *Alternative Fluorocarbons Environmental Acceptability Study*, AFEAS, 1997.

Anderson, M. L., and B. D. Johnson, Gas transfer: A gas tension method for studying equilibrium across a gas-water interface, *J. Geophys. Res.*, 97, C11, 17,899-17,904, 1992.

Andrews, J. N., The isotopic composition of radiogenic helium and its use to study groundwater movement in confined aquifers, *Chem. Geol.*, 49, 339-351, 1985.

Andrews, J. N., Mechanisms for noble gas dissolution by groundwaters, in *Isotopes of Noble Gases as Tracers in Environmental Studies. Proceedings of a Consultants Meeting on Isotopes of Noble Gases as Tracers in Environmental Studies*, May 29 to June 2, 1989, IAEA, Vienna, 305 p.p., 1992.

Andrews, J. N., and D. J. Lee, Inert gases in groundwater from the Bunter Sandstone of England as indicators of age and paleoclimatic trends., *J. Hydrology*, 41, 233-252, 1979.

Andrews, J. N., I. S. Giles, R. L. F. Kay, and D. J. Lee, Radioelements, radiogenic helium, and age relationships for groundwater from the granites at Stripa, Sweden, *Geochim. Cosmochim. Acta*, 46, 1533-1543, 1982.

Araguas Araguas, L., Danesi, P., Fröhlich, K., and K. Rosanski, Global monitoring of the isotopic composition of precipitation, J. *Radioact. Nucl. Chem.*, 205, 189-200, 1996.

Balderer, W., and B.E. Lehmann, $^{3}He/^{4}He$-ratios as indicators of the origin of helium in groundwater; examples from the deep Nagra boreholes in northern Switzerland., In *6th International Symposium on Water Rock Interaction in Malvern*, edited by D. L. Miles, 45-47, British Geological Survey, 1989.

Ballentine, C. J., and C. M. Hall, Determining paleotemperature and other variables by using an error-weighted, nonlinear inversion of noble gas concentrations in water, *Geochim. et Cosmochim. Acta*, 63, 2315-2336, 1999.

Ballentine, C. J., R. K. O'Nions, E. R. Oxburgh, F. Horvath, and J. Deak, Rare gas constraints on hydrocarbon accumulation, crustal degassing and groundwater flow in the Pannonian Basin, *Earth Planet. Sci. Lett.*, 105, 229-246, 1991.

Baxter, J. R., *An Environmental Isotope Survey of the Fresh Water Aquifer in Kent County, Ontario*, B.A. Sc. Thesis, Dept. of Geology, University of Windsor, Ontario, 1987.

Beaton, B., *An Isotopic and Geochemical Survey of the Fresh Water Aquifer in Lambton County*, M. Sc. Thesis, Univ. of Waterloo, Ontario, 1994.

Benson, B. B., and D. Krause Jr., Empirical laws for dilute aqueous solutions of nonpolar gases, *J. Chem. Physics*, 64, 689-709, 1976.

Bottomley, D. J., M. Gascoyne, and D. C. Kamineni, The geochemistry, age, and origin of groundwater in a mafic pluton, East Bull Lake, Ontario, Canada, *Geochim. Cosmochim. Acta*, 54, 993-1008, 1990.

Bu, X., and M. J. Warner, Solubility of chlorofluorocarbon 113 in water and seawater, *Deep Sea Res.*, 42, 1151-1161, 1995.

Bullister, J. L., and R. F. Weiss, Determination of CCL_3F and CCL_2F in seawater and air, *Deep Sea Res.*, 35, 839-854, 1988.

Busenberg, E., and L. N. Plummer, Use of chlorofluorocarbons (CCL_3F and CCL_2F) as hydrologic tracers and age-dating tools: the alluvium and terrace system of Central Oklahoma, *Water Resour. Res.*, 28, 2257-2883, 1992.

Capasso, G., and S. Inguaggiato, A simple method for the determination of dissolved gases in natural waters; an application to thermal waters from Vulcano Island, *Appl. Geochem.*, 13, 631-642, 1998.

Carignan, R., Automated determination of carbon dioxide, oxygen, and nitrogen partial pressures in surface waters, *Limnol. and Ocean.*, 43, 969-975, 1998.

Carter, R. C., W. J. Kaufman, G. T. Orlob, and D. K. Todd, Helium as a ground-water tracer, *J. Geophys. Res.*, 64, 2433-2439, 1959.

Clarke, W. B., W. J. Jenkins, and Z. Top, Determination of tritium by mass spectrometric measurements of ^3He, *Int. J. Appl. Radiat. Isot.*, 27, 515-522, 1976.

Cook, P. G., Solomon, D. K., Plummer, L. N., Busenberg, E., and S. L. Schiff, Chlorofluorocarbons as tracers of groundwater transport processes in a shallow, silty sand aquifer, *Water Resour. Res.*, 31, 425-434, 1995.

Crank, J., *The Mathematics of Diffusion*, 347 pp., Oxford University Press, Oxford, 1956.

Crnokrak, B., *An Environmental Isotope and Computer Flow Model Investigation of the Freshwater Aquifer in the Lake Huron to Lake Erie Corridor*. M. Sc. Thesis, Dept. of Geology, University of Windsor, Ontario, 1990.

Crooks, V. E., and R. M. Quigley, Saline leachate migration through clay: a comparative laboratory and field investigation, *Canad. Geotech. J.*, 21, 349-363, 1984.

Cserepes, L., and L. Lenkey, Modelling of helium transport in groundwater along a section in the Pannonian basin, *J. of Hydrol.*, 225, 185-195, 1999.

D'Aoust, B. G., and M. J. R. Clark, Analysis of supersaturated air in natural waters and reservoirs, *Trans. of the Amer. Fisheries Soc.*, 109, 708-724, 1980.

D'Astous, A. Y., W. W. Ruland, J. R. G. Bruce, J. A. Cherry, and R. W. Gillham, Fracture effects in the shallow groundwater zone in weathered Sarnia clay, *Can. Geotech. J.*, 27, 43-56, 1989.

Damon, P. E., and J. L. Kulp, Excess helium and argon in beryl and other minerals, *The American Mineralogist*, 43, 433-459,1958.

Davis, S. N. and R. J. M. DeWiest, *Hydrogeology*. 463 pp., J. Wiley and Sons, Inc., New York, 1966.

Deipser, A., and R. Stegmann, Biological degradation of VCCs and CFCs under simulated anaerobic landfill conditions in laboratory test digesters, *Environ. Sci. Pollut. Res. Int.*, 4, 209-216, 1997.

Desaulniers, D. E., *Groundwater Origin, Geochemistry and Solute Transport in Three Major Glacial Clay Plains of East Central North America*, Ph.D. Thesis, University of Waterloo, Ontario, 1986.

Desaulniers, D. E., J. A. Cherry, and P. Fritz, Origin, age and movement of pore water in argillaceous Quaternary deposits at four sites in Southwestern Ontario, *J. of Hydrol.*, 50, 231-257, 1981.

Desaulniers, D. E., R. S. Kaufmann, J. A. Cherry, and H. W. Bentley, ^{37}Cl-^{35}Cl variations in a diffusion controlled groundwater system., *Geochim. Cosmoshim. Acta*, 50, 1757-1764, 1986.

Dunkle, S. A., Plummer, L. N., Busenberg, E., Phillips, P. J., Denver, J. M., Hamilton, P. A., Michael, R. L., and T. B. Coplen, Chlorofluorocarbons (CCL_3F and CCL_2F) as dating tools and hydrologic tracers in shallow ground water of the Delmarva Peninsula, Atlantic Coastal Plain, United States, *Water Resour. Res.*, 29, 3837-3860, 1993.

Dyck, W., and F. G. Da Silva, The use of ping-pong balls and latex tubing for sampling the helium content of lake sediments, *J. Geochem. Explor.*, 14, 41-48, 1981.

Ekwurzel, B., Schlosser, P., Smethie, W. M., Plummer, L. N., Busenberg, E., Michel, R. L., Weppernig, R., and M. Stute, Dating of shallow groundwater: comparison of the transient tracers $^{3}H/^{3}He$, chlorofluorocarbons, and ^{85}Kr, *Water Resour. Res.*, 30, 1693-1708, 1994.

Elkins, J. W., Thompson, T. M., Swanson, T. H., Butler, J. H., Hall, B. D., Cummings, S. O., Fisher, D. A., and A. G. Raffo, Decrease in growth rates of atmospheric chlorofluorocarbons 11 and 12, *Nature*, 364, 780-783, 1993.

Erdmann, R., *An Environmental Isotope Survey of the Fresh Water Aquifer in St. Clair and Macomb Counties*, Michigan, B.A. Sc. Thesis, Dept. of Geology, University of Windsor, Windsor, Ontario, 1987.

Farvolden, R. N., and J. A. Cherry, Region 15, St. Lawrence lowland, in *The geology of North America*, edited by W. Back, J.S. Rosenshein, and P.R. Seaber, 133-140, Geological Society of America, Boulder, Colorado, 1988.

Fitzgerald, W. D., M. Mundry, and D. J. Storrison, Drift thickness of Sarnia-Bright Groove area, Southern Ontario, Ontario Geological Survey, Preliminary Map P-2368, scale 1:50,000, 1979.

Flint, R. F., *Glacial and Quaternary Geology*, 892 pp., John Wiley and Sons, Inc., New York, 1971.

Ford, D. C., and S. R. H. Worthington, Assessment of matrix diffusion in Silurian dolostone using stable isotopes ratios in rock cores, *Geol. Soc. Amer., 1998 Ann. Meeting, Abstracts with Programs*, 30, 225, 1998.

Galletti, P. M., M. T. Snider, and D. Silbert-Aiden, Gas permeability of plastic membranes for artificial lungs, *Med. Res. Engineer.*, 20, 20-23, 1966.

Gascoyne, M., and M. I. Sheppard, Evidence of terrestrial discharge of deep groundwater on the Canadian Shield from helium in soil gases, *Environ. Sci. and Technol.*, 27, 2420-2426, 1993.

Gelhar, L. W., Stochastic subsurface hydrology from theory to applications, *Water Resourc. Res.*, 22, 135S-145S, 1986.

Golder Associates Ltd., *Results of Geological and Hydrogeological Investigation and Contaminant Plume Delineation Study 1987*, Clean-up of abandoned PCB storage facility, Smithville, Ontario. Golder Associates Ltd., Ref. 871-1156, 1988.

Golder Associates Ltd., *Hydrogeologic Data Compilation and Assessment, CWML Site. Smithville, Ontario*. Golder Associates Ltd., Report No. 941-9033, 1995.

Goodall, D. C., and R. M. Quigley, Pollutant migration from two sanitary landfill sites near Sarnia, Ontario, *Can. Geotech. J.*, 14, 223-236, 1977.

Hall, C. M., and C. J. Ballentine, A rigorous mathematical method for calculating paleotemperature, excess air, and paleo-salinity from noble gas concentrations in groundwater, *Eos Trans*, Amer. Geophys. Union, 77, Fall Meeting Suppl., F178, 1996.

Hanna, T. H., Engineering properties of glacial lake clays near Sarnia, Ontario, *Ontario Hydro Research Quarterly*, 18, 1-12, 1966.

Harper, M. P., W. Davidson, and W. Tych, Temporal, spatial, and resolution constraints for in situ sampling devices using diffusional equilibration: dialysis and SET, *Environ. Sci. and Technol.*, 31, 3110-3119, 1997.

Harrington, G. A., P. G. Cook, and N. I Robinson, Equilibrium times of gas-filled diffusion samplers in slow-moving ground water systems, *Ground Water Mon. and Remed.*, Spring, 60-65, 2000.

Harris, S. M., *Characterization of the Hydraulic Properties of a Fractured Clay Till*, Unpublished M.Sc. Thesis, Department of Civil Engineering, University of Waterloo, Ontario, 1994.

Heaton, T. H. E., and J. C. Vogel, "Excess air" in groundwater, *J. Hydrol.*, 50, 201-216, 1981.

Hunt, A.G., *Diffusional Release of Helium-4 From Mineral Phases as Indicators of Groundwater Age and Depositional History*. Ph.D. Dissertation, University of Rochester, Department of Earth and Environmental Sciences, New York, 2000.

Hurley, P. M., The helium age method and migration of helium in rocks, in *Nuclear Geology*, edited by H. Faul, 301-329, John Wiley and Sons, Inc., New York, 1954.

Husain, M. M., *Origin and Persistence of Pleistocene and Holocene Water in a Regional Clayey Aquitard and Underlying Aquifer in Part of Southwestern Ontario*, PhD Thesis, Univ. of Waterloo, Ontario, 1996.

Husain M. M., J. A. Cherry, S. Fidler, and S. K. Frape. On the long-term hydraulic gradient in the thick clayey aquitard in the Sarnia region. *Can. Geotech. J.*, 35, 986-1003, 1998.

Husain M. M., J. A. Cherry, and S. K. Frape. Persistence of a Large Zone of Pleistocene Water in the Regional Freshwater Aquifer, Southwestern Ontario. *J. Hydrol.*, in press.

IAEA, *Statistical Treatment of Data on Environmental Isotopes in Precipitation*, IAEA, Vienna, Tech. Rep. No. 331, 1992.

Interra Technologies Ltd., *Hydrogeologic Study of the Freshwater Aquifer and Deep Geological Formations, Sarnia, Ontario*, Vol. 1, Final report to the Ontario Ministry of the

Environment, Detroit/St. Clair/St. Mary's Rivers Project, 214 pp., Interra Technologies Ltd., 1989.

Jagger Hims, Ltd., Geologic, *Hydrogeologic, and Geotechnical Compliance Considerations*, 1993 Annual Report to Laidlaw Environmental Services, January, 1994.

Jähne, B., H. Gerhard, and W. Dietrich, Measurement of the diffusion coefficients of sparingly soluble gases in water, *J. Geophys. Res.*, 92, 10767-10776, 1987.

Johnson, R. L., J. A. Cherry, and J. F. Pankow, Diffusive contaminant transport in natural clay: a field example and implications for clay-lined waste disposal sites, *Environ. Sci. and Tech.*, 23, 340-349, 1989.

Johnson, R. L., J. P. Pankow, and J. A Cherry, Design of a ground-water sampler for collecting volatile organics and dissolved gases in small-diameter wells, *Ground Water*, 25, 448-454, 1987.

Karp, K. E., A diffusive sampler for passive monitoring of volatile organic compounds in ground water, *Ground Water*, 31, 735-719, 1993.

Katz, B. G., Lee, T. M., Plummer, L. N., and E. Busenberg, Chemical evolution of groundwater near a sinkhole lake, northern Florida. 1. Flow patterns, age of groundwater, and influence of lakewater leakage, *Water Resour. Res.*, 31, 1549-1564, 1995.

Kim, C. K., Rho, B. H., and K. J. Lee, Environmental tritium in the areas adjacent to the Wolsong Nuclear Power Plant, *J. Environ. Radioact.*, 41, 217-231, 1998.

Klint, K. E. S., *Fractures and Depositional Features of the St. Joseph Till and Upper Part of Black Shale Till at the Laidlaw site, Lambton County, Ontario*, Geological Survey of Denmark and Greenland, report 1996/9, submitted to Waterloo Centre for Groundwater Research, University of Waterloo, Canada, 1996.

Lapcevic, P., Novakowski, K., Bickerton, G., and J. Voralek, *Preliminary Results of the Fall 1995 Drilling and Hydraulic Testing Program at the Smithville Phase IV Bedrock Remediation Site*, NWRI Contribution No. 96-50, 36, 1996.

Lewis, C. F. M., T. C. Moore Jr, D. K. Rea, D. L. Dettman, A. L. Smith, and L. A. Mayer, Lakes of the Huron Basin: their record of runoff from the Laurentide ice sheet, *Quat. Sci. Rev.*, 13, 891-922, 1994.

Lovelock, J. E., Atmospheric fluorine compounds as indicators of air movements. *Nature*, 230, 379, 1971.

Mamyrin, B. A., and I. N. Tolstikhin, *Helium Isotopes in Nature*, 273 pp., Elsevier, New York, 1984.

Manning, A. H., personal communication, University of Utah, 2002.

Manning, A. H., A. L. Sheldon, and D. K. Solomon, A new method of noble gas sampling that improves excess air determinations, p. 449, *Eos, Transactions,* 81, Fall Meet. Suppl., American Geophysical Union, Washington, D.C., 2000.

Marine, I. W., The use of naturally occurring helium to estimate groundwater velocities for studies of geologic storage of radioactive waste, *Water Resour. Res.*, 15, 1130-1136, 1979.

Martel, D. J., J. Deák, P. Dövényi, F. Horváth, R. K. O'Nions, E. R. Oxburgh, L. Stegena, and M. Stute, Leakage of helium from the Pannonian Basin, *Nature*, 342, 908-912, 1989.

Marty, B., T. Torgersen, V. Meynier, R. K. O'Nions, and G. de Marsily, Helium isotope fluxes and groundwater ages in the Dogger Aquifer, Paris Basin, *Water Resour. Res.*, 29, 1025-1035, 1993.

Masarik, J., and R.C. Reedy, Terrestrial cosmogenic-nuclide production systematics calculated from numerical simulations, *Earth Planet. Sci. Lett.*, 136, 381-395, 1995.

Mazor, E., and A. Bosch, Dynamics of groundwater in deep basins; ^{4}He dating, hydraulic discontinuities, and rates of drainage, In *Proceedings of the International Conference on Groundwater in Large Sedimentary Basins*, 380-389, Australian Water Resources Council, Australia, 1991.

Mazor, E., and A. Bosch, Helium as a semi-quantitative tool for groundwater dating in the range of 10^4 to 10^8 years, in *Isotopes of Noble Gases as Tracers in Environmental Studies Consultants Meeting on Isotopes of Nobles Gases as Tracers in Environmental Studies*, May 29 to June 2, 1989, IAEA, Vienna, 305 p.p., 1992.

McCarthy, R. L., Bower, F. A., and J. P. Jesson, The fluorocarbon-ozone theory, 2. World production and release of CCl_3F and CCl_2F (fluorocarbons 11 and 12) through 1975, *Atmos. Environ.*, 11, 491-497, 1977.

McKay, L., *Groundwater Flow and Contaminant Transport in a Fractured Clay Till*, Ph.D. Thesis, Univ. of Waterloo, Ontario, 1991.

McKay, L. D., R. W. Gillham, and J. A. Cherry, Field experiments in a fractured clay till: 2. Solute transport and colloid transport, *Water Resour. Res.*, 29, 1149-1162, 1993.

McKay, L. D., and J. Fredericia, Distribution, origin, and hydraulic influence of fractures in a clay rich glacial deposit, *Can. Geotech. J.*, 32, 957-975, 1995.

Mellary, A. A., and E. P. Kilburn, Groundwater Probability, County of Lambton, Ontario, Water Res. Comm., Map 3118-1, 1969.

Misra, C., D. R. Nielsen, and J. W. Biggar, Nirtogen transformation in soil during leaching, Theoretical considerations, *Soil Sci. Soc. Amer. Proc.*, 38, 289-293, 1974.

Murphy, J. J., *A Geochemical and Hydrogeological Study of the Interface Zone Aquifer at the Laidlaw Site, Lambton County, Ontario*, Unpublished B.Sc. Thesis, Department of Earth Sciences, University of Waterloo, Ontario, 1994.

Novakowski, K. S., and P. Lapcevic, Regional hydrogeology of the Silurian and Ordovician sedimentary rock underlying Niagara Falls, Ontario, Canada. *J. Hydrol.*, 104, 211-236, 1988.

Novakowski, K., Lapcevic, P., Bickerton, G., Voralek, J., Xanini, L., and C. Talbot, *The Development of a Conceptual Model for Contaminant Transport in the Dolostone Underlying Smithville, Ontario*, Prepared for the Smithville Phase IV Bedrock Remediation Program. 67pp. Final, December, 2000.

O'Brien, K., Secular variations in the production of cosmogenic isotopes in the Earth's atmosphere, *J. Geophys. Res.*, 84, 423-431, 1979.

O'Neill, J. E., and I. Brindle, Development and application of innovative remediation technologies at DNAPL contaminated sites in fractured bedrock (Smithville PCB site), *Geol. Soc. Amer., 1998 Ann. Meeting, Abstracts with Programs*, 30, 279, 1998.

O'Nions, R. K., and E. R. Oxburgh, Helium, volatile fluxes and the development of continental crust, *Earth Planet. Sci. Lett.*, 90, 331-347, 1988.

Pearson, F. J., Jr. W. Balderer, H. H. Loosli, B. E. Lehmann, A. Matter, T. Peters, H. Schmassmann, and A. Gautschi, Applied isotope hydrology; a case study in Northern Switzerland, *Stud. Environ. Sci.*, 43, 439, Elsevier, Netherlands, 1991.

Plummer, L. N., and E. Busenberg, *Chlorofluorocarbons, in Environmental Tracers in Subsurface Hydrology*, Kluwer Academic Publishers, Boston, 441-478, 2000.

Plummer, L. N., Busenberg, E., McConnell, J. B., Drenkard, S., Schlosser, P., and R. L. Michel, Flow of river water into a karstic limestone aquifer. 1. Tracing the young fraction in groundwater mixtures in the Upper Floridan aquifer near Valdosta, Georgia, *Appl. Geochem.*, 13, 995-1015, 1998a.

Plummer, L.N., Busenberg, E., Drenkard, S., Schlosser, P., McConnell, J. B., Michel, R.L., Ekwurzel, B., and R. Weppernig, Flow of river water into a karstic limestone aquifer. 2. Dating the young fraction in groundwater mixtures in the Upper Floridan aquifer near Valdosta, Georgia, *Appl. Geochem.*, 13, 1017-1043, 1998b.

Poreda, R. J., Cerling, T. E., and D. K. Solomon, Tritium and helium isotopes as hydrologic tracers in a shallow unconfined aquifer, *J. Hydrology*, 103, 1-9, 1988.

Rasmussen, R. A., and M. A. K. Khalil, Atmospheric trace gases: trends and distributions over the last decade, *Science*, 232, 1623-1624, 1986.

Remenda, V. H., J. A. Cherry, and T. W. D. Edwards, Isotopic composition of old groundwater from Lake Agassiz: implications of late Pleistocene climate, *Sci.*, 266,1975-1978, 1994.

Ronen, D., M. Magaritz, and I. Levy, An in situ multilevel sampler for preventive monitoring and study of hydrochemical profiles in aquifers, *Ground Water Monitor. and Remed.*, 7, 69-74, 1987.

Rowe, R. K., C. J. Caers, and F. S. Barone, Laboratory determination of diffusion coefficient of contaminants using undisturbed clayey soil, *Canad. Geotech. J.*, 25, 108-118, 1988.

Rudd, J. W. M., and R. D. Hamilton, Two samplers for monitoring dissolved gases in lake water and sediments, *Limnol. And Ocean.*, 20, 902-906, 1975.

Ruland, W. W., J. A. Cherry, and S. Feenstra, The depth of fractures and active groundwater flow in a clayey till plain in southwestern Ontario, *Groundwater*, 29, 405-417, 1991.

Sanford, B. V., Thompson, F. J., and G. H. McFall, Plate tectonics – A possible controlling mechanism in the development of hydrocarbon traps in southwestern Ontario, *Bull. Canad. Petrol. Geol.*, 33, 52-71, 1985.

Sanford, W. E., R. G. Shropshire, and D. K. Solomon, Dissolved gas tracers in groundwater: simplified injection, sampling, and analysis, *Water Resour. Res.*, 32, 1635-1642, 1996.

Sano, Y., Helium flux from the solid earth, *Geochem. J.*, 20, 227, 1986.

Sano, Y., H. Wakita, and C. W. Huang, Helium flux in a continental land area estimated from $^{3}He/^{4}He$ ratio in northern Taiwan, *Nature*, 323, 55, 1986.

Schlosser, P., Stute, M., Dorr, H., Sonntag, C., and K. M. Oto, Tritium/^{3}He dating of shallow groundwater, *Earth and Planet. Sci. Lett.*, 89, 353-362, 1988.

Schlosser, P., M. Stute, C. Sonntag, and K. O. Munnich, Tritogenic ^{3}He in shallow groundwater, *Earth Planet. Sci. Lett.*, 94, 245-254, 1989.

Selim, H. M., and R. S. Mansell, Analytical solution of the equation for transport of reactive solutes through soils, *Water Resourc. Res.*, 12, 528-532, 1976.

Semprini, L., Hopkins, G. D., Roberts, P. V., and P. L. McCarty, In-situ biotransformation of carbon tetrachloride, 1,1,1,-trichloroethane, Freon-11, and Freon-12 under anoxic conditions, *EOS Trans.*, Am. Geophys. Union, 71, 1324, 1990.

Sherwood-Lollar, B., S. K. Frape, and S. M. Weise, New sampling devices for environmental characterization of groundwater and dissolved gas chemistry (CH_4, N_2, He), *Environ. Sci. Technol.*, 28, 2423-2427, 1994.

Sklash, M., S. Mason, S. Scott, and C. Pugsley, An investigation of the quantity, quality and sources of groundwater seepage into the St. Clair River near Sarnia, Ontario, Canada, *Water Pollution Res. J.*, 21(3), 351-367, 1986.

Slough, K. J., Sudicky, E. A., and P. A. Forsyth, Importance of rock matrix entry pressure on DNAPL migration in fractured geologic materials, *Ground Water*, 37, 237-244, 1999.

Soderman, L. G., and Y. D. Kim, Effect of groundwater levels on stress history of St. Clair clay till deposits, *Canad. Geotech. J.*, 7, 173-187, 1970.

Solomon, D. K., *The Use of Tritium and Helium Isotopes to Determine Groundwater Recharge to Unconfined Aquifers*, Ph.D. Thesis, University of Waterloo, Waterloo, Ontario, 213 pp., 1992.

Solomon, D. K., and P. G. Cook, ^{3}H and ^{3}He, in *Environmental Tracers in Subsurface Hydrology*, Kluwer Academic Publishers, Boston, 397-424, 2000.

Solomon, D. K., P. G. Cook, and W. E. Sanford, Dissolved gases in subsurface hydrology, in Isotope Tracers in Catchment Hydrology, eds., C. Kendall and J. J. McDonnell, Elsevier Science, Amsterdam, 291-318, 1998.

Solomon, D. K., Hunt, A., and R. J. Poreda, Source of radiogenic helium 4 in shallow aquifers: implications for dating young groundwater, *Water Resour. Res.*, 32, 1805-1813, 1996.

Stephenson, M., W. J. Schwartz, T. W. Melnyk, and M. F. Motycka, Measurement of advective water velocity in lake sediment using natural helium gradients, *J. Hydrol.*, 154, 63-84, 1994.

Stute, M., Sonntag, C., Deak, J., and P. Schlosser, Helium in deep circulating groundwater in the Great Hungarian Plain: flow dynamics and crustal and mantle helium fluxes, *Geochim. Cosmochim. Acta*, 56, 2051-2067, 1992.

Strutt, R. J., Helium and radioactivity in rare and common minerals, *Roy. Soc. London Proc.*, 80A, 572-594, 1908a.

Strutt, R. J., The accumulation of helium in geologic time, *Roy. Soc. London Proc.*, 81A, 272-277, 1908b.

Strutt, R. J., The leakage of helium from radioactive minerals, *Roy. Soc. London Proc.*, 82A, 166-169, 1909.

Stute, M., C. Sonntag, J. Deak, and P. Schlosser, Helium in deep circulating groundwater in the Great Hungarian Plain: flow dynamics and crustal and mantle helium fluxes, *Geochim. Cosmochim. Acta*, 56, 2051-2067, 1992.

Sudicky, E. A., Slough, K. J., and P. A. Forsyth, DNAPL migration in fractured porous rock media; parameter sensitivity, prediction uncertainty and implications for remediation, *Groundwater Quality; Remediation and Protection*, 250, 157-165, 1998.

Sugisaki, R., and K. Taki, Simplified analyses of He, Ne, and Ar dissolved in natural waters, *Geochem. J.*, 21, 1, 23-27, 1987.

Swanson, S. K., personal communication, University of Wisconsin, 2000.

Takahata, N., and Y. Sano, Helium flux from a sedimentary basin, *Applied Rad. and Isotopes*, 52, 985-992, 2000.

Takaoka, N., and Y. Mizutani, Tritiogenic ^{3}He in groundwater in Takaoka, *Earth and Planet. Sci. Lett.*, 85, 74, 1987.

Therrien, R., and E. A. Sudicky, Three-dimensional analysis of variably-saturated flow and solute transport in discretely-fractured porous media, *J. Contam. Hydrol.*, 23, 1-44, 1996.

Thompson, G. M., and J. M. Hayes, Trichloromethane in ground water: A possible tracer and indicator of ground water age, *Water Resour. Res.*, 15, 546-554, 1979.

Tolstikhin, I. N., and I. L. Kamensky, Determination of groundwater age by the T-^{3}He method, *Geochem Int.*, 6, 810-811, 1969.

Torgersen, T., Controls on pore fluid concentration of ^{4}He and ^{222}Rn and the calculation of ^{4}He/Rn ages, *J. Geochem. Explor.* 13, 57-75, 1980.

Torgersen, T., Terrestrial helium degassing fluxes and the atmospheric helium budget: Implications with respect to the degassing processes of the continental crust, *Chem. Geol.*, 79, 1-14, 1989.

Torgersen, T., and W. B. Clarke, Helium accumulation in groundwater, I. An evaluation of sources and the continental flux of crustal ^{4}He in the Great Artesian Basin, Australia, *Geochim. Comochim. Acta*, 49, 1211-1218,1985.

Torgersen, T., and G. N. Ivey, Helium accumulation in groundwater, 2, A model for the accumulation of the crustal ^{4}He degassing flux, *Geochim. Cosmochim. Acta,* 49, 2445-2452, 1985.

Torgersen, T. and J. O'Donnell, The degassing flux from the solid earth: Release by fracturing, *Geophys. Res. Lett.*, 18, 951-954, 1991.

Torgersen, T., Zop, T., Clarke, W. B., Jenkins, W. J., and W. S. Broeker, A new method for physical limnology –tritium-helium-3 ages –results for Lakes Erie, Huron and Ontario, *Limnol. Oceanog.*, 22, 181-193, 1977.

Warner, M. J., and R. F. Weiss, Solubilities of chlorofluorocarbons 11 and 12 in water and seawater, *Deep Sea Res.*, 32, 1485-1497, 1985.

Watten, B. J., D. R. Smith, and W. J. Ridge, Continuous monitoring of dissolved oxygen and total dissolved gas pressure based on head-space partial pressures, *J. of the World Aquaculture Soc.*, 28, 316-333, 1997.

Weaver, T. R., *Groundwater Flow and Solute Transport in Shallow Devonian Bedrock Formations and Overlying Pleistocene Units, Lambton County, Southwestern Ontario*, PhD. Thesis, Dept Earth Sci., Univ. of Waterloo, Ontario, 1994.

Webster, I. T., P. R. Teasdale, and N. J. Grigg, Theoretical and experimental analysis of peeper equilibration dynamics, *Environ. Sci. and Technol.*, 32, 1727-1733, 1998.

Weiss, R. F., Helium isotope effect in solution in water and seawater, *Science*, 168, 247-248, 1970.

Weiss, R. F., Solubility of helium and neon in water and seawater, *J. Chem. Eng. Data*, 16, 235-241, 1971.

Weiss, R. F., and B. A. Price, Nitrous oxide solubility in water and seawater, *Mar. Chem.*, 8, 347-359, 1980.

Weiss, R. F., and B. A. Price, Dead Sea gas solubilities, *Earth and Planet. Sci. Lett.*, 92, 7-9, 1989.

Weiss, W., Bullacher, J., and W. Roether, Evidence of pulsed discharges of tritium from nuclear energy installations in central European precipitation, in, *Behaviour of Tritium in the Environment*, 17-30, IAEA, Vienna, 1979.

Wilkowske, C., *Chlorofluorocarbons as Hydrologic and Geochemical Tracers in Fractured Shales and Saprolite, Oak Ridge Reservation, Tennessee*, M.Sc. Thesis, University of Utah, 116 pp., 1998.

Wilkowske, C. D., and D. K. Solomon, Evaluation of a simple copper tube sampler for dating ground water with chlorofluorocarbons (CFCs), *Geol. Soc. Amer., 1997 Ann. Meeting, Abstracts with Programs*, 29, A-77, 1997.

Wilson, G. B., *Isotope Geochemistry and Denitrofication Processes in Groundwaters*, Ph.D. Thesis, University of Bath, U.K., 1986.

Wilson, G. B., and G. W. McNeill, Noble gas recharge temperatures and excess air component, *Appl. Geochem.*, 12, 747-762, 1997.

Worthington, S. R. H., and D. C. Ford, An equilibrium channel network model for carbonate aquifers, *Geol. Soc. Amer., 1998 Ann. Meeting, Abstracts with Programs*, 30, 69, 1998.

Worthington, S. R. H., and D. C. Ford, Test methods for developing a conceptual model for a PCB-contaminated carbonate aquifer, in, *Geotechnical and environmental applications of karst geology and hydrology, Proceedings - Multidisciplinary Conference on Sinkholes and the Engineering and Environmental Impacts of Karsts*, A. A. Balkema, Boston, 333-338, 2001.

Worthington, S. R. H., Ford, D. C., and G. J. Davies, Techniques for estimating scaling effects associated with channeling in carbonate aquifers, *Geol. Soc. Amer., 1999 Ann. Meeting, Abstracts with Programs*, 31, 287, 1999.

Yanful, E. K., and R. M. Quigley, Tritium, oxygen-18 and deuterium diffusion at the Confederation Road landfill site, Sarnia, Ontario, Canada, *Canad. Geotech. J.*, 27, 271-275, 1990.

Yatsevich, I., and M. Honda, Production of nucleogenic neon in the Earth from natural radioactive decay, *J. Geophys. Res.*, 102, 10291-10298, 1997.

Zanini, L., Novakowski, K., and P. Lapcevic, *Inorganic Geochemistry of the Groundwater at the Smithville Site – Phase I Investigation*, NWRI Control No. 97-128, 39 pp., 1997.

Zanini, L., Novakowski, K. S., Lapcevic, P., Bickerton, G. S., Voralek, J., and C. Talbot, Groundwater flow in a fractured carbonate aquifer inferred from combined hydrogeologic and geochemical measurements, *Ground Water*, 38, 350-360, 2000.